5-1-2014

Evaluation of Non-functionalized Single Walled Carbon Nanotubes Composites for Bone Tissue Engineering

Ashim Gupta
Southern Illinois University Carbondale, ashim6786@gmail.com

Follow this and additional works at: http://opensiuc.lib.siu.edu/dissertations

Recommended Citation

EVALUATION OF NON-FUNCTIONALIZED SINGLE WALLED CARBON NANOTUBES

COMPOSITES FOR BONE TISSUE ENGINEERING

By

Ashim Gupta

B.Pharm, University of Delhi, Delhi, INDIA , 2008

M.S., Southern Illinois University Carbondale, IL, USA, 2010

A Dissertation

Submitted in Partial Fulfillment of the Requirements for the

Doctor of Philosophy

Department of Molecular Biology, Microbiology and Biochemistry

in the Graduate School

Southern Illinois University Carbondale

May 2014

DISSERTATION APPROVAL

EVALUATION OF NON-FUNCTIONALIZED SINGLE WALLED CARBON NANOTUBES

COMPOSITES FOR BONE TISSUE ENGINEERING

By

Ashim Gupta

A Dissertation Submitted in Partial

Fulfillment of the Requirements

for the Degree of

Doctor of Philosophy

in the field of Molecular Biology, Microbiology and Biochemistry

Approved by:

Dr. Deliang Cao, Chair

Dr. Saadiq F. El-Amin III, Advisor

Dr. Daotai Nie

Dr. Linda Toth

Dr. Mary Ellen McAsey

Graduate school

Southern Illinois University Carbondale

March 10th, 2014

AN ABSTRACT OF THE DISSERTATION OF

ASHIM GUPTA, for the Doctor of Philosophy degree in MOLECULAR BIOLOGY, MICROBIOLOGY AND BIOCHEMISTRY, presented on March 10th, 2014, at Southern Illinois University Carbondale.

TITLE: EVALUATION OF NON-FUNCTIONALIZED SINGLE WALLED CARBON NANOTUBES COMPOSITES FOR BONE TISSUE ENGINEERING

MAJOR PROFESSOR: Dr. Saadiq F. El-Amin III

Introduction: Bone defects and non-unions caused by trauma, tumor resection, pathological degeneration, or congenital deformity pose a great challenge in the field of orthopedics. Traditionally, these defects have been repaired by using autografts and allografts. Autografts have set the gold standard for clinical bone repair because of their osteoconductivity, osteoinductivity and osteogenicity. Nevertheless, the application of autografts is limited because of donor availability and donor site morbidity. Allografts have the advantage that the tissues are readily available and can be easily applied, especially when large segments of bone are to be reconstructed. However, their use is also limited by the risk of disease transfer and immune rejection. To circumvent these limitations tissue engineering has evolved as a means to develop viable bone grafts. An ideal bone graft should be both osteoconductive and osteoinductive, biomechanically strong, minimally antigenic, and eliminates donor site morbidity and quantity issues. The biodegradable polymer, Poly lactic-co-glycolic acid (PLAGA) was chosen because of its commercial availability, biocompatibility, non-immunogenicity, controlled degradation rate, and its ability to promote optimal cell growth. To improve the mechanical properties of PLAGA, Single Walled Carbon Nanotubes (SWCNT) were used as a reinforcing material to fabricate composite scaffolds. The overall goal of this project is to develop a Single Walled Carbon Nanotube composite (SWCNT/PLAGA) for bone regeneration and to examine the interaction of MC3T3-E1 cells (mouse fibroblasts) and hBMSCs (human bone marrow derived stem cells) with the SWCNT/PLAGA composite via focusing on extracellular matrix production

and mineralization; and to evaluate its toxicity and bio-compatibility *in-vivo* in a rat subcutaneous implant model. We hypothesize that reinforcement of PLAGA with SWCNT to fabricate SWCNT/PLAGA composites increases both the mechanical strength of the composites as well as the cell proliferation rate on the surface of the composites while expressing osteoblasts phenotypic, differentiation and mineralization markers; and SWCNT/PLAGA composites are biocompatible and non-toxic, and are ideal candidates for bone tissue engineering.

Methods: PLAGA and SWCNT/PLAGA composites were fabricated with various amounts of SWCNT (5, 10, 20, 40 and 100mg), characterized and degradation studies were performed. PLAGA (poly lactic-co-glycolic acid) and SWCNT/PLAGA microspheres and composites were fabricated; characterized and mechanical testing was performed. Cells were seeded and cell adhesion/morphology, growth/survival, proliferation and gene expression analysis were performed to evaluate biocompatibility. Sprague-Dawley rats were implanted subcutaneously with Sham, poly lactic-co-glycolic acid (PLAGA) and SWCNT/PLAGA composites, and sacrificed at 2, 4, 8 and 12 week post-implantation. The animals were observed for signs of morbidity, overt toxicity, weight gain, food consumption, hematological and urinalysis parameters, and histopathology.

Results: Imaging studies demonstrated uniform incorporation of SWCNT into the PLAGA matrix and addition of SWCNT did not affect the degradation rate. Composites with 10mg SWCNT resulted in highest rate of cell proliferation ($p<0.05$) among all composites. Imaging studies demonstrated microspheres with uniform shape and smooth surfaces, and uniform incorporation of SWCNT into PLAGA matrix. The microspheres bonded in a random packing manner while maintaining spacing, thus resembling trabeculae of cancellous bone. Addition of 10mg SWCNT led to greater compressive modulus and ultimate compressive strength. Imaging

studies revealed that MC3T3-E1 cells adhered, grew/survived, and exhibited normal, non-stressed morphology on the composites. SWCNT/PLAGA composites exhibited higher cell proliferation rate and gene expression compared to PLAGA. No mortality and clinical signs were observed. All the groups showed consistent weight gain and rate-of-gain for each group was similar. All the groups exhibited similar pattern for food consumption. No difference in urinalysis parameters, hematological parameters; and absolute and relative organ weight was observed. A mild to moderate summary toxicity (sumtox) score was observed for animals treated with the PLAGA and SWCNT/PLAGA whereas the sham animals did not show any response. At all the time intervals both PLAGA and SWCNT/PLAGA showed a significantly higher sumtox score compared to the Sham group. However, there was no significant difference between PLAGA and SWCNT/PLAGA groups.

Conclusion: Our SWCNT/PLAGA composites, which possess high mechanical strength and mimic the microstructure of human trabecular bone, displayed tissue compatibility similar to PLAGA, a well known biocompatible polymer over the 12 week study. Thus, the results obtained demonstrate the potential of SWCNT/PLAGA composites for application in BTE and musculoskeletal regeneration. Future studies will be designed to evaluate the efficacy of SWCNT/PLAGA composites in bone regeneration in a non-union ulnar bone defect rabbit model. As interest in carbon nanotube technology increases, studies must be performed to fully evaluate these novel materials at a nonclinical level to assess their safety. The ability to produce composites capable of promoting bone growth will have a significant impact on tissue regeneration and will allow greater functional recovery in injured patients.

DEDICATION

I dedicate my thesis to my parents, brother and friends. Also to the person who made all

of this possible, my mentor: Saadiq El-Amin, M.D. Ph.D.

TABLE OF CONTENTS

CHAPTER   **PAGE**

LIST OF TABLES

LIST OF FIGURES

x

CHAPTER 1

BACKGROUND

Bone

Bone, or osseous tissue, is an active, rigid living organ, which forms an important part of the endoskeleton of vertebrates. It is lightweight in comparison to the work it performs to support the body. It is basically composed of the hard part of the bone, marrow, which is the soft tissue present as red and yellow marrow, bone cells present in both cortex and medulla, nerves which carry information to and from the brain, blood vessels for the supply of essential nutrients and cartilage for attachment with bones and joint formation. Bones provide some or all of the following functions:

1) A shell for the protection of our internal organs.

2) A structure to support and shape our body.

3) A lever to create movements like walking, with the coordinated help from muscles, ligaments, tendons and joints.

4) A base for the production of blood cells from its marrow content.

5) A reservoir for essential elements and compounds like calcium, phosphorous and fatty acids.

6) A buffer for blood pH levels.

7) A filter for toxic elements and also for their removal from the system.

The three most substantial properties that this dense, semi-rigid, porous, calcified connective tissue provides to vertebrate survival are mechanical, synthetic and metabolic functions.

Mechanical Functions of Bone

The mechanical functions of the bone include protection, structure and movement. Bones such as the skull and ribs are known to protect the brain and the lungs and heart respectively. The framework provided by bone lends to its structural function and provides support for the entire body. Finally, bones work in conjunction with skeletal muscles, ligaments and joints to generate and transfer forces in its mechanical function of 'movement'. In this way, individual body parts or the whole body can be adjusted and moved in a variety of ways.

Synthetic Function of Bone

Another major role of bone is the production of blood. This function is accomplished by the marrow, located within the medullary cavity of long bones and interstices of cancellous bone. These areas of the bone produce blood cells in a complex process known as hematopoiesis.

Metabolic Functions of Bone

Bone serves many metabolic functions in the body as well. Bone acts as a reserve for important minerals that the body requires such as calcium and phosphorus. Similarly, bones store growth factors like insulin-like growth factors, transforming growth factor and bone morphogenic proteins in their mineralized matrices. Additional storage capacities that bone has include the storage for fatty acids in the yellow bone marrow.

Bones further support the metabolic functions of the body by buffering the blood against excessive pH changes by absorbing or releasing alkaline salts. Bone has detoxification abilities since it can store heavy metals and other foreign elements, thus removing them from the blood and reducing their negative effects on other tissues of the body.

Bone can be thought of as an endocrine organ of sorts because it controls phosphate metabolism by releasing fibroblast growth factor – 23 (FGF-23), which acts on the kidneys in

2

order to reduce a hormone released from bone known as osteocalcin, contributes to the regulation of blood sugar (glucose) and fat deposition. It increases both the insulin secretion and sensitivity, in addition to boosting the number of insulin-producing cells and reducing stores of fat (Lee et al., 2007).

Structure of Bone

Morphologically bones exist in two different structural forms: compact and trabecular. Compact or cortical bone forms the cortex, or outer shell, of most bones and contributes to about 80 percent of the weight of a human skeleton. Cortical bone is made of a system of functional units called osteons (or Haversian system), each formed by concentric lamellae of compact bone surrounding the Haversian canal, in which blood vessels and nerves are contained. In between the lamellae osteocytes are laid down, the most abundant cells found in compact bone, which intercommunicate via long cytoplasmic extensions that occupy tiny canals called canaliculi. Each osteon is in direct contact with the periosteum, the bone marrow and other osteons through the Volkmann's canals. Trabecular or cancellous bone instead consists of a series of fine spicules (trabeculae) forming an interconnected network of bone tissue. Each trabecula is made of several concentric lamellae with osteocytes located between the lamellae. The cavities of the cortical bone are filled with bone marrow and occupied by blood vessels. The surface of bones is covered by the periosteum (outer) and endosteum, two membranes of connective tissue containing the osteoprogenitor cells, which develop into osteoblasts and provide a continuous supply of cells supporting bone growth, remodeling and repair.

Cellular Structure of Bone

Bones are mainly constituted of three different cell types, categorized as osteoblasts, osteocytes and osteoclasts. Osteoblasts, which derive from mesenchymal stem cells (MSCs), are cuboidal

3

post-proliferative cells with high synthetic activity and responsible for bone extracellular matrix deposition and mineralization. Osteocytes are star-shaped mature osteoblasts, smaller in size, which are embedded in a mineralized matrix and represent 90 percent of all cells in bone. Osteoclasts are instead multinucleated cells of hematopoietic origin with osteolytic properties, and are responsible for bone resorption. The coordinated action of osteoblasts and osteoclasts secure bone homeostasis during development and remodeling throughout lifetime.

Molecular Structure of Bone

The majority of the bone is made up of the bone matrix. It consists of inorganic and organic parts. Bone is formed by the hardening of this matrix entrapping the cells (Osteoblasts).

Inorganic: The inorganic composition of bone (bone mineral) is formed from carbonated hydroxyapatite ($Ca_{10}(PO_4)_6(OH)_2$) with lower crystallinity (Legros, Balmain, & Bonel, 1987; Field, Riley, Mello, Corbridge, & Kotula, 1974). The matrix is initially laid down as unmineralized osteoid (manufactured by osteoblasts). Mineralization involves osteoblasts secreting vesicles containing Alkaline Phosphatase. This cleaves the phosphate groups and acts as the foci for calcium and phosphate deposition. The vesicles then rupture and act as a centre for crystals to grow on. More particularly, bone mineral is formed from globular and plate structures, distributed among the collagen fibrils of bone and forming yet larger structure.

Organic: The organic part of matrix is mainly composed of Type I collagen. This is synthesized intracellularly as tropocollagen and then exported, forming fibrils. The organic part is also composed of various other factors such as glycosaminoglycans, osteocalcin, osteonectin, bone-sialo protein, osteopontin and Cell Attachment Factor.

4

Histologically/Microscopically, two types of bone can be identified based on the pattern of collagen forming the osteoid.

Woven Bone: which is characterized by haphazard organization of collagen fibers and is mechanically weak

Lamellar Bone: which has a regular parallel alignment of collagen into sheets (lamellae) and is mechanically strong

Woven bone is produced when osteoblasts produce osteoid rapidly, which occurs initially in all the fetal bones (but is later replaced by more resilient lamellar bone). In adults woven bone is created after fractures or in the Paget's disease. Woven bone is weaker, with a smaller number of randomly oriented collagen fibers, but forms quickly. It is soon replaced by lamellar bone, which is highly organized in concentric sheets with a much lower proportion of Osteocytes to surrounding tissue. Lamellar bone is stronger and filled with many collagen fibers parallel to other fibers in the same layer (these parallel columns are called osteons). In cross-section, the fibers run in opposite directions in alternating layers, assisting in the bone's ability to resist torsion forces. After a fracture, woven bone forms initially and is gradually replaced by lamellar bone during a process known as "bony substitution."

<div align="center">

Bone Formation

</div>

Bone formation is considered to be one of the most fascinating forms of tissue development throughout the body. It requires a process shared by a controlled mechanism of regeneration and remodeling that exists coherently to maintain the skeletal framework. The formation of bone during the fetal stage of development occurs by two processes:

Intramembranous Ossification: It mainly occurs during the formation of the flat bones of the skull, mandible, maxilla, and clavicles. The bone is formed from the connective tissue such as mesenchymal connective tissue rather than from cartilage. The steps in Intramembranous ossification are:

  a. Development of ossification center

  b. Calcification

  c. Formation of trabeculae

  d. Development of periosteum

Endochondral Ossification: It occurs in long bones and most of the rest of the bones in the body. It involves an initial hyaline cartilage that continues to grow. The steps in involved in Endochondral ossification are:

  a. Development of cartilage model

  b. Growth of cartilage model

  c. Development of the primary ossification center

  d. Development of the secondary ossification center

  e. Formation of articular cartilage and epiphyseal plate

Tissue Engineering of Bone

Bone defects and non-unions caused by congenital deformity, trauma, tumor resection, peri-prosthetic fractures or pathological deformation pose a great challenge in the field of orthopedics. Traditionally, these have been treated using autografts and allografts. Autografts are described as tissue/organ that is taken from the same individual to repair a specific medical problem (R. S. Langer & Vacanti, 1999). The autografts have set the gold standard for clinical bone repair because of their osteoconductivity, osteoinductivity and osteogenicity (C. T.

6

Laurencin, Ambrosio, Borden, & Cooper, 1999). Allografts, on the other hand, are described as organs transferred from one individual to another individual of same species (R. S. Langer & Vacanti, 1999). This is currently the most widely used method of organ transplantation and replacement today (Berggren, Weiland, & Dorfman, 1982). Although, the use of autografts is limited by donor shortage and donor site morbidity, whereas, the use of allografts is limited by the risk of disease transfer and immune rejection (Burg, Porter, & Kellam, 2000). To circumvent these limitations, tissue engineering has evolved as a more effective means for bone defect repair and regeneration.

Tissue engineering can be described as a compilation of several different disciplines of science utilized to create a functional organ or tissue with specific emphasis on ameliorating an individual's existence and alleviating musculoskeletal defects and disorders. Laurencin defined tissue engineering as, "an application of biological, chemical and engineering principles towards the repair, restoration, or regeneration of living tissues using biomaterials, cells, and factors alone or in combination" (Laurencin et al., 1999). The fundamentals of tissue engineering allow a unique discipline to be studied because all facets of science can be incorporated simultaneously to create a new form of research to better understand the musculoskeletal conditions.

The ability to decipher the intricate underlying factors of tissue engineering will introduce a new way of approaching tissue and organ growth. Tissue engineering applications offer biocompatibility, availability, and diversity when being applied to various areas of bone and tissue regeneration. Over the last decade there has been an increased push for the use of alternative materials in the fields of medicine and science, especially in Orthopedics with an emphasis on addressing musculoskeletal disorders (Jackson & Simon, 1999). Such interests have led to the introduction of synthetic materials for use in various tissue engineering

7

applications. The understanding for such needs has generated a keen interest in developing

biodegradable polymers based on various monomers combined to achieve a specific polymer

type (Ignatius & Claes, 1996).

<div align="center">**Biodegradable Polymers**</div>

The success of the scaffold-based bone regeneration approach relies heavily on effectiveness of

the biodegradable scaffold (Hutmacher, 2000). The use of biodegradable polymers for tissue

engineering offers several advantages. Polymeric materials are unlimited in quantity, can be

fabricated to promote optimal cellular compatibility (Attawia, Uhrich, Botchwey, Langer, &

Laurencin, 1996), can be surface treated to resemble tissue like qualities (Brekke & Toth, 1998),

and can eliminate the need for surgical removal once placed *in vivo* (Royals et al., 1999). With

all of the aforementioned advantages, biodegradable polymers offer a new and exciting challenge

for the field of medicine, particularly in the areas of cartilage and bone regeneration. The ability

to create matrices capable of promoting bone growth will produce unlimited potential for both

the molecular and engineering sides of research.

The polyesters are a group of biodegradable polymers that include polyglycolic acid

(PGA), polylactic acid (PLA) and the copolymer, polylactic-co-glycolic acid (PLAGA). These

polymers are currently approved by the Food and Drug Administration for certain orthopedic

applications (Mikos, Sarakinos, Leite, Vacanti, & Langer, 1993), and are currently on the market

as suture materials, fixation pins and staples (Grizzi, Garreau, Li, & Vert, 1995; Ignatius &

Claes, 1996). The advantages of these materials are their ability to degrade via bulk erosion into

harmless by-products (Grizzi et al., 1995; Migliaresi, Fambri, & Cohn, 1994).

The PGA polymer is highly crystalline, thus giving the material a high melting point and

decreased solubility in organic solvents. The PGA polymer was one of the first polymers used as

surgical suture material and is currently on the market as DEXON®. Its reported degradation rate is between 6 and 8 months, causing the material to lose mechanical strength at an accelerated rate (Ignatius & Claes, 1996).

The addition of a methyl group to PGA led to the introduction of a lactic acid group, leading to formation of PLA polymer. This cyclic dimer exists in both the L and D isoforms, which can also be combined in a mixture to create the synthetic polymer D, L-PLA. PLA is also a semi-crystalline polymer that possesses a more hydrophobic profile with a higher molecular weight and melting point (Migliaresi et al., 1994). This allows a longer degradation time that is reported to take more than 2.5 years (Migliaresi et al., 1994). Degradation studies have revealed that PLA is broken down through hydrolytic cleavage, where the monomeric lactide groups are removed via the glycolytic process occurring in the surrounding muscle (Vert, Li, & Garreau, 1994; Vert, Mauduit, & Li, 1994). Currently, PLA material is on the market as suture anchors and interference screws.

In an attempt to obtain a more controllable material with better characteristics, the combination of both PLA and PGA was introduced in various ratios such as 50:50, 25:75 and 85:15. Poly lactic-co-glycolic acid (PLAGA) is used as a scaffold material because of its excellent biocompatibility and bioresorbability, commercial availability, non-immunogenicity, controlled degradation rate, and its ability to promote optimal cell growth (Athanasiou, Niederauer, & Agrawal, 1996; Lu, Garcia, & Mikos, 1999). Several studies have examined the uses of PLAGA matrices as evidenced by the literature describing the polymer's acceptance in the areas of tissue engineering and orthopedics (Thomson, Yaszemski, Powers, & Mikos, 1995; Cohen, Alonso, & Langer, 1994). Currently, the combined material is on the market for craniomaxillofacial fixation devices and interference screws (R. Zhang & Ma, 1999). Studies by

various laboratories have demonstrated good biological fixation with the copolymers and the ability to use these materials for drug delivery devices as well (Cohen et al., 1994; Jalil & Nixon, 1990; Miyamoto et al., 1993; Vert, Mauduit, et al., 1994).

Carbon Nanotubes (CNT)

One of the essential requirements of the scaffold material is to have the desired mechanical properties (elastic modulus and tensile strength) which can be increased by reinforcing with a second-phase material. Carbon Nanotubes (CNT) due to their unprecedented properties in terms of size, strength and surface area have made them a potential reinforcement in the production of nanocomposites with ceramics, metals and polymers, including biodegradable polymers (N. Sinha & Yeow, 2005; Armentano, Dottori, Puglia, & Kenny, 2008). Data from literature reveals that CNT that were incorporated into a polymer matrix substantially improve upon the original mechanical properties of that material (Hu, Ni, Montana, Haddon, & Parpura, 2004; Schwartz et al., 1999; Bagambisa, Kappert, & Schilli, 1994). CNT combined with chitosan generated a matrix that enhanced the mechanical properties, including the Young's modulus, and tensile strength as much as 93% and 99% respectively (Mattson, Haddon, & Rao, 2000). Similar results were seen when CNT were uniformly distributed into a brittle hydroxyapatite bioceramic coating. The improved fracture toughness of 56% was attributed to the incorporation of the CNT (Webb, Hlady, & Tresco, 2000). Apart from the polymer enhancement, they have also been used to reinforce the ceramic matrices, where the addition of CNT increased the fracture toughness (Arsecularatne & Zhang, 2007).

In addition, a lot of researchers have reported that CNT act as an excellent substrate for cell growth and differentiation (Shi Kam, Jessop, Wender, & Dai, 2004; Liopo, Stewart, Hudson, Tour, & Pappas, 2006; Hu et al., 2004). CNT are allotropes of carbon with a cylindrical

10

nanostructure. They have been constructed with length-to-diameter ratio of up to 132,000,000:1 (X. Wang et al., 2009) which is significantly larger than compared to any other material. Nanotubes are members of the fullerene structural family. Their name is derived from their long, hollow structure with the walls formed by one-atom-thick sheets of carbon, called graphene. These sheets are rolled at specific and discrete ("chiral") angles, and the combination of the rolling angle and radius decides the nanotube properties, for example, whether the individual nanotube shell is a metal or semiconductor. Nanotubes are categorized as single-walled nanotubes (SWCNT) and multi-walled nanotubes (MWCNT).

SWCNT have a diameter close to 1 nanometer, with a tube length that can be many millions of times longer. The structure of a SWCNT can be conceptualized by wrapping a one-atom-thick layer of graphite called graphene into a seamless cylinder. MWCNT consist of multiple rolled layers (concentric tubes) of graphene. There are two models that can be used to describe the structures of multi-walled nanotubes. In the **Russian Doll model**, sheets of graphite are arranged in concentric cylinders whereas in the **Parchment model**, a single sheet of graphite is rolled in around itself, resembling a scroll of parchment or a rolled newspaper (Dai, 2002).

The material of interest in our laboratory is SWCNT. They are solely made up of carbon with same scale size of DNA and the fact that all living entities are carbon based makes them an ideal candidate for introduction into the biological systems (Dai, 2002).

Cell adhesion receptors (Integrins)

For the PLAGA/SWCNT composites to be successful in the field of bone tissue engineering, their interaction with the cellular tissue needs to be examined. One way to examine the interaction of these composites with the surrounding tissue is to look into the receptors involved in the cellular adhesion, integrins. Integrins are transmembrane heterodimeric proteins that

contains α and β subunits which localize to form a receptor that has been demonstrated to be involved in the cellular adhesion, signal transduction and gene expression (Ruoslahti, 1996; Hughes, Salter, Dedhar, & Simpson, 1993; Gronowicz & McCarthy, 1996).

The integrins were first introduced to the field of science and molecular biology during the discovery of the RGD sequence found in the fibronectin gene. Studies by Pytela et al. (Pytela, Pierschbacher, & Ruoslahti, 1985) discovered that the RGD sequence, which stands for Arg-Gly-Asp, adheres directly to the integrin $\alpha_5\beta_1$. Further studies on chicken receptors, platelet adhesion proteins GP IIb/IIIa and lymphocytic adhesion proteins, all of which have structural similarities to the fibronectin integrin receptor (Ruoslahti, 1996) further supports the presence of integrins. The aforementioned finding demonstrated that integrins are a large family of related adhesion proteins from different species performing the same function. Ruoslahti states that the term "integrin" is appropriately given because of the receptor's ability to integrate with the extracellular matrix proteins that were found to adhere to these receptors (Ruoslahti, 1996). These findings were important and led to the increased investigation of the integrins in the field of medicine, science, and orthopedics. The structural diversity of integrins is important to the receptor function. The integrin receptor consists of α and β subunits that combines to form a transmural receptor that functions together. The carboxyl end of the subunit is located on the extracellular side of the receptor and is involved in adhesion, whereas the N-terminal region that contains NH_2 is located intracellularly and is involved in signal transduction and communication. To date over 12 different α subunits and over 8 different β subunits have been reported that form to create a receptor that is specific for a certain ligand sequence (T. Saito, Albelda, & Brighton, 1994). For example, the pairing of $\alpha_2\beta_1$ is specific for the abundant extracellular matrix molecule collagen, whereas $\alpha_5\beta_1$ is more specific for fibronectin (Hautanen, Gailit, Mann, & Ruoslahti,

1989; Pierschbacher & Ruoslahti, 1984; R. K. Sinha & Tuan, 1996). It is this specific pairing of the integrin subunits that gives the receptor the specificity that allows it to bind, as well as the diversity that has been described to date (Hynes, 1992).

Several studies have confirmed integrins involvement in the following: cell adhesion to the surface, cell-cell adhesion, platelet function, leukocyte activity, wound repair and embryological development of muscle (Fernandez, Clark, Burrows, Schofield, & Humphries, 1998; Gullberg, Velling, Lohikangas, & Tiger, 1998; Johansson, Svineng, Wennerberg, Armulik, & Lohikangas, 1997). Studies by El-Amin et al. have demonstrated that Integrin expression is critical to human osteoblast cell adhesion to biomaterials, including the biodegradable polyesters. These results introduced the concept that adhesion of osteoblasts could be up-regulated depending on the surface of the polymer and composition. Other researchers such as Sinha et al. described the abundant accumulation and expression of integrins on orthopedically-related metals, such as titanium and cobalt chrome (R. K. Sinha & Tuan, 1996), which are currently used to produce implants for hip arthroplasty. The human osteoblasts' expression of integrins on metallic surfaces occurred at varied levels depending on the surface of the material and the type of metal employed, again supporting integrins' role in cellular attachment. In addition to biomaterial surfaces designed from either polymers or metals, growth on matrices created with either various protein or peptides were also investigated. Saito et al. demonstrated that in the presence of surfaces coated with type I collagen, fibronectin, vitronectin and poly-D-lysine, cell adhesion was enhanced 60-70% for cells seeded on these surfaces, whereas only 40-50% was observed for cells plated on surfaces covered with type IV collagen, laminin and gelatin (T. Saito et al., 1994). In addition, they demonstrated an increase in the specific integrin receptors ($\alpha_1\beta_1$, $\alpha_3\beta_1$, $\alpha_5\beta_1$, and $\alpha_v\beta_1$) that bind to the previously mentioned proteins (T. Saito et al., 1994). They

13

also reported that integrins interaction in bone cells are important in determining skeletal development, bone matrix production, the pathological processes of fracture repair, osteogenic tumors, and metabolic bone diseases. Additionally, integrins involvement in various other cells, ranging from neural to endothelial cells, has been demonstrated by several investigators (Hynes, 1992). However, to obtain a deeper understanding of the connection with tissue engineered bone, Integrin expression by osteoblasts needs to be more thoroughly evaluated in the orthopedic realm.

Several other studies have looked at the type of integrins expressed from various types of osteoblasts that are currently being used in the field of cellular adhesion (Attawia et al., 1996; Puleo & Nanci, 1999). Albeda et al. reported that the following integrins: α_1, α_5, α_6, α_v, β_1 and β_2, were observed at various levels on rat calvarial cells. They also reported a negative staining for the α_2 and α_3 integrins, indicating their absence. When evaluating Integrin expression in fetal bone *in vivo*, a large amount of α_4, α_5, α_v, β_1 and β_3 were detected, but other integrins such as α_1, α_2 and α_3 were not investigated, thus leaving their presences unknown (Albelda & Buck, 1990). When evaluating Integrin expression on human osteoblasts isolated *in vitro*, studies by Sinha et al. reported the presence of α_2, α_3, α_4 α_5, α_v, β_1 and β_3, thus demonstrating that various growth methods lead to the production of a vast repertoire of integrins (R. K. Sinha & Tuan, 1996).

Alkaline Phosphatase

Alkaline phosphatase (ALP) is a hydrolase enzyme responsible for removing phosphate groups from many molecules like nucleotides, proteins, and alkaloids. The process of removing the phosphate group is called dephosphorylation. ALPs are most effective in an alkaline environment. It is sometimes used synonymously as a basic phosphatase. In humans, alkaline phosphatase is present in all tissues throughout the entire body, but is particularly concentrated in

liver, bile duct, kidney, bone, and the placenta.

The growth of preosteoblastic cells to mature osteoblasts has been correlated with levels of alkaline phosphatase (ALP) expression, which has widely been used as a bone marker to evaluate bone formation (Aubin, Liu, Malaval, & Gupta, 1995). Even though it is widely used, few studies have demonstrated the role of ALP but many have speculated its involvement in mineralization. Aubin et al. demonstrated poor levels of alkaline phosphatase in bone-metabolizing diseases such as Hypophosphatasia and Ricketts due to the inability to mineralize bone (Coelho & Fernandes, 2000). From a basic science research perspective, ALP is present in preosteoblasts and appears in differentiating osteoblasts before expression of matrix proteins, such as osteocalcin. Overall, the ALP protein is associated with the cellular membrane and plays a role in the regulation of osteoprogenitor/ osteoblast migration and or differentiation (Coelho & Fernandes, 2000).

Osteocalcin

Osteocalcin, also known as bone gamma-carboxyglutamic acid-containing protein (BGLAP), is a noncollagenous protein found in bone and dentin. In humans, the osteocalcin is encoded by the BGLAP gene (Puchacz et al., 1989; Cancela, Hsieh, Francke, & Price, 1990). Osteocalcin is secreted solely by osteoblasts and thought to play a role in the body's metabolic regulation and is pro-osteoblastic, or bone-building, by nature (Lee et al., 2007). It is implicated in bone mineralization and calcium ion homeostasis. Osteocalcin, described as a member of the gla protein group, is referred to as both bone gla protein and matrix gla protein (Reinholt, Hultenby, Oldberg, & Heinegård, 1990). The gla proteins are secreted by both osteoblasts and chondrocytes and are a family of mineral binding–ECM proteins. The family of gla proteins contains glutamic acid residues that help in the binding of Ca^{2+} and hydroxyapatite crystals. The osteocalcin has

15

been reported to be involved in regulating bone remodeling (Reinholt et al., 1990), where the levels are increased during the growth of mineral crystal formation.

In addition to bone formation, osteocalcin has also been reported to affect osteoclast activity. Studies have demonstrated that osteocalcin increases osteoclast activity leading to bone resorption. The ability of osteocalcin to affect osteoclast activity can also be supported by its binding to another ECM protein, osteopontin (Reinholt et al., 1990). The binding of both molecules leads to a complex that initiates the recruitment of Osteoclasts to a particular area of bone and induces cellular attachment.

Osteocalcin also acts as a hormone in the body, causing beta cells in the pancreas to release more insulin, and at the same time directing fat cells to release the hormone adiponectin, which increases sensitivity to insulin (Lee et al., 2007; Pi, Wu, & Quarles, 2011; Fulzele et al., 2010). Another study by Oury et al. demonstrated endocrine function of Osteocalcin in male fertility regulation. They reported that by binding to a G protein-coupled receptor expressed in the Leydig cells of the testes, osteocalcin regulates in a CREB-dependent manner the expression of enzymes that is required for testosterone synthesis thus promoting germ cell survival (Oury et al., 2011).

RUNX2

Runt-related transcription factor 2 (RUNX2) or core-binding factor subunit alpha-1 (CBF-alpha-1) is a protein which in humans is encoded by the RUNX2 gene. RUNX2 is a key transcription factor associated with osteoblast differentiation. This protein is a member of RUNX family of transcription factors and has a Runt DNA-binding domain. RUNX2 is essential for the osteoblastic differentiation and skeletal morphogenesis and acts as a scaffold for nucleic acids and regulatory factors involved in the skeletal gene expression. The protein can bind DNA either

as a monomer or, with more affinity, as a subunit of a heterodimeric complex. Transcript variants of the gene that encode different protein isoforms result from the use of alternate promoters as well as alternate splicing. Differences in RUNX2 are hypothesized to be the cause of the skeletal differences between modern humans and early humans such as Neanderthals. These differences include a different shape of the skull, a bell-shaped chest in Neanderthals (Green et al., 2010). The binding interactions of RUNX2 change as cells go through mitosis, with binding affinity increasing as chromosomes condense and then decreasing through subsequent mitotic phases. The increased residence of RUNX2 at mitotic chromosomes may reflect its epigenetic function in "bookmarking" of target genes in cancer cells (Pockwinse et al., 2011; Tandon et al., 2012).

Collagen

Collagen is a group of naturally occurring proteins found in animals, especially in the flesh and connective tissues of vertebrates (Müller, 2003). It is the main component of connective tissue, and is the most abundant protein present in the ECM in mammals (Groessner-Schreiber & Tuan, 1992; Di Lullo, Sweeney, Korkko, Ala-Kokko, & San Antonio, 2002). The collagen family consists of more than 15 different types that have been described in vertebrates and are divided into subgroups. Some of the most important ones are fibrillar collagen, which includes Type I, II, III, V and XI; the fibril-associated class, which includes IX and XII; the network forming group IV; and the filamentous group VI. The collagen families contain a triple helix, which is composed of folded alpha chains that assume a proper helical formation involving glycine at every third amino acid residue (Shoulders & Raines, 2009). The alpha chains that make up the triple helix can be found to possess a triplet sequence of Gly-X-Y, where the X is usually proline and the Y is found to be hydroxyproline. The abundance of the hydroxyproline adds stability to the helical structure and its presence has been described as crucial for collagen to have good

17

structural integrity (Shoulders & Raines, 2009). Another key amino acid is lysine, which has been shown to be involved in the cross-linking between the alpha chains that comprise the collagen framework.

The fibrillar class, which contains the more abundant types of collagen, has been reported to be involved in various locations in the body. For instance, Type I collagen has been found primarily in skin, bone, tendon, corneas, and fibrous matrices. However, very little has been reported in cartilage. On the other hand, Type II collagen is found in abundance in cartilage and is associated with both corneal stroma and the notochord. Type III is a main component of reticular fibers (Waldrop, Puchtler, Meloan, & Younker, 1980).

In addition to the several classes of collagen molecules found and reported throughout the body, collagen has also been demonstrated to be involved in cellular adhesion. Studies have exhibited cellular adhesion to collagen and collagen-coated surfaces via receptors such as the integrins.

Osteopontin

Osteopontin (OPN) is another bone protein that is mainly involved in, but not limited to, matrix mineralization (Reinholt et al., 1990). It has been described as a glycoprotein known to be involved in many tissue and organ types. Moreover, it has been demonstrated to be expressed in a variety of tissues, such as kidney, chondrocytes, odontoblasts, both bone and bone-derived marrow gland cells, and a whole host of other epithelial types of tissues (Butler, 1989). In particular, the main expression of osteopontin is in bone and related cellular tissues and structures. Early analysis of osteopontin revealed that this acidic glycoprotein contains high amounts of sialic acid synthesized by a variety of tissue types including fibroblasts (Ashizawa et al., 1996), preosteoblasts, osteoblasts, osteocytes (Reinholt et al., 1990; Butler, 1989; Denhardt

18

& Guo, 1993), odontoblasts, some bone marrow cells, hypertrophic chondrocytes, dendritic cells, macrophages (Murry, Giachelli, Schwartz, & Vracko, 1994), smooth muscle (Ikeda, Shirasawa, Esaki, Yoshiki, & Hirokawa, 1993), skeletal muscle myoblasts (Uaesoontrachoon et al., 2008), endothelial cells, and extraosseous (non-bone) cells in the inner ear, brain, kidney, deciduum, and placenta. Synthesis of osteopontin is stimulated by calcitriol (1, 25-dihydroxy-vitamin D_3).

OPN has been described to be involved in the early stages of osteogenesis where-by osteoblasts bind to the ECM matrix (Denhardt & Guo, 1993), in osteoclast attachment which is a key factor during bone absorption via the regulation of bone crystal size (Reinholt et al., 1990). Intracellular signaling events have also been described to be regulated by OPN through its GRGDS amino acid binding sequence involvement with the $\alpha_v\beta_3$ integrin receptor. This was confirmed through studies performed in the presence of OPN and other RGD-peptides involving the $\alpha_v\beta_3$ receptor where osteoclast chicken cells, secreted Ca^{2+} via ATPase in a calmodulin-dependent manner (Butler, 1989).

Osteopontin also plays an important role in chemotaxis by recruiting neutrophils in alcoholic liver diseases (Banerjee, Apte, Smith, & Ramaiah, 2006; Apte, Banerjee, McRee, Wellberg, & Ramaiah, 2005). OPN causes cell activation by inhibiting production of Th2 cytokine IL-10 thus leading to enhanced Th1 response; enhance B cell immunoglobulin production and proliferation; and induces mast cells degranulation (K. X. Wang & Denhardt, 2008; Nagasaka et al., 2008). OPN is also an important anti-apoptotic factor in many circumstances. It blocks the activation-induced cell death of macrophages and T cells as well as fibroblasts and endothelial cells exposed to harmful stimuli (Denhardt, Noda, O'Regan, Pavlin, & Berman, 2001; Standal, Borset, & Sundan, 2004) and prevent non-programmed cell death in inflammatory colitis (Da Silva et al., 2006).

19

Bone Sialoprotein

Bone Sialoprotein (BSP) is a component of mineralized tissues such as bone, dentin, cementum and calcified cartilage. It is a significant component of the bone ECM and has been suggested to constitute approximately 8% of all non-collagenous proteins found in bone and the cementum (Fisher, McBride, Termine, & Young, 1990). The amount of BSP in bone and dentin is nearly equal (Qin et al., 2001), however the function of BSP in these mineralized tissues is not known. One possibility is that it acts as a nucleus for the formation of the first apatite crystals (Hunter & Goldberg, 1994) and as the apatite forms along the collagen fibres within the ECM, it could then help direct, redirect or inhibit the crystal growth. Additional roles of BSP are MMP-2 activation, angiogenesis, and protection from complement-mediated cell lysis. Therefore, the regulation of the BSP gene is important to bone matrix mineralization, osteoblasts differentiation and tumor growth in bone (Ogata, 2008).

RESEARCH OBJECTIVE

The overall goal of this project is to develop a Single Walled Carbon Nanotube composite (SWCNT/PLAGA) for bone regeneration and to examine the interaction of MC3T3-E1 cells and hBMSCs with the SWCNT/PLAGA composite via focusing on extracellular matrix production and mineralization; and to evaluate its toxicity and bio-compatibility *in-vivo* in a rat subcutaneous implant model.

HYPOTHESIS

We hypothesize that:

1. Reinforcement of PLAGA with SWCNT to fabricate SWCNT/PLAGA composites increases both the mechanical strength of the composites as well as the cell proliferation rate on the surface of the composites while expressing osteoblasts phenotypic, differentiation and mineralization markers.

2. SWCNT/PLAGA composites are biocompatible and non-toxic, and are ideal candidates for bone tissue engineering.

SPECIFIC AIMS

1. To fabricate the two-dimensional Poly lactic acid (PLA) and Poly (lactic-co-glycolic) acid (PLAGA) polymeric scaffolds, and to determine the cellular adhesion and proliferation rate on these scaffolds.

2. To fabricate and evaluate the two-dimensional Single Walled Carbon Nanotubes (SWCNT) composites (SWCNT/PLAGA) for bone tissue engineering.

3. To fabricate, characterize and evaluate the three-dimensional SWCNT/PLAGA composites for bone tissue engineering.

4. To evaluate the toxicity and bio-compatibility *in-vivo* in a rat subcutaneous implant model.

CHAPTER 2

EVALUATION OF TWO DIMENSIONAL PLA AND PLAGA COMPOSITES FOR

BONE TISSUE ENGINEERING

CHAPTER 2-1

INTRODUCTION

Bone defects and non-unions caused by congenital deformity, trauma, tumor resection, peri-prosthetic fractures or pathological deformation pose a great challenge in the field of orthopedics. Traditionally, these bone defects have been treated using autografts and/or allografts, with or without the use of biological agents. Autografts have been traditionally thought of as the gold standard for use in bony defects because of their osteoconductivity, osteoinductivity and osteogenicity (R. S. Langer & Vacanti, 1999; C. T. Laurencin et al., 1999). Allografts provide a good osteoconductive environment, however their osteoinductive capabilities are poor. Autograft use is limited by donor shortage and donor site morbidity, whereas, the use of allografts is limited by the risk of disease transfer, immune rejection and the lack of adequate osteoinductivity and osteogenicity (R. S. Langer & Vacanti, 1999; Burg et al., 2000). To circumvent the limitations posed by autografts and allografts, tissue engineering has evolved as a means to develop viable bone grafts.

Bone tissue engineering has evolved in order to attempt to provide a gold standard synthetic bone substitute for which large bony defects can be adequately addressed. Bone tissue engineering involves the combination of biodegradable scaffolds with or without the use of cells and growth factors to regenerate bone (Petite et al., 2000). The success of the scaffold-based bone regeneration approach relies heavily on the effectiveness of the biodegradable scaffold (Hutmacher, 2000). The use of biodegradable polymers for tissue engineering offers several

22

advantages. Polymeric materials are unlimited in quantity, can be fabricated to promote optimal cellular compatibility (Attawia et al., 1996), can be surface treated to resemble tissue like qualities (Brekke & Toth, 1998), and can eliminate the need for surgical removal once placed *in vivo* (Royals et al., 1999). With all of the aforementioned advantages, biodegradable polymers offer a new and exciting challenge for the field of medicine, particularly in the areas of cartilage and bone regeneration. The ability to create matrices capable of promoting bone growth will produce unlimited potential for both the molecular and engineering sides of the research.

Some of the important classes of polymers are polyanhydrides, polyphosphazenes and polyesters. Polyanhydrides are synthesized through the dehydration of diacid molecules via polycondensation (C. T. Laurencin & Langer, 1987). They have been described as being very hydrolytically unstable and they degrade by surface erosion which leads to a faster degradation rate (R. Langer, 1995). Polyanhydrides have been approved as implantable devices in the brain by the FDA for controlled drug delivery of the chemotherapeutic agent (BCNU) to treat brain tumors (R. Langer & Vacanti, 1993). Studies from literature also showed that addition of imide group leads to enhanced mechanical properties (Uhrich, Ibim, Larrier, Langer, & Laurencin, 1998). Another study by Fan et al. reported that, mild inflammatory reactions were observed after implantation of the polymer (Fan, Li, Jiang, Tang, & Wang, 2008).

Polyphosphazenes consists of an inorganic phosphorous-nitrogen backbone connected to various amino acid groups, such as glycine. They have an amorphous profile with a molecular weight in the millions and it degrades by both bulk and surface erosion (Elgendy, Norman, Keaton, & Laurencin, 1993). Study by Laurencin et al. showed the biocompatible nature of polyphosphazenes (C. T. Laurencin, El-Amin, et al., 1996). They are still a new class of polymers and their applications for tissue engineering are yet to be established.

Another important class is the polyesters, which are a group of biodegradable polymers that include polyglycolic acid (PGA), polylactic acid (PLA) and the copolymer, polylactic-co-glycolic acid (PLAGA). These polymers are currently approved by the Food and Drug Administration for certain orthopedic applications (Mikos et al., 1993), and are currently on the market as suture materials, fixation pins and staples (Grizzi et al., 1995; Ignatius & Claes, 1996). The advantages of these materials are their ability to degrade via bulk erosion into harmless by-products (Grizzi et al., 1995; Migliaresi et al., 1994).

The PGA polymer is highly crystalline, thus giving the material a high melting point and decreased solubility in organic solvents. Its reported degradation rate is between 6 and 8 months, causing the material to lose mechanical strength at an accelerated rate (Ignatius & Claes, 1996). The addition of a methyl group to PGA led to the introduction of a lactic acid group, leading to formation of PLA polymer. PLA is a semi-crystalline polymer that possesses a more hydrophobic profile with a higher molecular weight and melting point (Migliaresi et al., 1994). This allows a longer degradation time that is reported to take more than 2.5 years (Migliaresi et al., 1994). In an attempt to obtain a more controllable material with better characteristics, the combination of both PLA and PGA was introduced in various ratios such as 50:50, 60:40, 75:25 and 85:15. Poly lactic-co-glycolic acid (PLAGA) is used as a scaffold material because of its excellent biocompatibility and bioresorbability, commercial availability, non-immunogenicity, controlled degradation rate, and its ability to promote optimal cell growth (Athanasiou et al., 1996). Several studies have examined the uses of PLAGA matrices as evidenced by the literature describing the polymer's acceptance in the areas of tissue engineering and orthopedics (Thomson et al., 1995; Cohen et al., 1994).

The purpose of this study was to develop 2-D PLA and PLAGA scaffolds and to determine the MC3T3-E1 and rMSCs (rat mesenchymal stem cells) cells adhesion and proliferation rate on these matrices. We hypothesize that the biodegradable polymers PLA and PLAGA with known biocompatibility and controlled degradability can be fabricated and optimized into suitable composites for bone tissue engineering applications.

25

METHOD

Biomaterials

Poly lactic acid (PLA) (Purasorb PL38, Purac Biomaterials, Netherlands) and Poly lactic-co-glycolic acid (PLAGA 85:15) (Purasorb PLG8523, Purac Biomaterials, Netherlands) were obtained and stored at -80^{0}C to prevent degradation.

Fabrication of PLA Scaffolds

PLA scaffolds were fabricated by dissolving 1g of PLA in 14ml solution of dichloromethane (Fisher Scientific, USA) in a 20ml scintillation vial. The solution was vortexed for 8 hours at a constant speed to dissolve the polymer. The dissolved polymer was then poured in a glass Petri-plate with Bytac paper and was immediately kept at -80^{0}C for 3 days. The plate was then kept at room temperature for 3 days or until the solvent was completely evaporated. The thin film obtained was bored into circular disks with a 12mm diameter and placed in a desiccator for 24 hours in order to remove the residual solvent.

Fabrication of PLAGA Scaffolds

PLAGA scaffolds were fabricated by dissolving 1g of PLAGA in 12ml solution of dichloromethane (Fisher Scientific, USA) in a 20ml scintillation vial. The solution was vortexed for 8 hours at a constant speed to dissolve the polymer. The dissolved polymer was then poured in a glass Petri-plate with Bytac paper and was kept under a vacuum hood for 30 minutes. The plate was then kept at -20^{0}C overnight and then brought to room temperature for complete evaporation of the solvent. The thin film obtained was bored into circular disks with a 12mm diameter and placed in a desiccator for 24 hours in order to remove the residual solvent.

Cell Culture

MC3T3-E1 cells were obtained from ATCC (MC3T3-E1 subclone 4). The cells were grown in Alpha Minimal Essential Medium (Alpha MEM) with ribonucleosides, deoxyribonucleosides, 2mM L-Glutamine, and 1mM sodium pyruvate (Hyclone, Thermo Scientific, USA) supplemented with 10% Fetal Bovine Serum (FBS) (Gibco, Invitrogen, USA) and 1% Penicillin-Streptomycin (PS) (Lonza, USA). The cells were kept in humidified air under 5% CO_2 at 37^0C.

Rat Mesenchymal Stem Cells (rMSCs) were cultured in Alpha Minimal Essential Medium (Alpha MEM) with ribonucleosides, deoxyribonucleosides, and 2mM L-Glutamine supplemented with 20% Fetal Bovine Serum (FBS) (Gibco, Invitrogen, USA) and 1% Penicillin-Streptomycin (PS) (Lonza, USA). The cells were kept in humidified air under 5% CO_2 at 37^0C. rMSCs were obtained from Dr. Cady's lab at Bradley University.

The PLA and PLAGA scaffolds were fabricated as described above and exposed to UV light for 15 minutes to insure sterilization. Tissue culture polystyrene (TCPS) (Fisherbrand Coverglass, Fisher Scientific, USA) served as a control. After sterilization the scaffold disks were placed in a 24 well plate and soaked in the complete culture medium for 1 hour. The desired number of cells (MC3T3-E1 and rMSCs) were counted using hemacytometer (Hausser Scientific, USA) and were then seeded on the disks for cell adhesion/morphology/proliferation studies.

Immunofluorescence Staining

MC3T3-E1 cells are flat and polygonal in shape and rMSCs are spindle like and fibroblastic in shape (Horikawa, Okada, Sato, & Sato, 2000; Chang et al., 2012). The morphology of the cells can be used to determine the cellular behavior on the polymeric scaffolds. Cellular morphology and adhesion (qualitatively) were determined by using Immunofluorescence staining. At day 3, 4

27

and 5; the scaffolds seeded with MC3T3-E1 cells were washed with PBS. The cells were then fixed with chilled 70% ethanol for 10 minutes. Post fixation, the cells were incubated with 1% Bovine Serum Albumin (BSA) in PBS having 0.05% Triton X-100 for 20 minutes at room temperature followed by immersing the samples in 1% Tween. The cells were then incubated overnight at 4^0C with monoclonal mouse Anti-β-actin antibody (1:400, catalog number- A5441, Sigma Aldrich, USA). They were then washed with 0.05% Tween and incubated with secondary antibody (goat anti-mouse F (ab') 2 fragment of IgG conjugated with an Alexa Fluor® 488 fluorescence probe, 1:400, catalog number- 4408, Cell Signaling, USA) for 1 hour at room temperature. This was followed by washing the cells with PBS, and staining for the nucleus (Hoechst dye), mounting using 80% Glycerol and viewing under a Confocal Microscope (Leica TCS SP5 spectral laser scanning confocal microscope) (Vandrovcová et al., 2011). Similarly, rMSCs were observed at day 3.

Scanning Electron Microscopy

Cell adhesion on the polymeric scaffolds surface was determined qualitatively by using SEM (Hitachi S-3000 scanning electron microscope). At day 3, the scaffolds seeded with cells (MC3T3-E1 and rMSCs) were washed with PBS. The cells were then fixed with 1.5% Glutaraldehyde in 0.1M Cacodylate buffer followed by post-fixation with 2.5% OsO_4 in 0.1M Cacodylate buffer. After fixation the cells were washed with 0.1M Cacodylate buffer and then dried using serial ethanol dehydration, followed by Hexamethyldisilazane (HMDS). The dried samples were then sputter coated with Gold/ palladium and viewed using the SEM.

Cell Proliferation Assay

Cell adhesion and proliferation was determined quantitatively using MTS assay at day 3, 5 and 7 post-seeding (5,000 rMSCs cells) on PLA and PLAGA scaffolds using TCPS as control. At

desired time points, media was removed, cells were washed with PBS and 20µl of Cell titer 96[®] AQ~~ueous~~ One solution reagent (Promega, USA) was added in each well having 100µl of culture medium followed by incubating the plate at 37^0C for 1-4 hours in a humidified; 5% CO_2 atmosphere. The absorbance/ optical density (O.D.) was measured at 490nm by using a microplate reader.

Statistical Analysis

MTS assay was performed three times in duplicate and mean ± SEM values along with statistical analysis using two-way ANOVA were performed. The results were considered significant when $p < 0.05$.

RESULTS

Fabrication of PLA and PLAGA Scaffolds

PLA and PLAGA two-dimensional (2-D) scaffolds were fabricated using solvent evaporation method. Figure 2-1 shows the fabrication process of these polymeric scaffolds and the film obtained. 12mm diameter disks were cut from the films obtained and used for cell adhesion/morphology and proliferation studies.
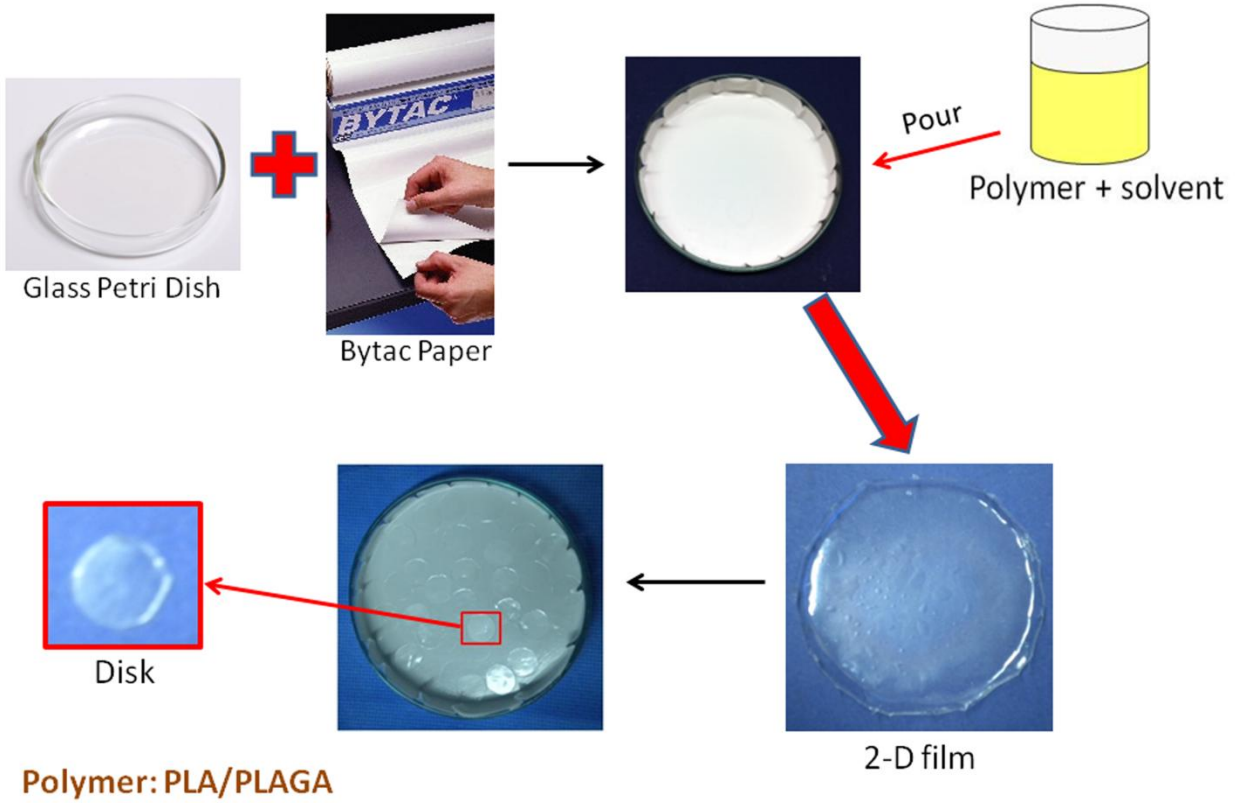
Figure 2-1: Schematic representation of steps involved in fabrication of 2-D PLA and

PLAGA scaffolds using solvent evaporation method.

Immunofluorescence Staining

The adhesion and the morphology of the MC3T3-E1 cells (Figure 2-2) on the various scaffold surfaces was observed using Immunofluorescence staining. The cells were stained with β-actin and nuclear hoechst stain and were observed at day 3, 4 and 5 under a confocal microscope. The images revealed that the cells adhered, grew and exhibited a normal, non-stressed morphological pattern on both the surfaces (PLA and PLAGA).

To make sure that the scaffolds fabricated are not cell type specific, rMSCs were observed at day 3 post-seeding (Figure 2-3). The results demonstrated that rMSCs also adhered and grew on the polymeric scaffold surface and exhibited their normal morphology.

Figure 2-2: Immunofluorescence staining (green: β-actin and blue: hoechst stain) images captured using a confocal microscope (at 10X 3.1 zoom) at day 3, 4 and 5. MC3T3-E1 cells adhered, grew and retained their morphology on PLA and PLAGA scaffolds.
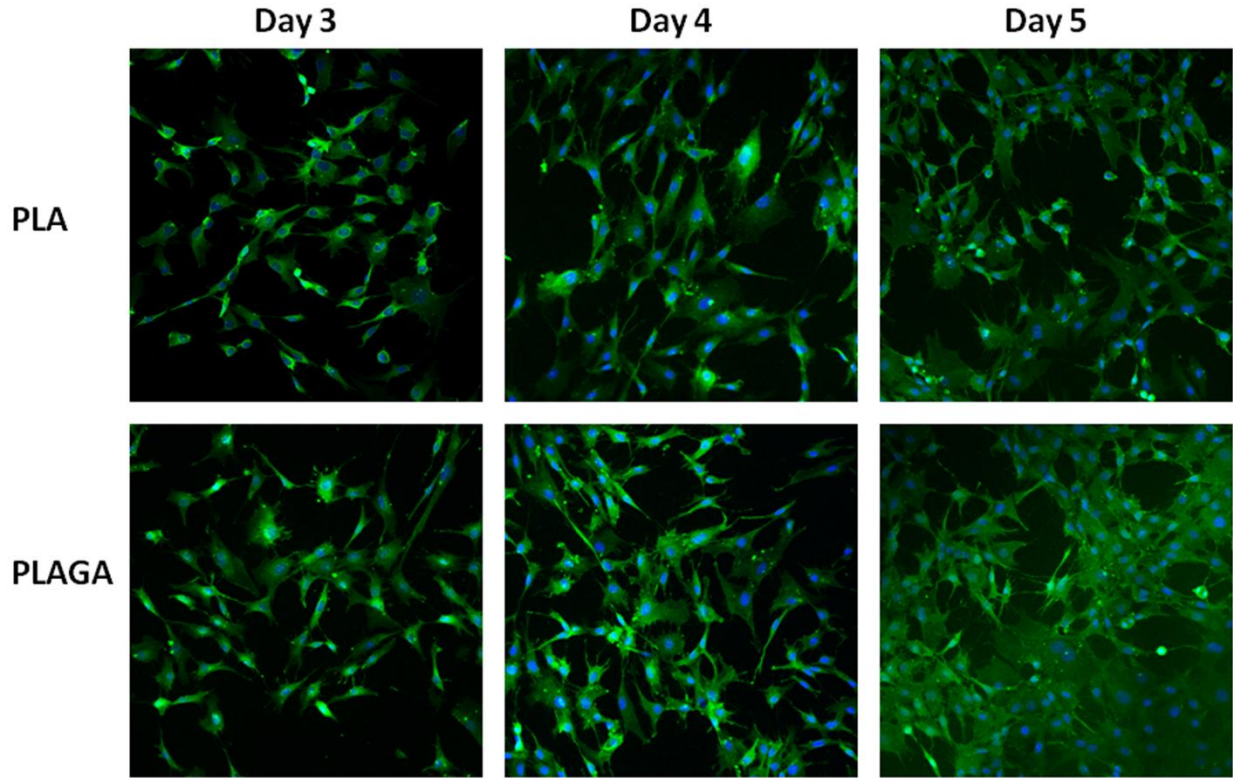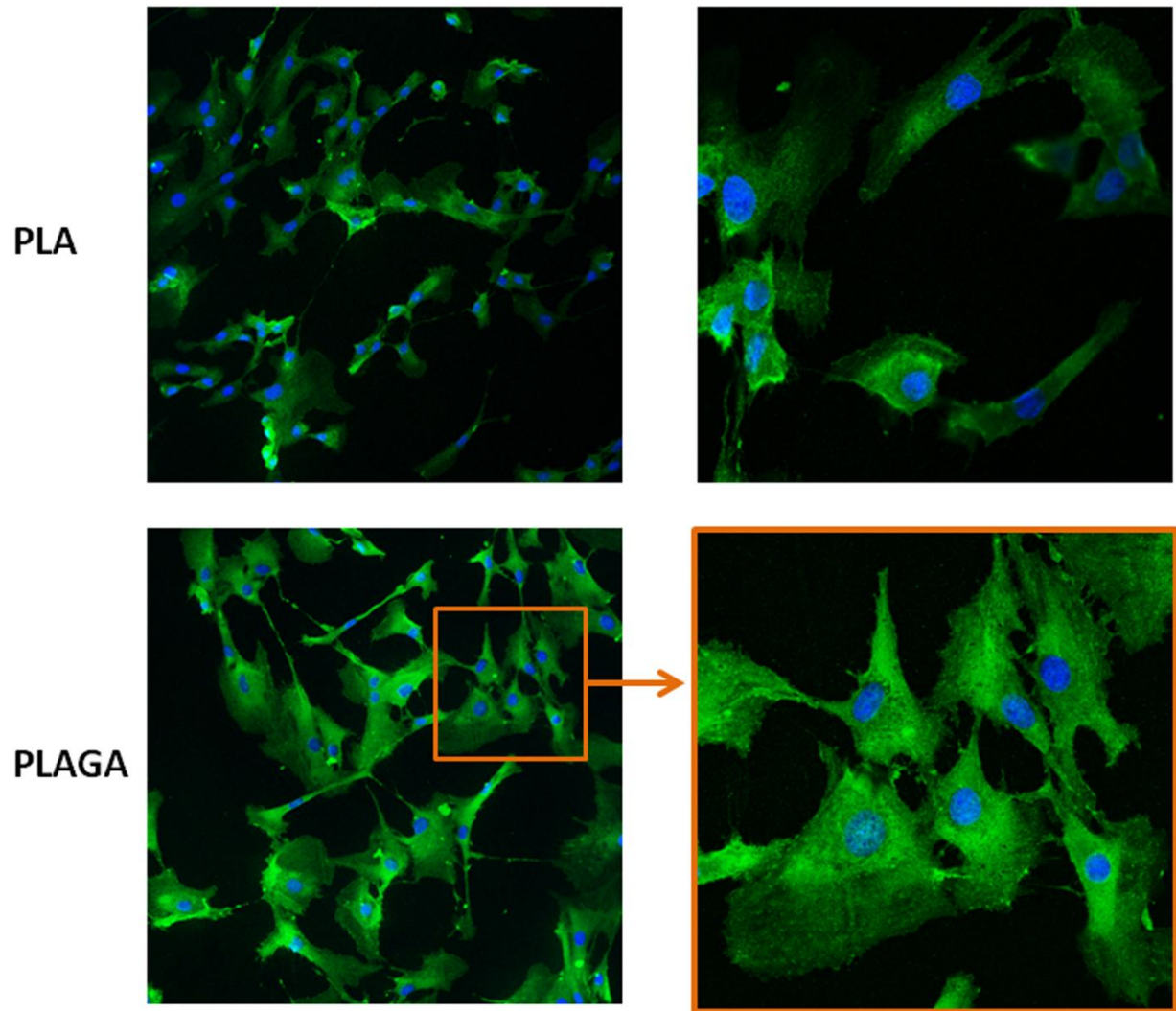
Figure 2-3: **Immunofluorescence staining (green: β-actin and blue: hoechst stain) images captured using a confocal microscope (at 10X 3.1 zoom) at day 3. rMSCs adhered, grew and retained their morphology on PLA and PLAGA scaffolds.**

Scanning Electron Microscopy

MC3T3-E1 cell and rMSCs adhesion on the PLA and PLAGA 2-D scaffolds was determined by

using Scanning Electron Microscopy (SEM) at day 3. Both MC3T3-E1 cells (Figure 2-4) and

rMSCs (Figure 2-5) adhered and grew on both the scaffolds. Cells covered almost the entire

surface of the scaffolds. The cells exhibited their characteristic morphology on both scaffold

surfaces.

PLA
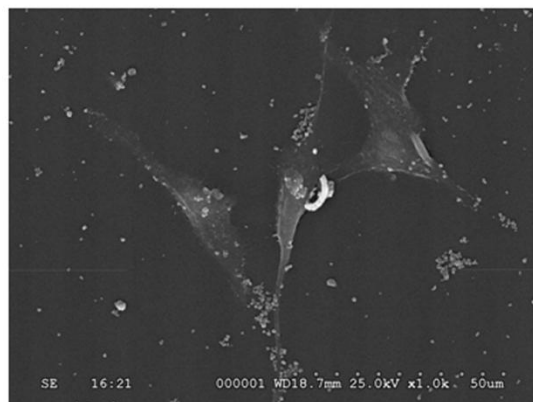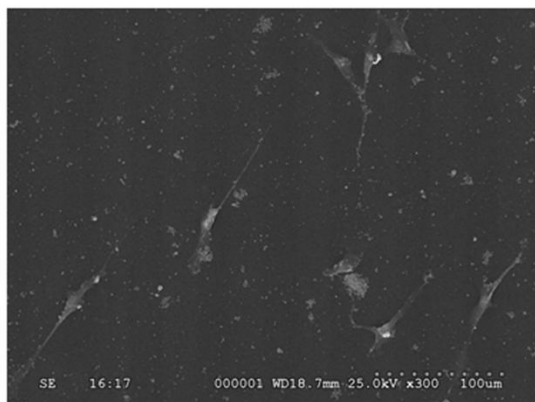
PLAGA
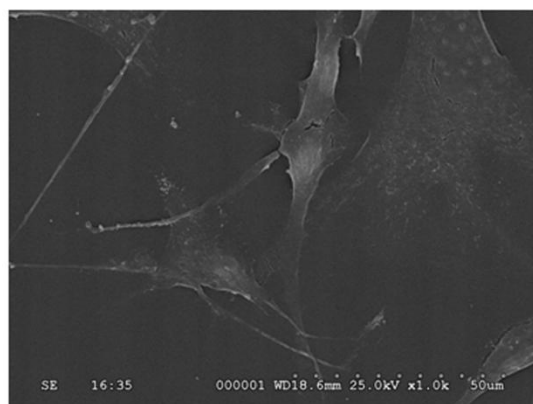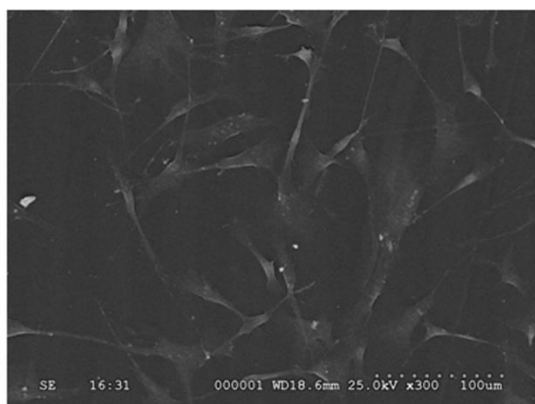
Figure 2-4: **SEM micrographs of MC3T3-E1 cells cultured on PLA and PLAGA scaffolds (at 300 and 1000X magnifications). MC3T3-E1 cells adhered and grew on all the surfaces.**

PLA
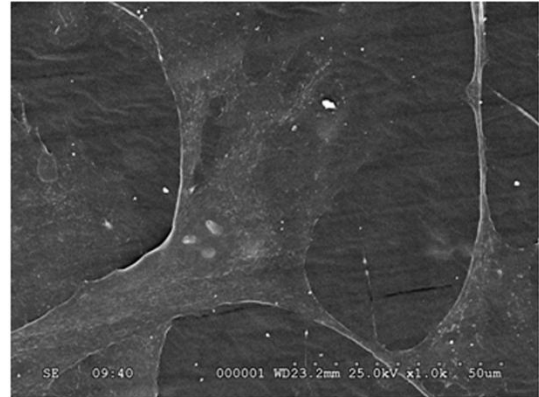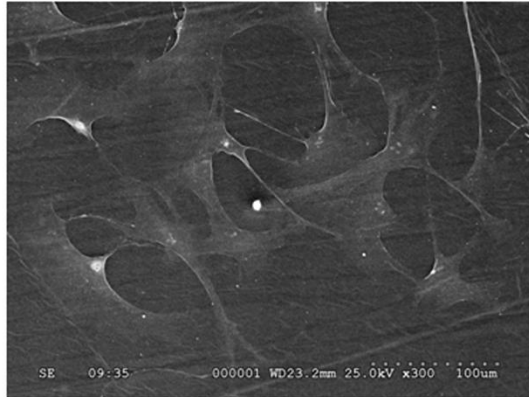
PLAGA
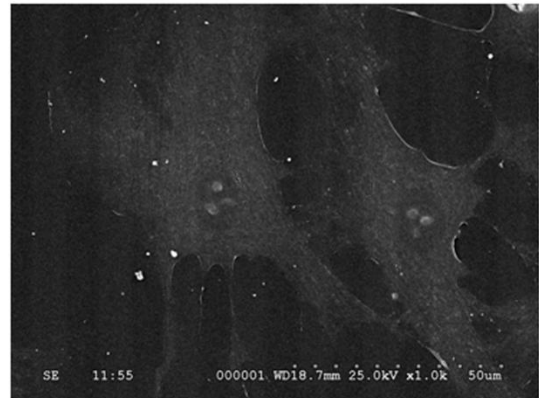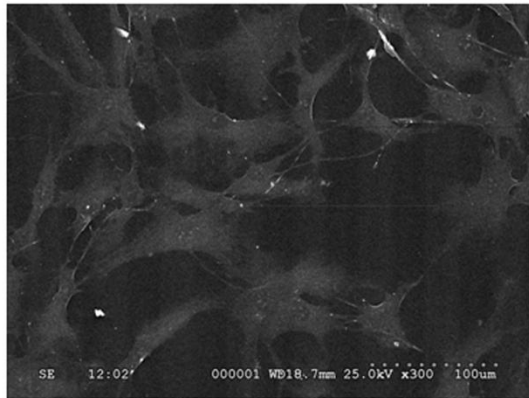
Figure 2-5: **SEM micrographs of rMSCs cultured on PLA and PLAGA scaffolds (at 300 and 1000X magnifications). rMSCs cells adhered and grew on all the surfaces.**

Cell Proliferation

Quantitatively cell proliferation for rMSCs was determined using MTS assay on both the polymeric scaffold surfaces and TCPS (as control) at day 3, 5 and 7. The results demonstrated significantly higher rate of cell proliferation on PLAGA compared to PLA at day 5 and day 7 ($p < 0.05$) and compared to control TCPS (Figure 2-6). The rate of cell proliferation was also higher on PLA compared to control TCPS.

Blank: No cells
Control: Cells cultured on TCPS
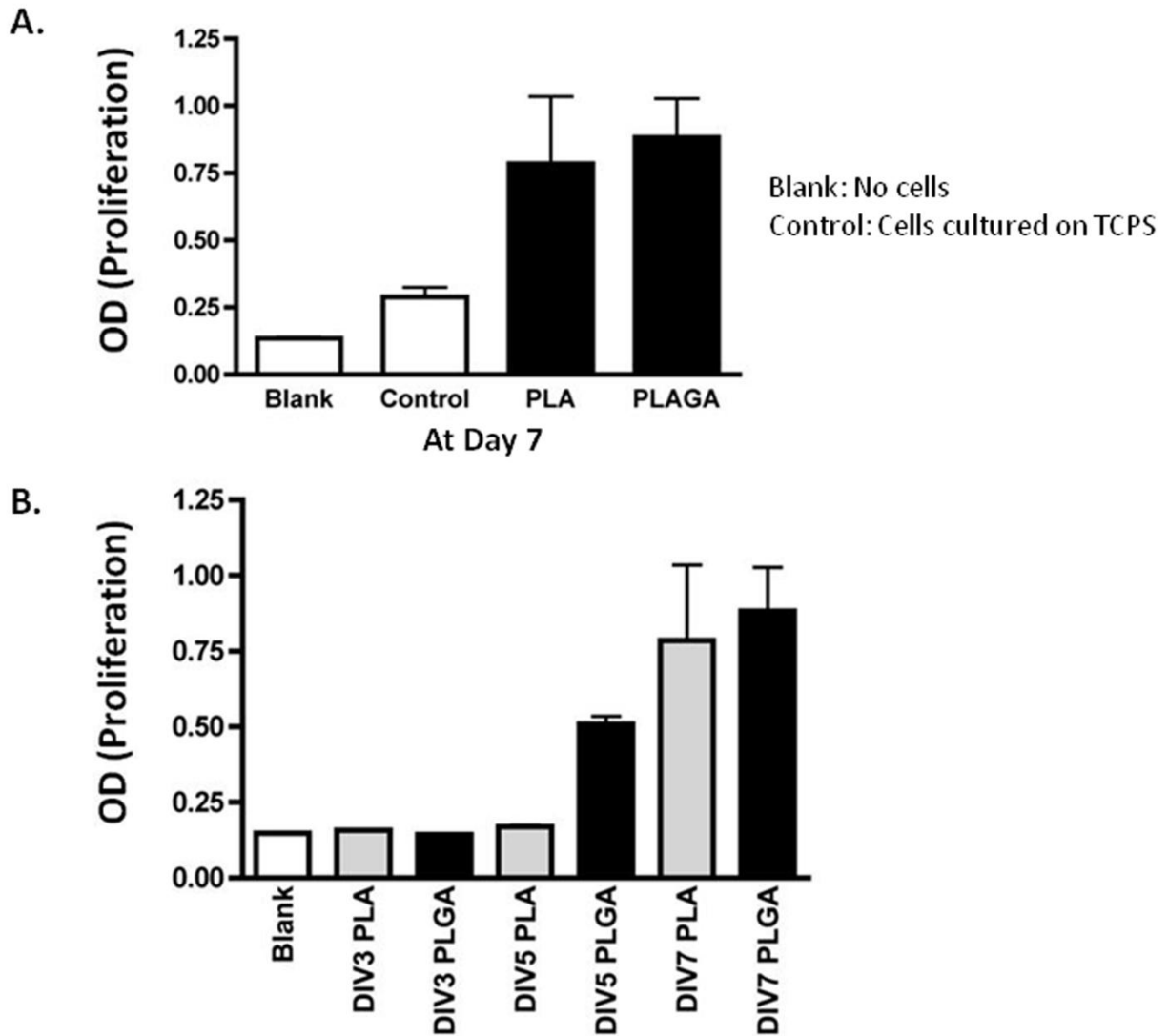
Figure 2-6: **(A & B) MTS assay for proliferation of rMSCs cultured on PLA and PLAGA scaffolds at day 3, 5 and 7. Results show higher proliferation rate on PLAGA compared to PLA and control TCPS. Data represents mean ± SEM and p<0.05 was considered significant.**

39

CHAPTER 2-4

DISCUSSION

We were able to successfully fabricate 2-D PLA and PLAGA scaffolds. Our results suggested that these tissue engineered PLA and PLAGA scaffolds promote cell adhesion and proliferation. Cells (MC3T3-E1 and rMSCs) adhered and grew on these scaffolds, and covered the entire surface of the scaffolds while maintaining their normal morphology. Higher rate of cell proliferation was observed on PLAGA compared to PLA and control TCPS at day 7. These results demonstrate the potential for use of PLAGA scaffolds for bone tissue engineering. Future studies will focus on optimizing these PLAGA scaffolds to enhance cell proliferation and mechanical strength, and to understand the biocompatibility of these scaffolds *in-vivo*.

CHAPTER 3

SINGLE WALLED CARBON NANOTUBES COMPOSITES FOR BONE TISSUE

ENGINEERING

CHAPTER 3-1

INTRODUCTION

Bone defects and non-unions caused by trauma, tumor resection, peri-prosthetic fractures or pathological deformation pose a great challenge in the field of orthopaedics. Traditionally, these bone defects have been treated using autografts and/or allografts, with or without the use of biological agents. Both autografts and allografts have certain pros and cons (C. T. Laurencin et al., 1999; Burg et al., 2000). To circumvent the limitations posed by them BTE has evolved to provide a gold standard synthetic bone substitute for which large boney defects can be adequately addressed. BTE involves the combination of biodegradable composites with or without the use of cells and growth factors to regenerate bone (Petite et al., 2000). The success of this approach relies heavily on the effectiveness of the biodegradable composite (Hutmacher, 2000). PLAGA is used as a composite material because of its excellent biocompatibility, bioresorbability, commercial availability, non-immunogenicity, controlled degradation rate, and ability to promote optimal cell growth (Athanasiou et al., 1996; Lu et al., 1999).

One of the essential requirements of composite material in BTE is to have the desired mechanical properties, which can be increased by reinforcement with a second-phase material. Carbon-based biomaterials have been used in the past as coatings and fillers in implants. Materials such as pyrolytic carbon, diamond-like carbon (DLC), carbon nitride (CN), and carbon fibers all have biomedical applications and have been found to produce blood biocompatibility with good adherence of endothelial cells. Both DLC and CN are considered options for coatings

41

and implants due to their inherent properties such as hardness, low coefficient of friction, chemical inertness, and high wear and corrosion resistance. Carbon nanotubes (CNT) are nanomaterials that have also been looked into for their use in biomedical systems and devices. CNT are an ideal second-phase material due to their unprecedented properties in terms of size, strength and surface area and possess high tensile strength, are ultra light weight and have excellent thermal and chemical stability which make them a potential reinforcement in the production of nanocomposites with ceramics, metals and polymers, including biodegradable polymers (N. Sinha & Yeow, 2005; Armentano et al., 2008). Due to these properties, CNT can be used as nanofillers in polymeric materials for mechanical property enhancement. In addition, researchers have reported that carbon nanotubes act as an excellent substrate for cell growth and differentiation (Shi Kam et al., 2004; Liopo et al., 2006; Hu et al., 2004). Both multi-walled carbon nanotubes-polyurethane composites and poly (carbonate urethanes) have an inert nature and biocompatible chemical surfaces that have shown excellent cellular adhesion and proliferation (Meng et al., 2005). The use of CNT for tissue engineering applications has presented several major drawbacks. CNT are difficult to align when they are used as reinforcement in composite fabrication and the result is a nanocomposite that cannot exhibit adequate mechanical properties. In order to circumvent this major hurdle, a multitude of innovations have been attempted, such as electrospinning a polymer based material in conjunction with the CNT and the incorporation of CNT into matrices of varying shapes (Koh, Rodriguez, & Venkatraman, 2009). Aside from fabrication, very little has been explored in terms of optimization and biocompatibility of these materials for orthopedic applications.

In this study, we used Single Walled Carbon Nanotubes (SWCNT) which are each a one-atom thick layer of graphite, called graphene, rolled into a cylinder. SWCNT are solely made up

of carbon with same scale size of DNA. The fact that all living entities are carbon based makes SWCNT an ideal candidate for introduction into the biological systems (Dai, 2002). The purpose of this study was to develop composites comprised of SWCNT and PLAGA and to evaluate the interaction of hBMSCs via cell adhesion/growth and proliferation, and MC3T3-E1 cells via cell adhesion/growth, survival, gene expression, extracellular matrix production and mineralization. We hypothesize that the novel SWCNT/PLAGA composites can be designed and optimized to support both hBMSCs and MC3T3-E1 cell growth, and represent potential candidates for synthetic BTE.

METHOD

Fabrication and Characterization of PLAGA and SWCNT/PLAGA Composites

SWCNT were obtained (Carbon nanotechnologies incorporated, USA) and stored in the desiccator. PLAGA (Purasorb PLG8523, Purac Biomaterials, Netherlands) was obtained and stored at -80^0C. PLAGA composites were fabricated by dissolving 1g of PLAGA in 12ml solution of dichloromethane (Fisher Scientific, USA) in a 20ml scintillation vial. The solution was vortexed for 8 hours at a constant speed to dissolve the polymer. It was then poured in a glass Petri-plate with Bytac paper and kept under a vacuum hood for 30 minutes. For SWCNT/PLAGA composites, once the PLAGA was dissolved various amounts of SWCNT (5mg, 10mg, 20mg, 40mg and 100 mg) were used in order to produce the desired composites. These amounts of SWCNT were added to the above polymer solution and the vials were vortexed for another 8 hours. This uniform mixture of PLAGA and SWCNT was then poured and kept under a vacuum hood for 30 minutes. For both composites, the plate were then kept at -20^0C overnight and then brought to room temperature for complete evaporation of the solvent. The thin films obtained were bored into circular disks with a 12mm diameter and placed in a desiccator for 24 hours to remove the residual solvent. For characterization, both the composites were mounted on a carbon coated SEM stub, sputter coated with Gold/Palladium and viewed under a SEM.

Degradation Studies

Degradation studies were performed on PLAGA and SWCNT/PLAGA composites over 21 days. The studies were performed in 0.1M Phosphate Buffered Saline (PBS) (pH= 7.4). Disks with diameters of 12mm were obtained, weighed and then placed in 15ml conical centrifuge tubes

44

containing 3ml PBS at 37^0C with constant stirring. The PBS was changed every 8 hours for first 24 hours, then once a day for the first week. For the remainder of the study, the PBS was changed once every 7 days. At days 1, 3, 5, 7, 14 and 21, disks were removed from the tubes, stored in a desiccator overnight and weighed to determine percentage mass loss over time.

Cell Culture

MC3T3-E1 cells were obtained from ATCC (MC3T3-E1 subclone 4, pre-osteoblasts). The cells were grown in Alpha Minimal Essential Medium (Alpha MEM) with ribonucleosides, deoxyribonucleosides, 2mM L-Glutamine, and 1mM sodium pyruvate (Hyclone, Thermo Scientific, USA) supplemented with 10% Fetal Bovine Serum (FBS) (Gibco, Invitrogen, USA) and 1% Penicillin-Streptomycin (PS) (Lonza, USA). Characterized hBMSCs were obtained from Prockop's lab (at the Center for Gene Therapy, Tulane University Health Sciences Center, New Orleans, USA) (Sekiya et al., 2002) and were cultured in same medium with 20% FBS. Both cells were kept in humidified air under 5% CO_2 at 37^0C (Sekiya et al., 2002). The PLAGA and SWCNT/PLAGA composites were fabricated as described above and exposed to UV light for 15 minutes to insure sterilization. Tissue-culture polystyrene (TCPS) served as a control. After sterilization the composite disks were placed in a 48 well plate and soaked in the complete culture medium for 1 hour. The desired number of cells were counted using hemacytometer and were then seeded on the disks for cell adhesion/morphology/proliferation, cell growth/ survival, and gene expression studies.

Scanning Electron Microscopy (SEM)

Cell adhesion on the polymeric composites surface was determined qualitatively by using SEM (Hitachi S-3000 scanning electron microscope). At day 3, the TCPS (control) and the composites seeded with 20,000 cells/ composite (MC3T3-E1 and hBMSCs) were washed with PBS. The

45

cells were then fixed with 1.5% Glutaraldehyde in 0.1M Cacodylate buffer followed by post-fixation with 2.5% OsO_4 in 0.1M Cacodylate buffer. After fixation the cells were washed with 0.1M Cacodylate buffer and then dried using serial ethanol dehydration, followed by Hexamethyldisilazane (HMDS). The dried samples were then sputter coated with Gold/ palladium and viewed using the SEM.

Immunofluorescence Staining

The morphology of the cells can be used to determine the cellular behavior on the polymeric composites. Cellular morphology and adhesion (qualitatively) were determined by using immunofluorescence staining as MC3T3-E1 cells are flat and polygonal in shape and hBMSCs are spindle shaped (Sekiya et al., 2002; Horikawa et al., 2000). At day 3, the TCPS (control) and the composites seeded with 20,000 cells/ composite were washed with PBS. The cells were then fixed with chilled 70% ethanol for 10 minutes. Post fixation, the cells were incubated with 1% Bovine Serum Albumin (BSA) in PBS having 0.05% Triton X-100 for 20 minutes at room temperature followed by immersing the samples in 1% Tween. The cells were then incubated overnight at 4^0C with monoclonal mouse Anti-β-actin antibody (1:400, Sigma Aldrich, USA). They were then washed with 0.05% Tween and incubated with secondary antibody (goat anti-mouse F (ab') 2 fragment of IgG conjugated with an Alexa Fluor® 488 fluorescence probe, 1:400, Cell Signaling, USA) for 1 hour at room temperature. This was followed by washing the cells with PBS, and staining for the nucleus (Hoechst dye), mounting using 80% Glycerol and viewing under a Confocal Microscope (Leica TCS SP5 spectral laser scanning confocal microscope) (Vandrovcová et al., 2011).

46

Cell Proliferation Assay

Cell adhesion and proliferation was determined quantitatively using MTS assay kit at day 3, 5 and 7 post-seeding (5,000 hBMSCs cells) on 20% BGS (Bovine Growth Serum)(negative control), PLAGA and SWCNT/PLAGA composites. At desired time points, media was removed, cells were washed with PBS and 20µl of Cell titer 96$^®$ AQueous One solution reagent (Promega, USA) was added in each well having 100µl of culture medium followed by incubating the plate at 37^{0}C for 1-4 hours in a humidified; 5% CO_2 atmosphere. The absorbance/ optical density (O.D.) was measured at 490nm by using a microplate reader.

Live/Dead Assay

LIVE/DEAD® Viability/Cytotoxicity kit (Invitrogen, Carlsbad, CA, USA) was used to determine the cell growth and survival in the PLAGA and SWCNT composites. 20,000 MC3T3-E1 cells/ composite were seeded. At day 3, 5 and 7, the cells were taken out of the culture, washed with PBS and stained for live-dead cells according to the manufacturer's instructions. The stained cells were visualized using a Confocal Microscope in which live cells were stained green and dead cells were stained red.

Real Time Reverse Transcriptase Polymerase Chain Reaction

20,000 MC3T3-E1 cells/ composite were seeded on TCPS, PLAGA and SWCNT/PLAGA composites and at day 7 after culturing the cells in the osteogenic medium (per osteogenesis kit, Millipore, USA), the cells were harvested and the RNA was isolated using Qiagen RNeasy mini kit. 200ng of isolated RNA was reverse transcribed into cDNA using Thermo Scientific maxima first strand cDNA synthesis kit. Real Time Reverse Transcriptase Polymerase Chain Reaction (RT-PCR) was carried out using the Taqman® (Invitrogen) gene expression assays to determine the expression of Alkaline Phosphatase (ALP), Osteocalcin (OC), Osteopontin (OPN), Bone

47

Sialoprotein (BSP), Runx-2, Type I collagen (TIC) and GAPDH (as control). The mouse primers were purchased from Applied Biosystems (Igwe, Mikael, & Nukavarapu, 2012) and RT-PCR was performed using an Eppendorf Realplex cycler.

Statistical Analysis

MTS assay was performed three times in duplicate and degradation study was performed two times in duplicate and mean ± SEM (Standard error of mean) values along with statistical analysis using two-way ANOVA were performed to assess the possible interaction between time and SWCNT concentration. Independent groups t -tests were performed at each time point to test pre-planned comparisons between the concentrations of SWCNT composites to control PLAGA scaffold. The results were considered significant when $p < 0.05$.

CHAPTER 3-3

RESULTS

Fabrication of PLAGA and SWCNT/PLAGA Composites

PLAGA and SWCNT/PLAGA two-dimensional composites were fabricated using solvent
evaporation method. Figures 2-1 and 3-1 shows the fabrication process of PLAGA and
SWCNT/PLAGA composites respectively and the films obtained (Figure 3-2). 12mm diameter
disks (Figure 3-3) were cut from the films obtained and used for cell adhesion/morphology,
growth, survival, and proliferation and gene expression studies.
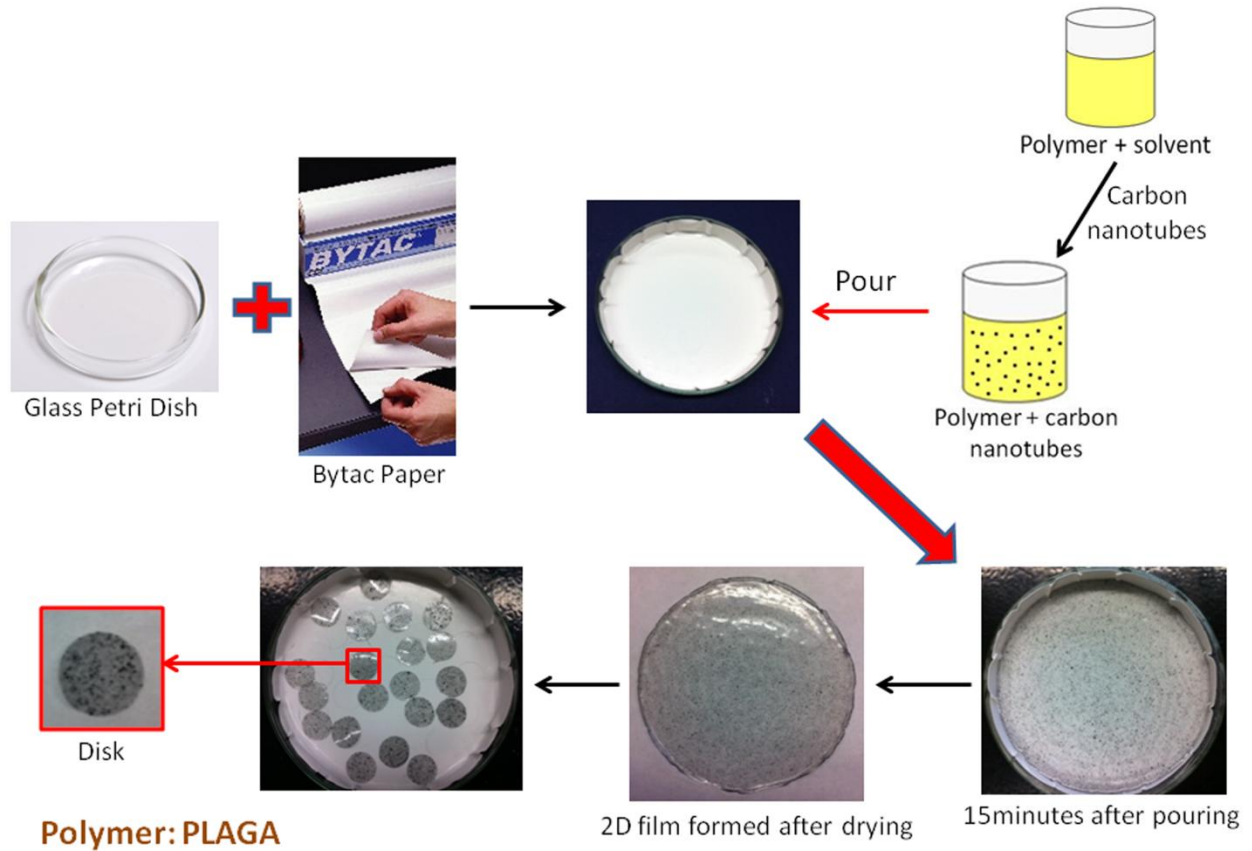
Figure 3-1: **Schematic representation of steps involved in fabrication of 2-D**

SWCNT/PLAGA scaffolds using solvent evaporation method.
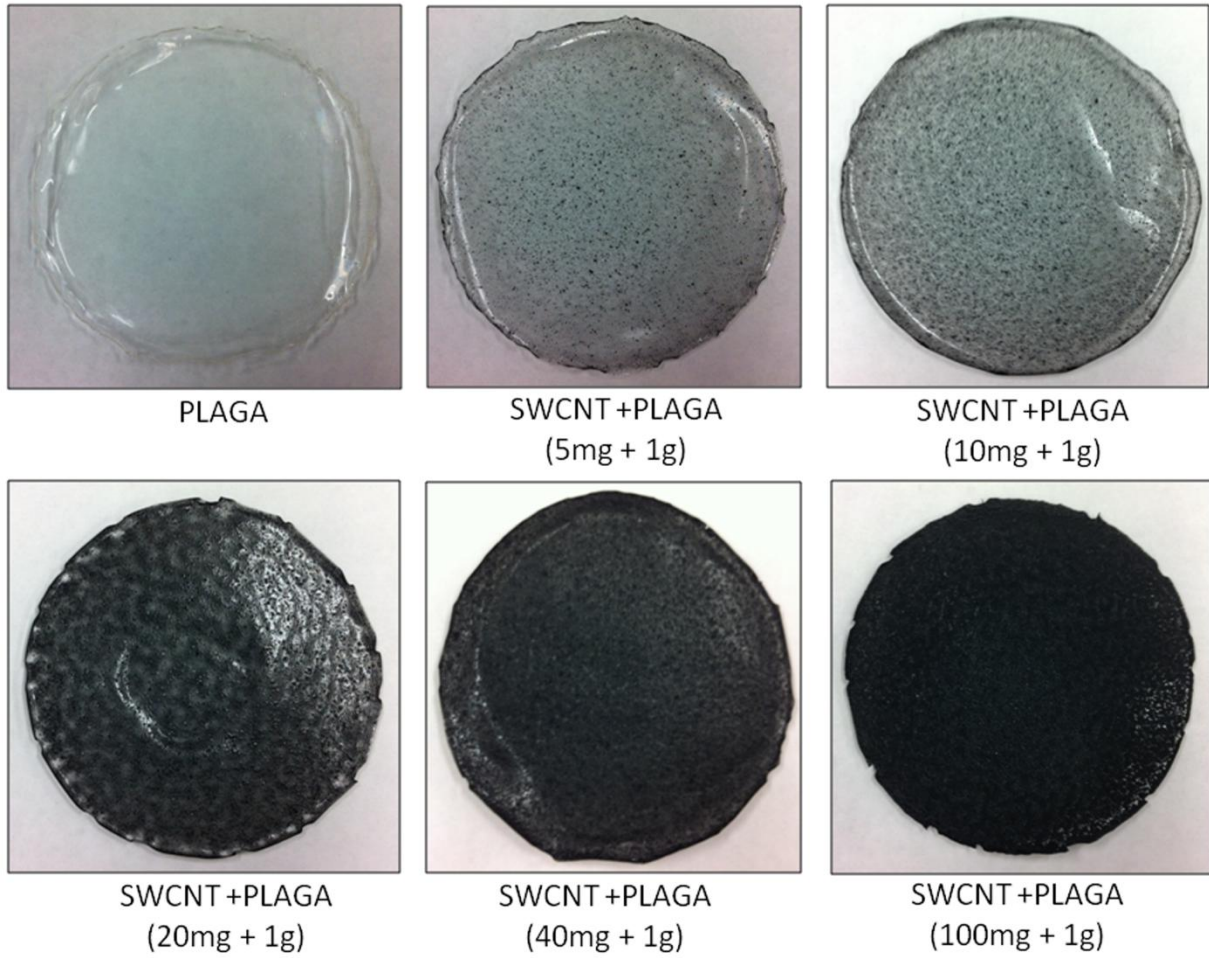
Figure 3-2: **Images of 2D PLAGA and SWCNT/PLAGA composites (100mm diameter) obtained.**

| PLAGA | SWCNT +PLAGA (5mg + 1g) | SWCNT +PLAGA (10mg + 1g) | SWCNT +PLAGA (20mg + 1g) | SWCNT +PLAGA (40mg + 1g) | SWCNT +PLAGA (100mg + 1g) |
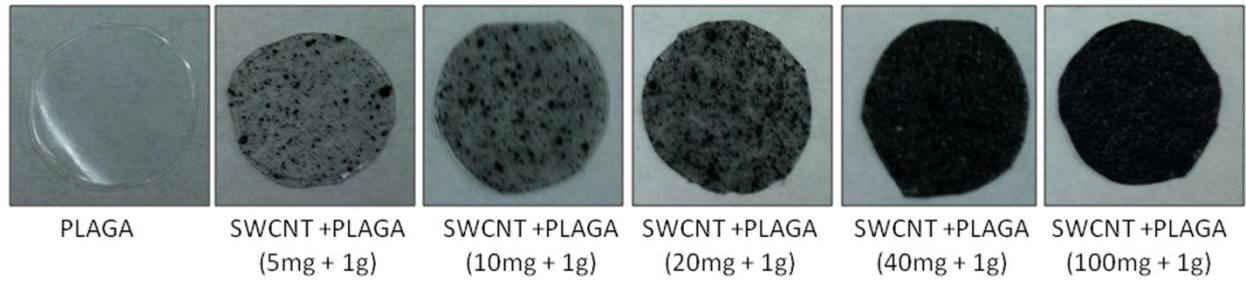
Figure 3-3: **Disks (12mm diameter) cut from the PLAGA and SWCNT/PLAGA composites.**

Characterization of PLAGA and SWCNT/PLAGA Composites

The SEM micrographs obtained for the SWCNT/PLAGA composites (Figure 3-4) demonstrated that the SWCNTs were embedded in the polymer matrix and appeared to be uniformly distributed throughout the composite. In some areas, the SWCNTs were emerging from the surface of matrix and the surface roughness of the composites increased with increasing SWCNT concentration, although SWCNT were still surrounded by PLAGA.
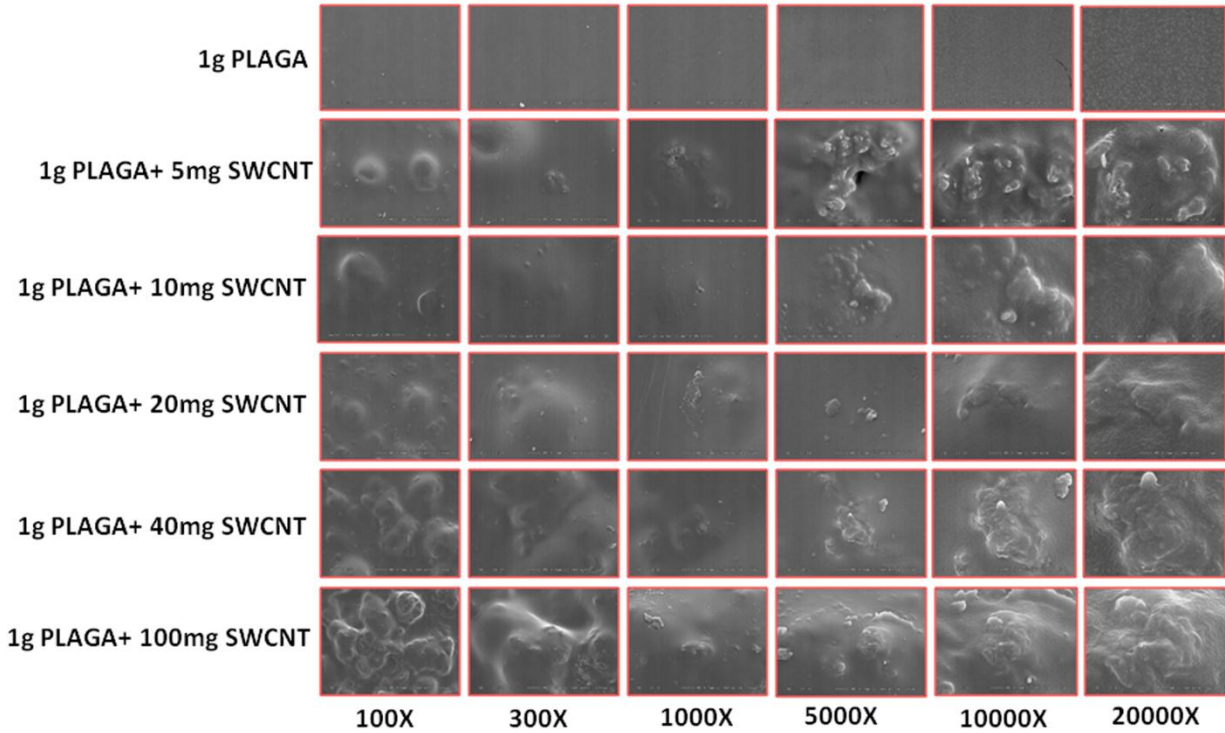
Figure 3-4: **SEM micrographs of PLAGA and SWCNT/PLAGA composites (at 100, 300, 1000, 5000, 10000 and 20000X magnifications). SWCNT can be seen homogenously distributed in PLAGA matrix.**

Degradation Studies

The degradation rate of PLAGA and SWCNT/PLAGA composites was investigated over a period of 21 days. Figure 3-5 demonstrates the percentage of mass lost over time. The results demonstrated that incorporation of SWCNT (in various concentrations) in PLAGA matrix did not have any significant effect ($p > 0.05$) on the degradation rate of the matrices when compared to the degradation rate of PLAGA alone.
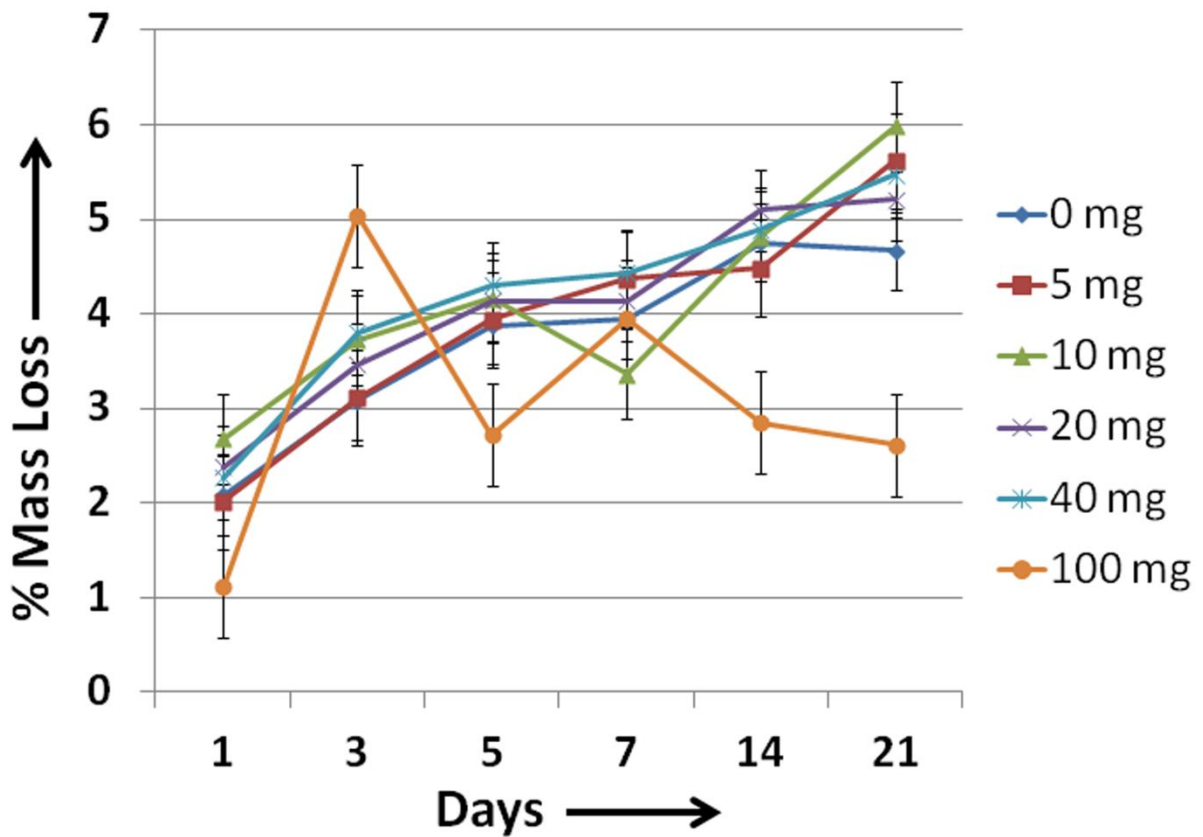
Figure 3-5: **Degradation profile of PLAGA and SWCNT/PLAGA composites as a function of % mass loss over time (days). Results show no significant difference in the degradation rate of SWCNT/PLAGA composites compared to PLAGA. Data represents mean ± SEM.**

<h1 style="text-align: center;">Scanning Electron Microscopy</h1>

Both hBMSCs (Figure 3-6) and MC3T3-E1 cells (Figure 3-7) adhered and grew on the PLAGA

as well as SWCNT/PLAGA composites. Cells were nearly confluent over the entire surface of

the composites. The cells exhibited their characteristic morphology on TCPS and were consistent

with all the polymeric composite surfaces.
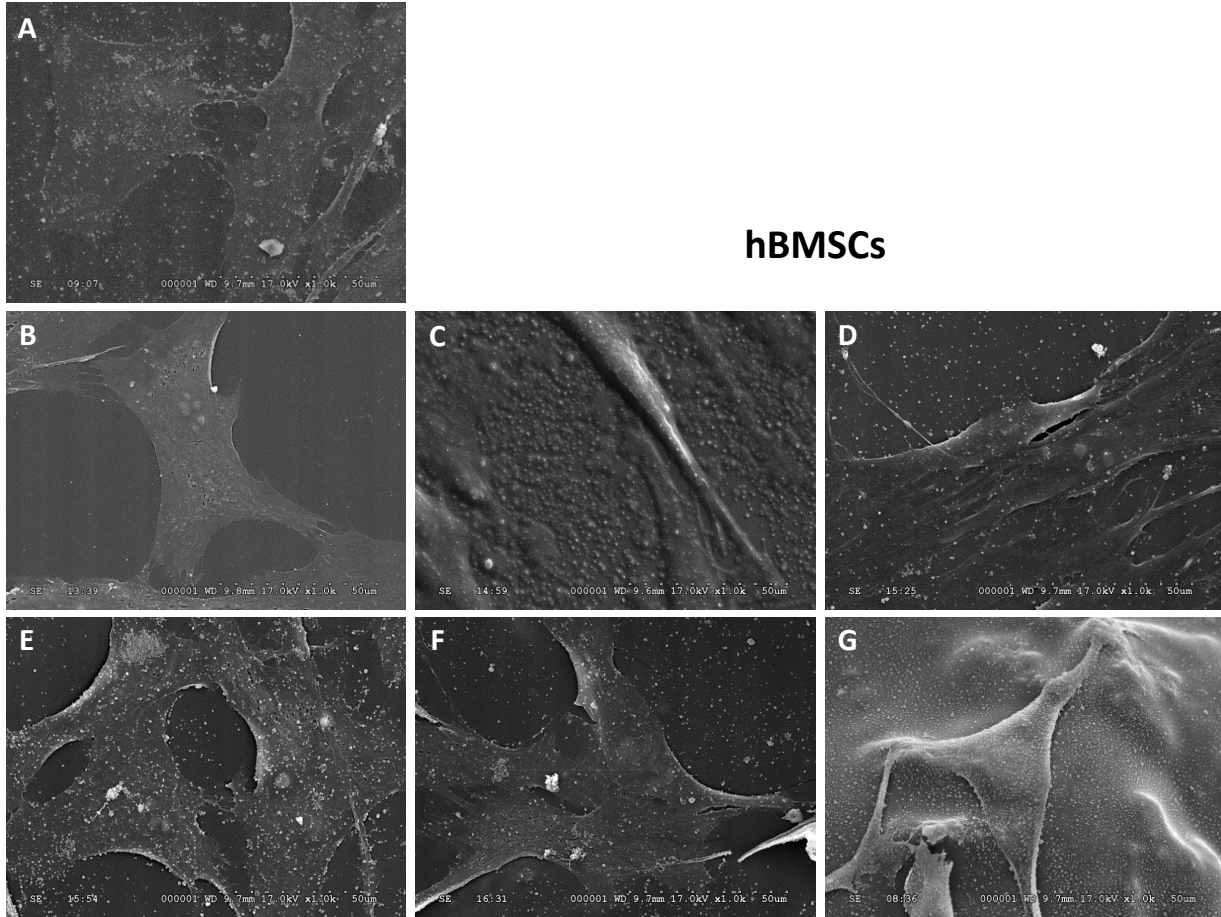
hBMSCs

Figure 3-6: **SEM images (at 1,000 X) of hBMSCs cultured on TCPS (A), PLAGA (B), and SWCNT/PLAGA composites (C–G). hBMSCs adhered and grew on all the surfaces.**
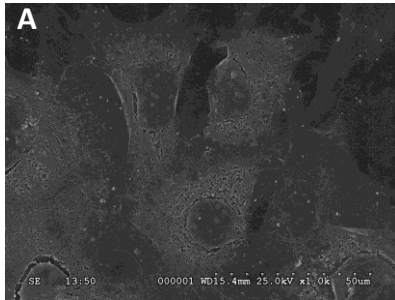
MC3T3-E1 Cells
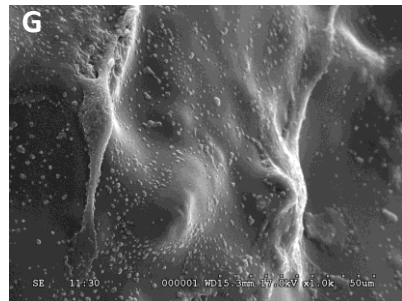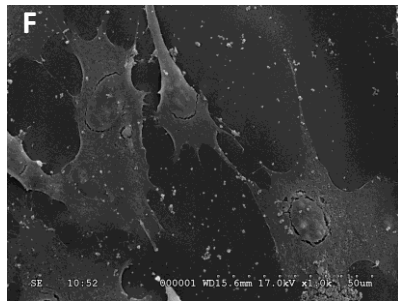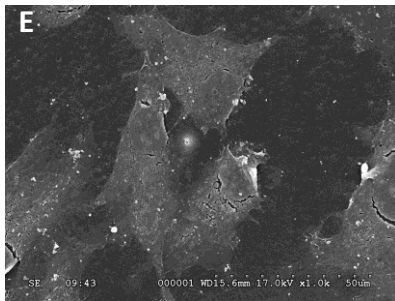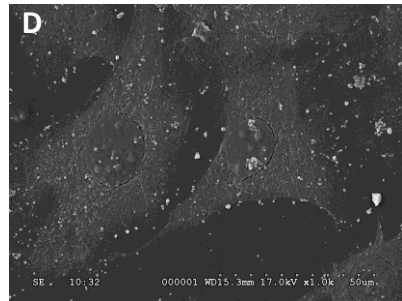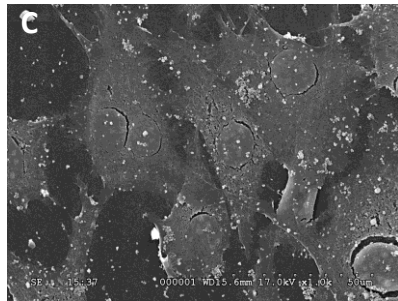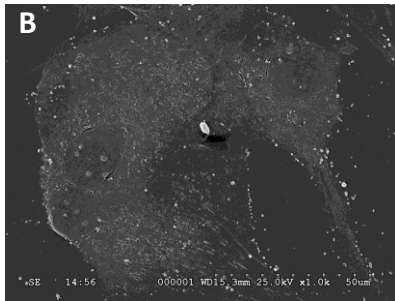
Figure 3-7: **SEM images (at 1,000 X) of MC3T3-E1 cells cultured on TCPS (A), PLAGA (B), and SWCNT/PLAGA composites (C–G). MC3T3-E1 cells adhered and grew on all the surfaces.**

Immunofluorescence Staining

The actin staining revealed that the hBMSCs (Figure 3-8) and MC3T3-E1 cells (Figure 3-9) adhered to all surfaces; grew and exhibited a normal, non-stressed morphological pattern (flat and polygonal morphology for MC3T3-E1 cells and spindle or elongated morphology for hBMSCs) observed by cells on both the experimental and control surfaces.
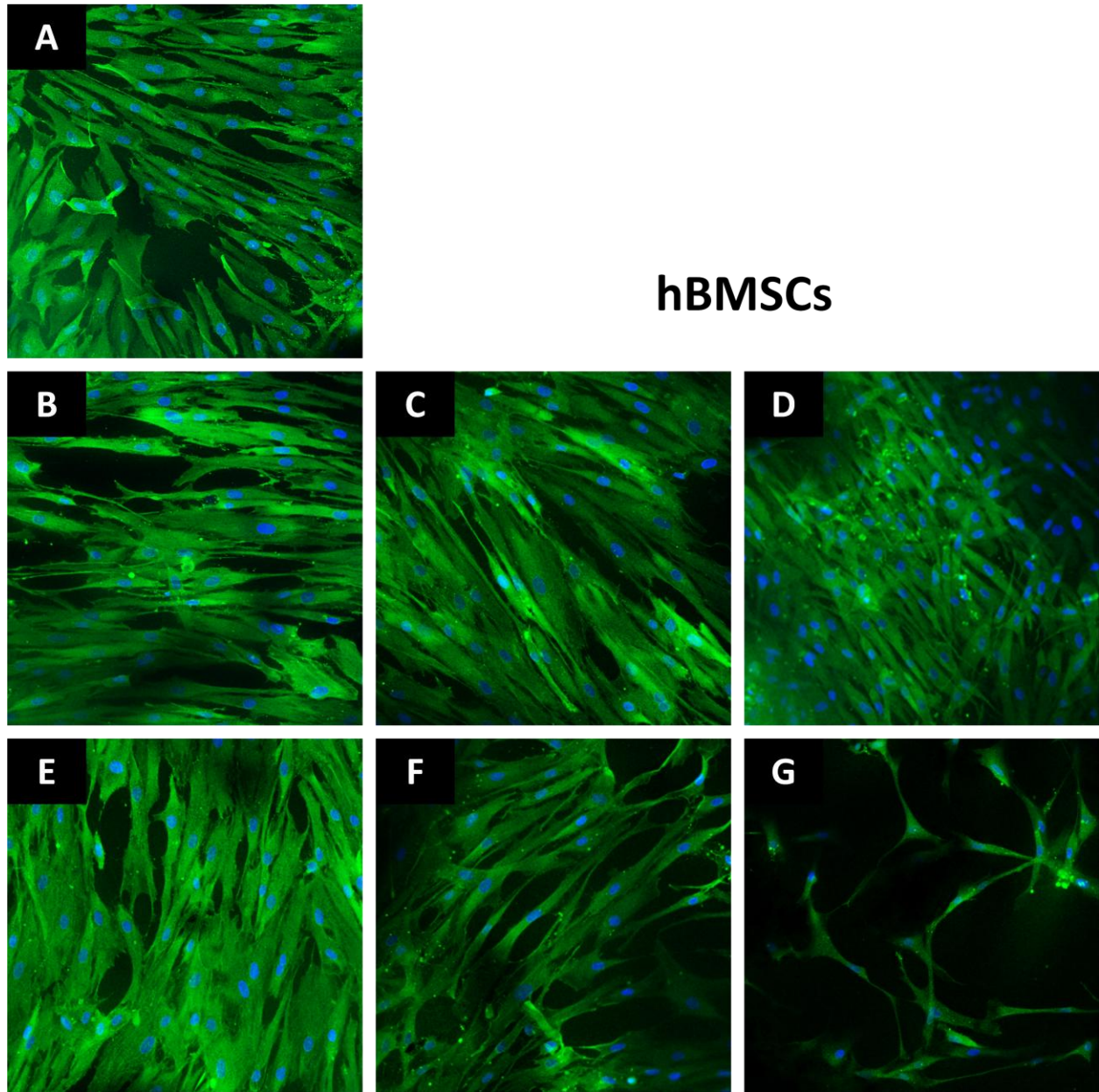
Figure 3-8: **Immunofluorescence staining (green: β-actin, blue: hoechst stain) images captured using a confocal microscope (at 10 X 3.1 zoom). hBMSCs adhered, grew and retained morphology on TCPS (A), PLAGA (B), and SWCNT/PLAGA composites (C–G).**
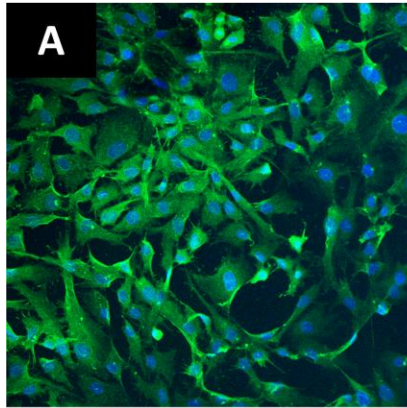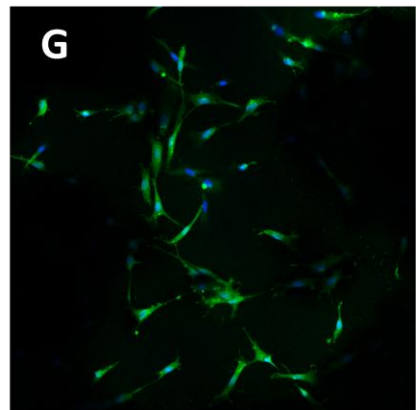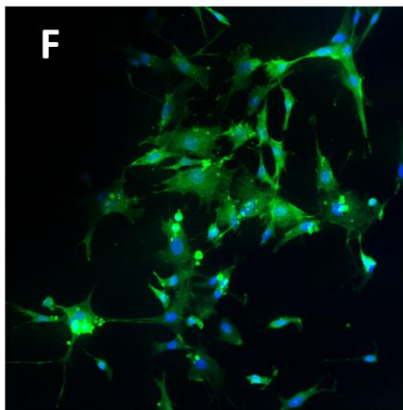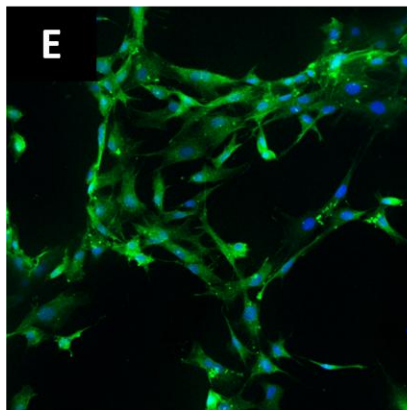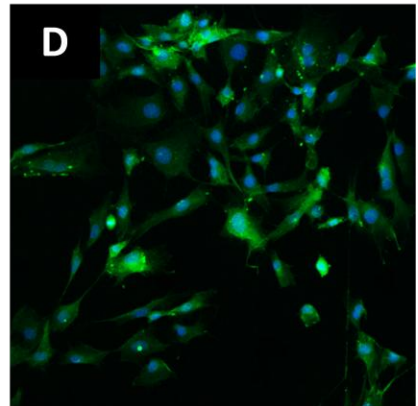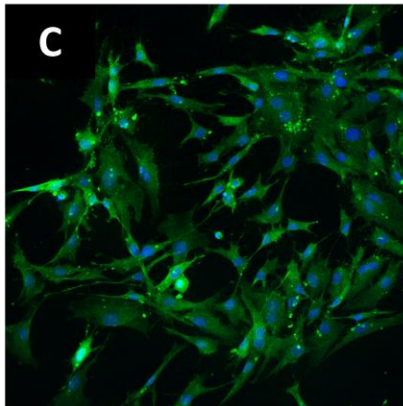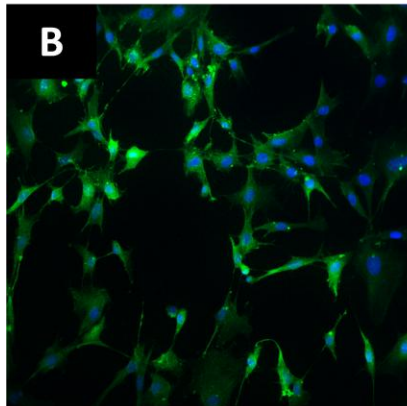
MC3T3-E1 Cells

Figure 3-9: **Immunofluorescence staining (green: β-actin, blue: hoechst stain) images captured using a confocal microscope (at 10 X 3.1 zoom). MC3T3-E1 cells adhered, grew and retained morphology on TCPS (A), PLAGA (B), and SWCNT/PLAGA composites (C–G).**

Live/Dead Assay

Live MC3T3-E1 cells were stained green and adhered and attained their normal polygonal morphology on all concentrations of the SWCNT/PLAGA composites. Dead cells were stained red and were very few in number (Figure 3-10). By day 7, the cell density increased on all the composite surfaces. No dead cells were observed by day 7.
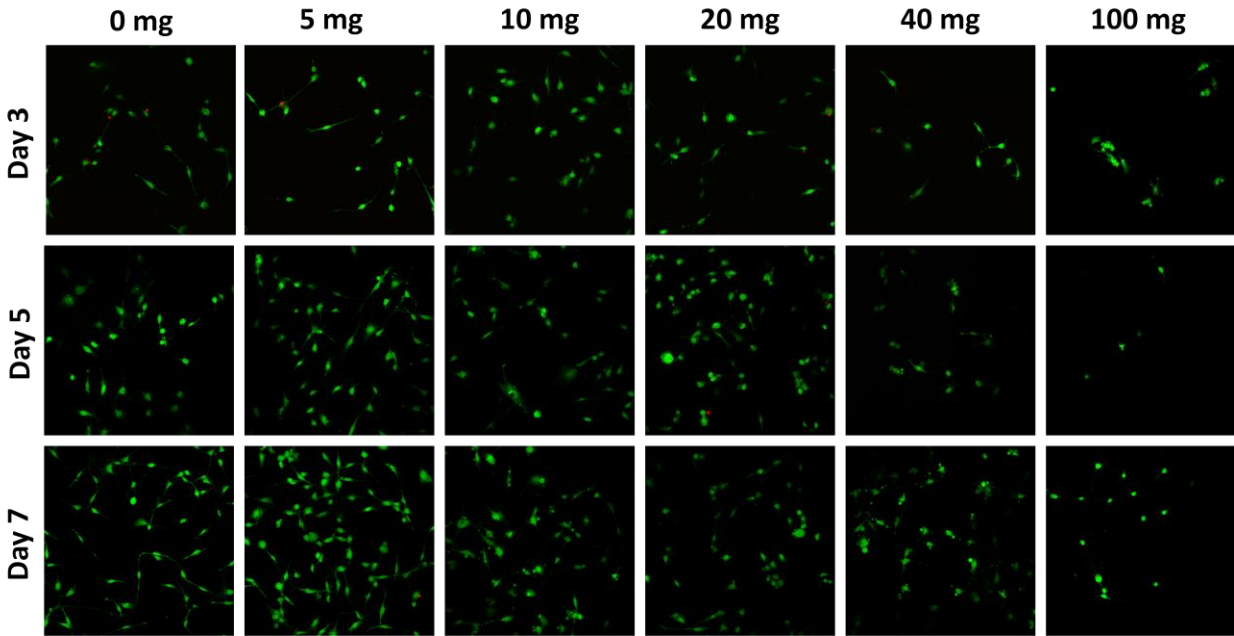
Figure 3-10: **Growth and survival of MC3T3-E1 cells on PLAGA and SWCNT/PLAGA composites (at 10 X 3.1 zoom). Images show live (green) and dead (red) cells cultured on the composites at day 3, 5, and 7.**

Cell Proliferation

At day 3, SWCNT/PLAGA composites with 5, 10 and 40mg of SWCNT showed higher rate of hBMSCs proliferation compared to other SWCNT/PLAGA composites, PLAGA alone and negative control BGS. At day 5, SWCNT/PLAGA composites with 10 and 40mg of SWCNT showed higher cell proliferation compared to other composites. At day 7, SWCNT/PLAGA composite with 10mg of SWCNT showed the highest rate of cell proliferation, which was statistically significant ($p < 0.05$), followed by SWCNT/PLAGA composites with 40, 20 and 100mg of SWCNT. SWCNT/PLAGA composites with 5mg of SWCNT showed similar proliferation rates as that of PLAGA alone, and higher proliferation compared to BGS (Figure 3-11).
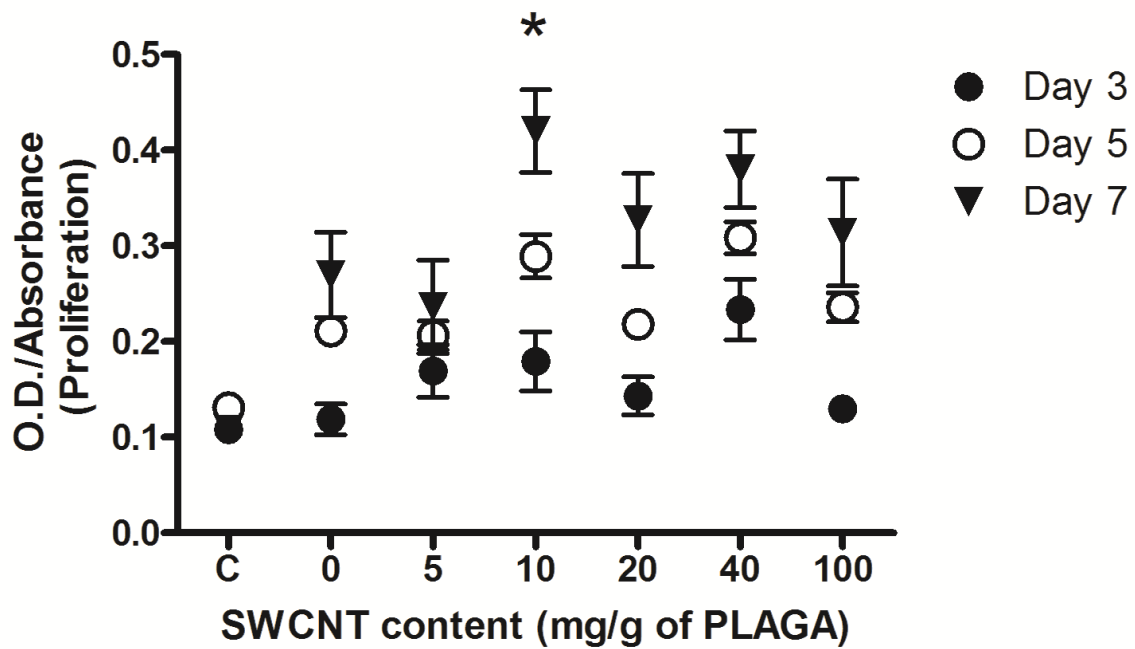
Figure 3-11: **MTS assay for proliferation of hBMSCs cultured on PLAGA and SWCNT/PLAGA composites at day 3, 5 and 7. Data represents mean ± SEM and $p < 0.05$ was significant (compared to hBMSCs cultured on PLAGA). * is significant over all groups.**

Gene Expression Analysis

The results demonstrated the expression of osteoblast phenotypic markers (Col I, OPN), mineralization markers (ALP1, OC, BSP) and osteoblast differentiation marker (Runx-2) on all the composites and the expression on all the SWCNT/PLAGA composites is similar to that of PLAGA and control TCPS by end of day 7 (Figure 3-12).

67
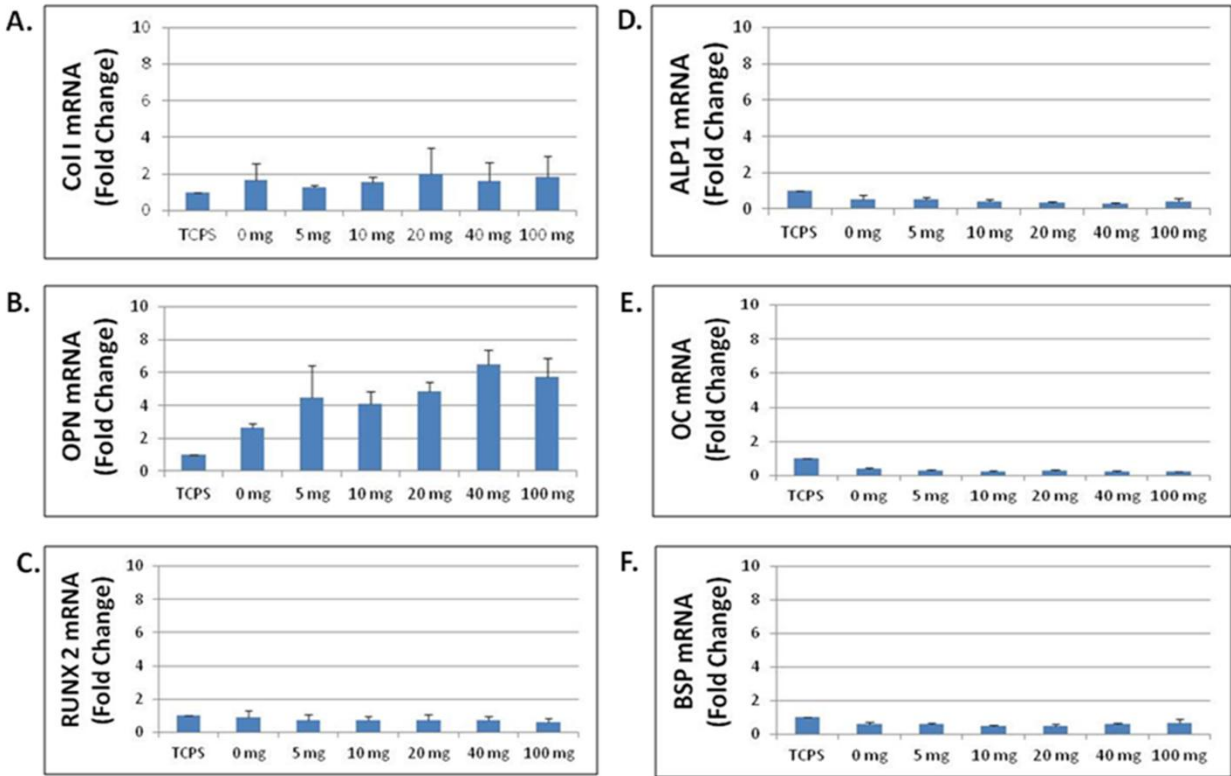
Figure 3-12: **Gene expression profile of MC3T3-E1 cells grown on PLAGA and SWCNT/PLAGA composites. Panels showing mRNA levels detected by qPCR for Col I (A), OPN (B), RUNX-2 (C), ALP 1 (D), OC (E) and BSP (F).**

CHAPTER 3-4

DISCUSSION

An ideal composite for BTE applications must be biodegradable, biocompatible, and promote cell growth and proliferation (Janicki & Schmidmaier, 2011). This study demonstrated that SWCNT/PLAGA composites imparted beneficial cellular (both MC3T3-E1 and hBMSCs) growth capabilities and gene expression, and mineralization abilities were well established. The most important finding of this study was that the addition of SWCNT to form SWCNT/PLAGA composites promoted cell proliferation as well as supported normal growth and gene expression of the cells.

In the development of ideal composites for bone defect, several key issues should be addressed, including the degradation rate of the composite. Optimally, the composite should degrade at a comparable rate to cell proliferation. The composite should also function as a temporary support, encouraging the proliferation process while providing the appropriate biomechanical stability (Jackson & Simon, 1999). One of the factors that attracted BTE to PLAGA in the past is the polymer's degradation rate, which is more ideal than other polymers for biological applications (Lu et al., 1999). This study showed that the SWCNT have the ability to be completely incorporated into a PLAGA matrix, while having no significant affect on the degradation rate of the composites when compared to those of PLAGA alone. This is in accordance with the study done by Armentano et al. which also showed that PLAGA and SWCNT/PLAGA composites have similar degradation rates (Armentano et al., 2008). Also, the uniform distribution and incorporation of SWCNT at all concentrations, indicates that these two materials are compatible and capable of existing together in a solid composite structure. It can also be deduced that the SWCNT did not impart any significant change to the chemical

69

composition of the PLAGA polymer, and thus the SWCNT/PLAGA composite may represent an ideal composite for bone regeneration.

Along with the need for a physiologically appropriate degradation rate, the composite must also allow for cellular attachment and proliferation. On all composites in this study, SEM and immunofluorescence demonstrated that both hBMSCs and MC3T3-E1 cells adhered to the surface and exhibited normal, healthy cell morphology. The cellular growth of hBMSCs and MC3T3-E1 cells was equally well-spread on the SWCNT/PLAGA composites as they appeared to be on the PLAGA composite alone. The successful growth of cells of differing types demonstrates that the surface of the SWCNT/PLAGA composites is potentially non-cell type specific based on the analysis of two cell types used. This study demonstrated the ability to preserve the inherent properties of PLAGA as well as increase its cellular proliferative capabilities by including SWCNT. Experimentation with various concentrations of the SWCNT, uncovered the fact that a concentration of 10mg actually increased the cellular proliferation of hBMSCs. This promotion of cellular proliferation provides further evidence to support the use of a SWCNT/PLAGA composite for tissue engineering purposes. Similar to cellular growth on PLAGA, gene expression of osteoblast phenotypic markers, mineralization markers, and osteoblast differentiation markers were seen on composites of all SWCNT concentrations using real time PCR. The expression of the genes and presence of these markers indicate that the MC3T3-E1 cells were able to thrive under the conditions provided by the SWCNT composites. This further supports the assertion that the presence of SWCNT in the composites does not alter the properties of the PLAGA and, in fact, imparts beneficial components to this material.

This study was the first step in evaluating the effectiveness of SWCNT/PLAGA composites as potential synthetic substitute for bone regeneration. Future studies are planned to

70

investigate the biomechanical compatibility of the SWCNT/PLAGA composite along with their cellular proliferation capabilities. The creation of 3-D composites for in vivo use will allow for bone defect models that will help in further determining the SWCNT/PLAGA composites ability to serve as a bone substitute. The incorporation of drugs or bioactive molecules to these composites will also be further explored, as these molecules may enhance new tissue formation and aid in targeting specific conditions, such as the treatment of bone defects following osteomyelitis, and will potentially enhance the clinical implications of SWCNT composites (Ambrose et al., 2004; Babensee, McIntire, & Mikos, 2000; Luginbuehl, Meinel, Merkle, & Gander, 2004).

In conclusion, this study showed that the addition of SWCNT to PLAGA 2-D composites resulted in a similar degradation rate as PLAGA alone and concentration of 10mg SWCNT resulted in the highest cell proliferation rate. The SWCNT imparted beneficial cellular growth capabilities to the SWCNT/PLAGA composites and the gene expressions and mineralization abilities were well established with these constructs. These results demonstrate the potential of SWCNT/PLAGA composites for musculoskeletal regeneration and bone tissue engineering.

CHAPTER 4

IN-VITRO EVALUATION OF THREE DIMENSIONAL SINGLE WALLED CARBON NANOTUBES COMPOSITES FOR BONE TISSUE ENGINEERING

CHAPTER 4-1

INTRODUCTION

Bone related injuries are among the most common orthopaedic injuries and account for more than three million surgeries annually (Giannoudis, Dinopoulos, & Tsiridis, 2005). More than half of these surgeries require bone grafting by either autograft or allograft (Greenwald et al., 2001). Although autografts and allografts are typically used to treat bone defects and non-unions caused by trauma, pathological deformation, or tumor resection (Thein-Han & Misra, 2009; C. T. Laurencin et al., 1999), bone grafts pose limitations due to the need of a secondary surgery, inadequate bone supply, risk of immunological response and disease transmission (Mistry & Mikos, 2005; Pellegrini, Seol, Gruber, & Giannobile, 2009).

To alleviate the limitations posed by autografts and allografts, bone tissue engineering (BTE) has evolved as an alternative strategy to develop bone grafts. This approach relies on the use of biodegradable polymers with or without the use of specific cell types and growth factors (Petite et al., 2000). The success of this strategy depends on the effectiveness of the biodegradable composite. An ideal composite must be commercially available, non-immunogenic, biodegradable, bioresorbable, biocompatible, and exhibit high mechanical strength (C. T. Laurencin et al., 1999; Gupta et al., 2013). PLAGA is used as a composite material because it exhibits all of these properties except high mechanical strength (Athanasiou et al., 1996; Lu et al., 1999).

Mechanical strength can be increased by reinforcing PLAGA with a second-phase material. Carbon based biomaterials such as pyrolytic carbon, diamond-like carbon, carbon nitride, and carbon fibers, all have been widely used as coatings and fillers in implants due to inherent properties like hardness, low coefficient of friction, chemical inertness, and high wear and corrosion resistance. These materials are highly applicable to the medical field due to their biocompatibility. Carbon Nanotubes (CNT) have also been looked into for their use in biomedical systems and devices due to their unprecedented properties in terms of size, strength and surface area. Additionally, CNT possess high tensile strength, are ultra light weight and have excellent thermal and chemical stability (N. Sinha & Yeow, 2005; Armentano et al., 2008; N. Saito et al., 2009). Due to these properties, CNT are excellent candidates for use as nanofillers in polymeric materials to increase mechanical properties. In addition, several researchers have reported that CNT act as an exceptional substrate for cell growth and differentiation (Hu et al., 2004; Zanello, Zhao, Hu, & Haddon, 2006).

In our previous study (Gupta et al., 2013) we demonstrated that addition of SWCNT to PLAGA formed a SWCNT/PLAGA composite with beneficial cellular growth capabilities, gene expression and mineralization. Degradation rate remained unaffected by addition of SWCNT. Although our results showed tremendous promise for BTE, the two-dimensional (2-D) design of the SWCNT/PLAGA composites must be modified to produce a three-dimensional (3-D) composite that facilitates cell proliferation and provides adequate mechanical strength.

Composite design and construction prove to be a difficult obstacle in BTE. Bone is a highly metabolic tissue that requires a constant supply of oxygen and essential nutrients. To accommodate these needs, highly porous scaffolds are often preferred (Dias, Fernandes, Guedes, & Hollister, 2012). Although highly porous scaffolds allow for greater perfusion of oxygen and

73

nutrients, a porous design may compromise the mechanical strength of the scaffold (Q. Zhang et al., 2012). A balance between structure and mechanical strength must be achieved to meet the strength and metabolic needs of bone.

In our previous study we demonstrated that composites reinforced with 10mg SWCNT imparted the highest cell proliferation rate (Gupta et al., 2013). The purpose of this study was to develop 3-D SWCNT/PLAGA composites using 10mg SWCNT, based on previous results, to determine the mechanical strength of the composites and to evaluate the interaction of MC3T3-E1 cells via cell adhesion, growth, survival, proliferation, and gene expression. We hypothesize that the 3-D SWCNT/PLAGA composites can be designed and optimized to support MC3T3-E1 cell growth, possess adequate mechanical strength, and can be applied for use in BTE.

74

CHAPTER 4-2

METHOD

Preparation of 1% PVA Solution

1.5g of poly vinyl alcohol (PVA) (Fisher Scientific, USA) was dissolved in 150ml of pre-warmed de-ionized (DI) water with continuous stirring on a magnetic stirrer. The solution was left on the stirrer for 2min and then again heated in the microwave for 40-45sec. The above steps were repeated until a homogenous solution was obtained. The solution was allowed to cool down and then moved to a steadystir machine.

Fabrication and Characterization of PLAGA and SWCNT/PLAGA Microspheres

PLAGA (Purac Biomaterials, Netherlands) and SWCNT (Sigma Aldrich, USA) were obtained and stored at -80^0C and in the desiccator, respectively. PLAGA and SWCNT/PLAGA microspheres were fabricated by an oil-in-water (o/w) emulsion method. For PLAGA microspheres, 1g of PLAGA was dissolved in 12ml solution of dichloromethane (Fisher Scientific, USA) in a 20ml scintillation vial and the solution was vortexed for 8hrs at a constant speed to dissolve the polymer. For SWCNT/PLAGA microspheres, once the PLAGA was dissolved, 10mg of SWCNT was added to the polymer solution and vortexed for another 8hrs. Both the solutions were then transferred to a 10ml syringe and, using an 18G 1½ inch needle, were injected at uniform speed to the continuously stirring PVA solution (at 300rpm). After 20hrs the stirring was stopped and the formed microspheres settled to the bottom. The microspheres were washed 3-4 times with DI water and then filtered using a Whatman filter paper. They were then air-dried for 24hrs and were stored in a desiccator. Scanning electron microscopy (SEM) was performed to study the surface and to determine the diameter of the

microspheres. They were mounted onto a carbon coated SEM stub, sputter coated with Gold/Palladium and viewed under the SEM.

Fabrication and Characterization of 3-D PLAGA and SWCNT/PLAGA Composites

PLAGA and SWCNT/PLAGA composites were fabricated via a thermal sintering technique. The microspheres, consisting of highly varied sizes, were packed into aluminum molds designed to produce 10mm diameter X 2mm thickness circular disks. The molds were heated at 100^0C for 4hrs to get desired disks and the disks were stored in a desiccator. SEM was performed to study the composites' surface. They were mounted onto a carbon coated SEM stub, sputter coated with Gold/Palladium and viewed under a SEM.

Composites Mechanical Characterization

Mechanical testing of PLAGA and SWCNT/PLAGA composites (n=6) was carried out using an Instron 5869 (Instron, USA) at 10% strain/min under physiological conditions. The calculated stress and strain were used to compute the compressive modulus and ultimate compressive strength.

Cell Culture

MC3T3-E1 cells (MC3T3-E1 subclone 4, precursor osteoblasts) were obtained from American Type Culture Collection (ATCC, USA). The cells were grown in Alpha Minimal Essential Medium (α-MEM) containing ribonucleosides, deoxyribonucleosides, 2mM L-Glutamine, and 1mM sodium pyruvate (Hyclone, Thermo Scientific, USA), and supplemented with 10% Fetal Bovine Serum (FBS) (Gibco, Invitrogen, USA) and 1% Penicillin-Streptomycin (P/S) (Lonza, USA). The 3-D PLAGA and SWCNT/PLAGA composites were fabricated as described above. Both sides were exposed to UV light for 15min each to insure sterilization. After sterilization the composites were placed in a 48-well plate and soaked in the complete culture medium for 1hr.

76

Cells were enzymatically lifted from the expansion flask, counted using a hemacytometer and 50,000 MC3T3-E1 cells/composite were seeded onto the composites and analyzed for cell adhesion/morphology/proliferation, cell growth/viability, and gene expression.

Scanning Electron Microscopy (SEM)

Cell adhesion on the composites surface was determined qualitatively by SEM (Hitachi S-3000 scanning electron microscope). At day 7, the composites seeded with 50,000 MC3T3-E1 cells/composite were washed with PBS. The cells were fixed with 1.5% Glutaraldehyde in 0.1M Cacodylate buffer, followed by 2.5% OsO_4 in 0.1M Cacodylate buffer for post-fixation. After fixation the cells were washed with 0.1M Cacodylate buffer and dried using serial ethanol dehydration and hexamethyldisilazane (HMDS). The dried samples were sputter coated with Gold/ palladium and viewed under SEM.

Immunofluorescence Staining

Normal unstressed MC3T3-E1 cells are flat and polygonal in shape and general cellular morphology was used to determine the cellular behavior (or stress) on the composites. Cellular morphology and adhesion (qualitatively) were determined by using immunofluorescence staining. At day 7, the composites were seeded with 50,000 MC3T3-E1 cells/composite and washed with PBS. The cells were then fixed with 70% ethanol at -20˚C for 10min. After fixation, the cells were incubated with 1% Bovine Serum Albumin (BSA) in PBS containing 0.05% Triton X-100 for 20min at room temperature (RT), followed by immersing in 1% Tween for 20min at RT. The cells were then incubated overnight at 4^0C with monoclonal mouse Anti-β-actin antibody (1:400, Sigma Aldrich, USA) followed by washing with 0.05% Tween. They were then incubated with secondary antibody (goat anti-mouse F (ab') 2 fragment of IgG conjugated with an Alexa Fluor® 488 fluorescence probe, 1:400, Cell Signaling, USA) for 1hr at RT. The

cells were then washed with PBS, and nuclei stained using Hoechst dye, mounted using 80% glycerol and viewed under a confocal microscope.

Live/Dead Assay

LIVE/DEAD® Viability/Cytotoxicity kit (Invitrogen, USA) was used to determine cell growth and survival on the PLAGA and SWCNT/PLAGA composites. 50,000 MC3T3-E1 cells/composite were seeded. At day 7, 14 and 21, the cells were taken out of the culture and washed with PBS. They were then stained for live-dead cells according to the manufacturer's instructions. The stained cells were visualized using a Confocal Microscope in which live cells were stained green and dead cells were stained red.

Cell Proliferation Assay

Cell proliferation was determined using CyQUANT® cell proliferation assay (Invitrogen, USA) as per manufacturer's instructions at day 7, 14 and 21 post-seeding 50,000 MC3T3-E1 cells/composite on 20% BGS (Bovine Growth Serum) as a negative control, PLAGA and SWCNT/PLAGA composites. Briefly, at desired time points, media was removed; cells were washed with PBS and trypsinized. The suspended cells were centrifuged and the cell pellet was stored at -80^0C. A total of 200μl of CyQUANT® GR dye/cell-lysis buffer was added to the pellet at RT. After incubating the samples for 2-5min at RT, protected from light, the 200μl sample was transferred to a microplate and fluorescence was measured at ~480nm excitation and ~520nm emission maxima using a microplate reader.

Real Time Reverse Transcriptase Polymerase Chain Reaction

50,000 MC3T3-E1 cells/ composite were seeded on control tissue-culture polystyrene (TCPS), PLAGA and SWCNT/PLAGA composites. At day 7, 14 and 21, after culturing the cells in the osteogenic medium (Igwe et al., 2012), the cells were harvested and the RNA was isolated using

RNeasy mini kit (Qiagen, USA). 200ng of isolated RNA was reverse transcribed into cDNA using maxima first strand cDNA synthesis kit (Thermo Scientific, USA). Real Time Reverse Transcriptase Polymerase Chain Reaction (RT-PCR) was carried out using the Taqman® (Invitrogen, USA) gene expression assays to determine the expression of Alkaline Phosphatase (ALP), Osteocalcin (OC), Osteopontin (OPN), Bone Sialoprotein (BSP), RUNX2, Type-I collagen (TIC) and GAPDH (as control). The mouse primers were purchased from Applied Biosystems (Igwe et al., 2012) and RT-PCR was performed using an Eppendorf Realplex cycler.

Statistical Analysis

CyQUANT® cell proliferation assay was performed two times in duplicate and gene expression analysis was performed three times in duplicate and mean $\pm$ SEM (Standard error of mean) values along with statistical analysis using two-way analysis of variance (ANOVA) with Tukey post hoc test were performed. Mechanical Testing was done with n=6 and a two-tailed, unpaired Student's t-test were performed to compare two groups, followed by one-way ANOVA with Tukey post hoc test. The results were considered significant when $p < 0.05$.

CHAPTER 4-3

RESULTS

Characterization of PLAGA and SWCNT/PLAGA Microspheres

The SEM micrographs for PLAGA (Figure 4-1) and SWCNT/PLAGA (Figure 4-2) microspheres demonstrated uniform shape and smooth surface with size ranging from 250-750µm. The light microscopy image for SWCNT/PLAGA microspheres (Figure 4-2) demonstrated that the SWCNT were incorporated and uniformly distributed in the PLAGA matrix.

80
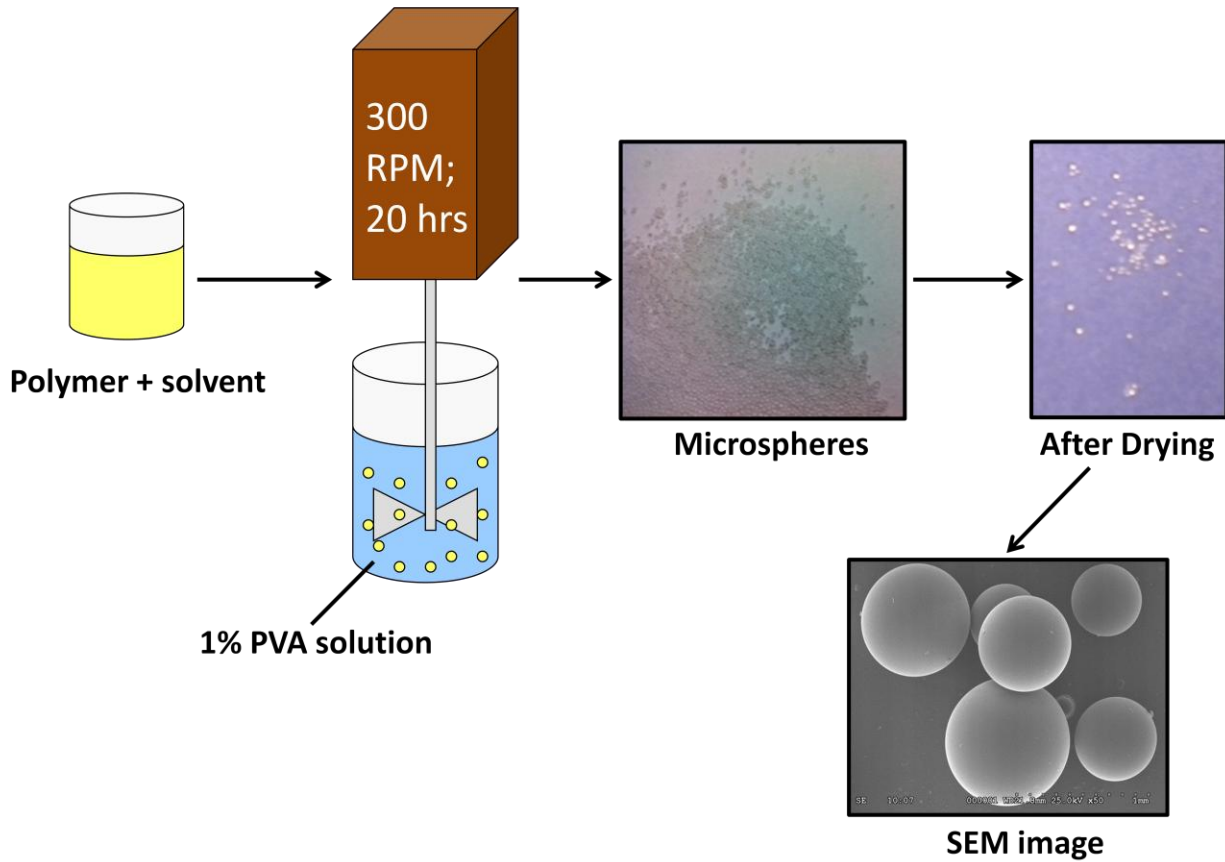
Figure 4-1: **Fabrication of PLAGA microspheres using oil-in-water emulsion method. In addition, figure also shows SEM image for PLAGA microspheres demonstrating uniform shape and smooth surface.**
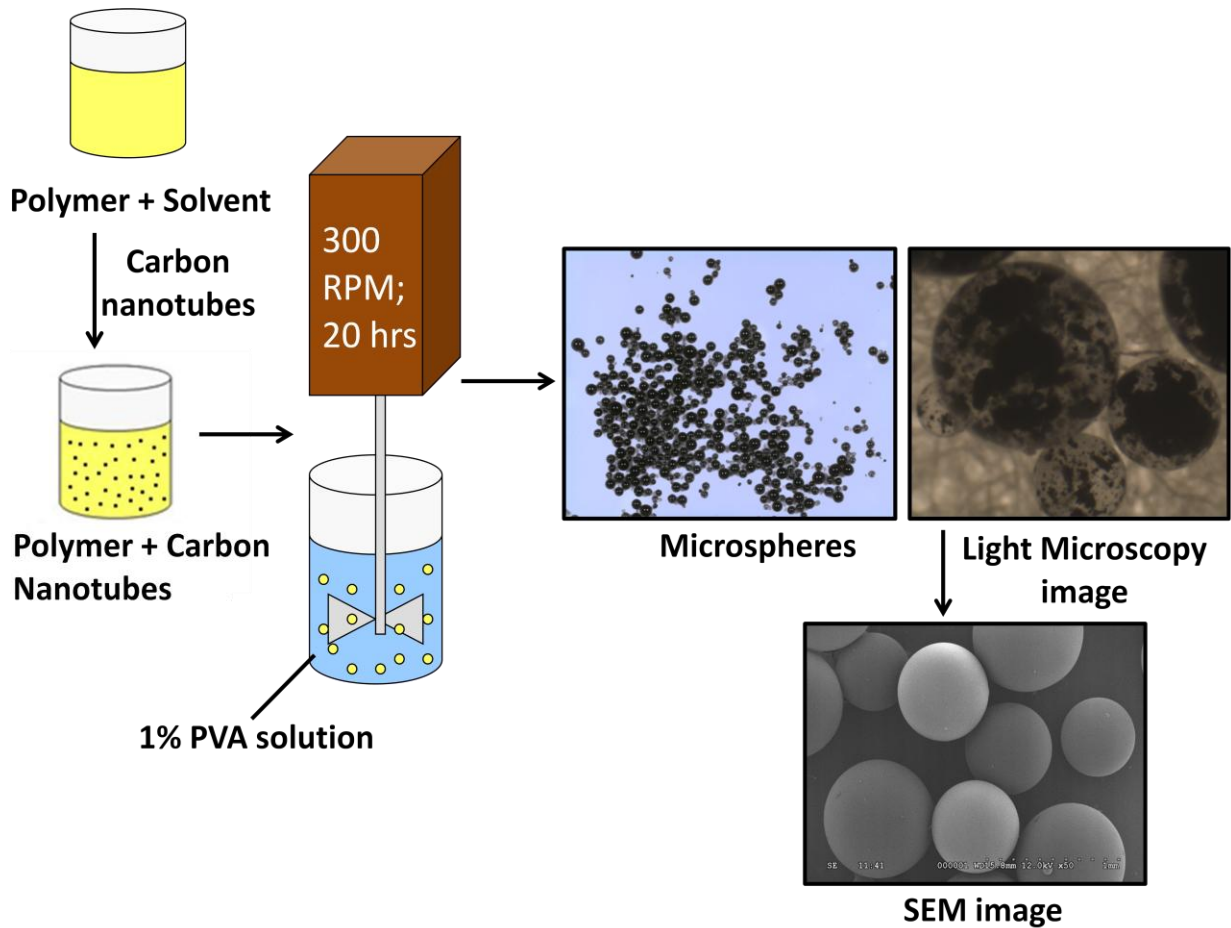
Figure 4-2: **Fabrication of SWCNT/PLAGA microspheres using oil-in-water emulsion method. In addition, figure also shows light microscopy and SEM image for SWCNT/PLAGA microspheres demonstrating uniform incorporation of SWCNT into PLAGA, and uniform shape and smooth surface of the microspheres.**

Fabrication and Characterization of PLAGA and SWCNT/PLAGA composites

The composites obtained via thermal sintering technique are shown in Figure 4-3. The SEM images for PLAGA and SWCNT/PLAGA composites showed bonding of the microspheres in random packing manner. The microspheres maintained their spacing, resembling trabeculae of cancellous bone (Figure 4-4).
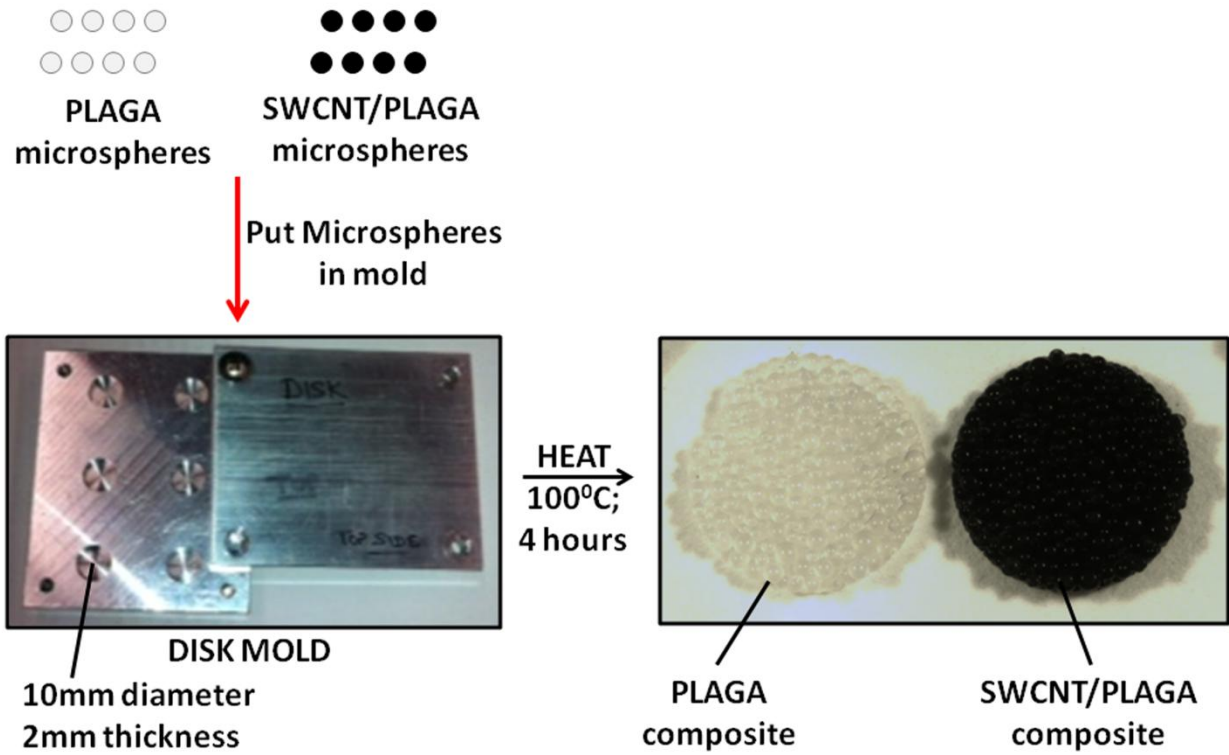
Figure 4-3: **Fabrication of 3-D PLAGA and SWCNT/PLAGA composites using thermal sintering technique.**

TOP VIEW   **SIDE VIEW**
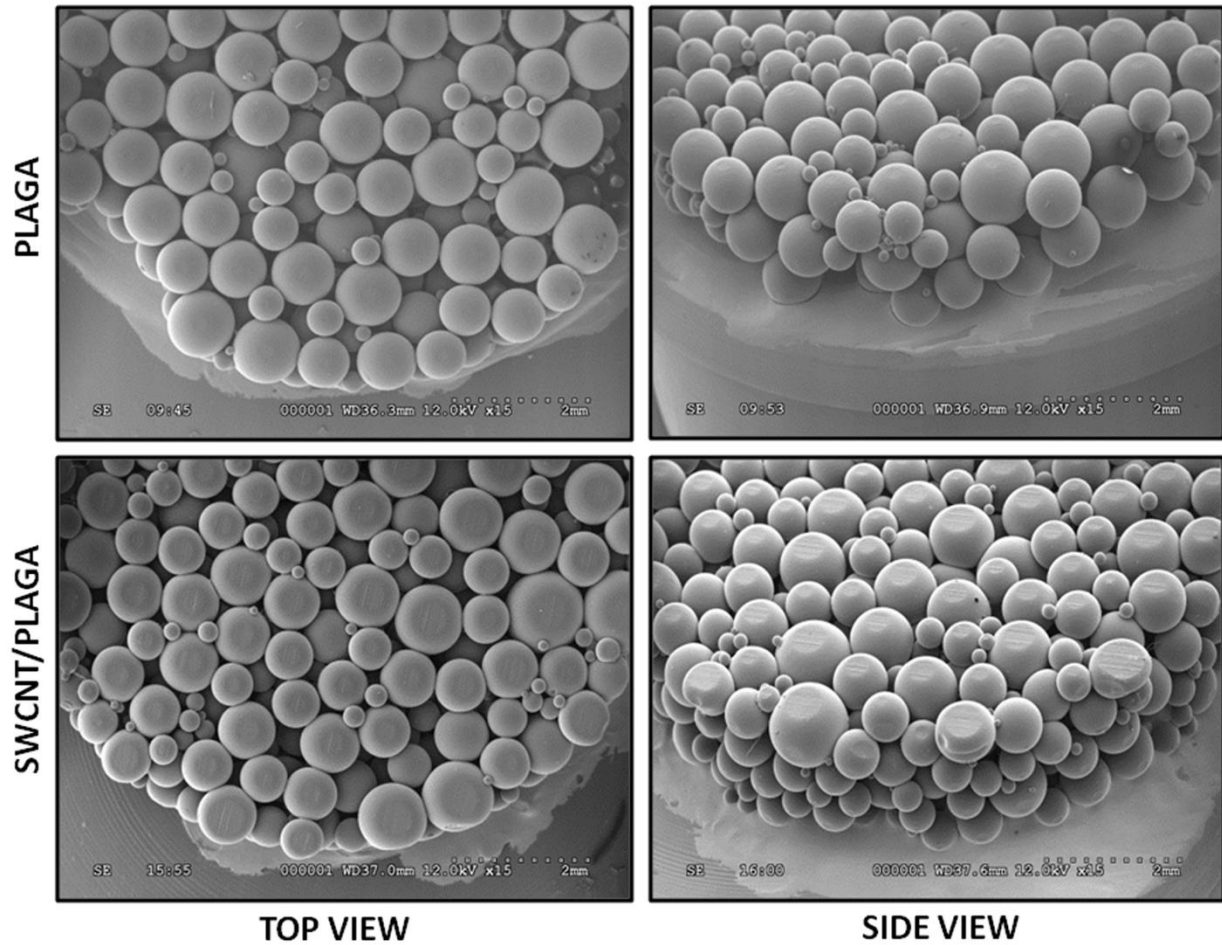
Figure 4-4: **SEM micrographs of PLAGA and SWCNT/PLAGA composites. The microspheres bonded in a random packing arrangement while maintaining spacing, resembling trabeculae of cancellous bone.**

Mechanical Characterization

SWCNT/PLAGA composites yielded a significantly greater compressive modulus and ultimate compressive strength compared to PLAGA composites. The computed compressive modulus and ultimate compressive strength for the SWCNT/PLAGA were 22.54±15.8MPa and 2.63±1.39MPa respectively, whereas the values for the PLAGA control were 7.65±3.97MPa and 0.663±0.24Mpa respectively (Figure 4-5).
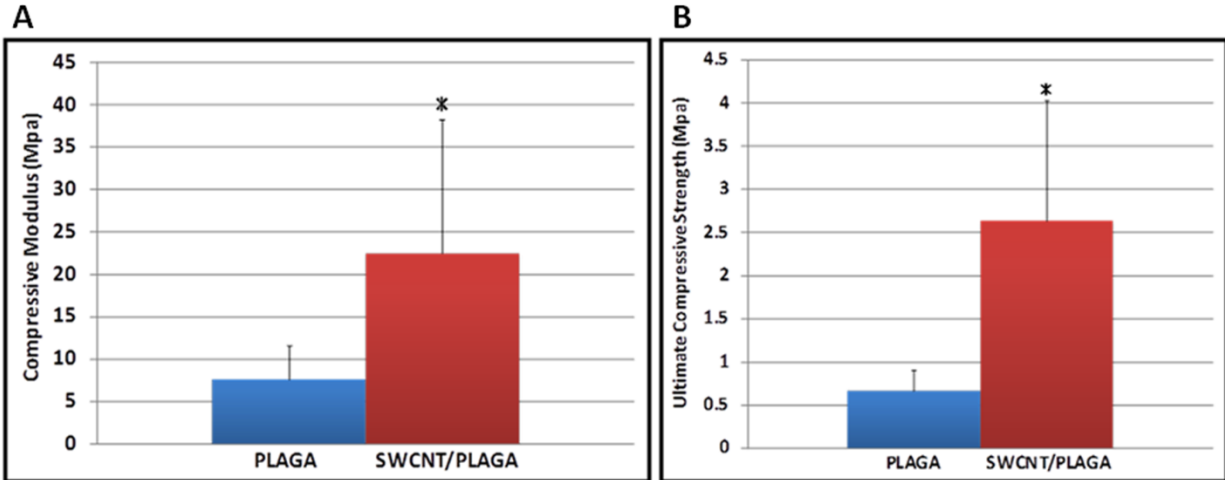
Figure 4-5: **Compressive Modulus (A) and Ultimate Compressive Strength (B) of PLAGA and SWCNT/PLAGA composites. * represents significant difference ($p < 0.05$) compared to PLAGA.**

Scanning Electron Microscopy

SEM images of MC3T3-E1 cells cultured on both PLAGA and SWCNT/PLAGA composites were taken at day 7. We observed that the cells adhered to the surface of the microspheres and also formed cytoplasmic extensions and bridged the gaps between the microspheres (Figure 4-6). At day 14 and 21, the proliferation progressed to the point where the entire surface of the microspheres was covered with the cells.
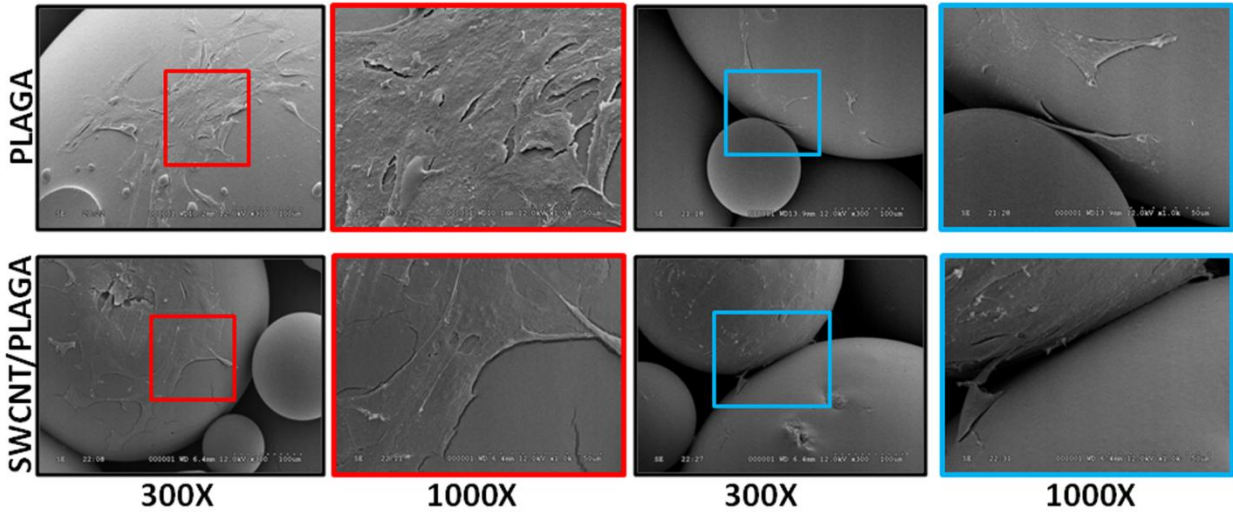
Figure 4-6: **SEM image (at 300X and 1000X) of MC3T3-E1 cells cultured on PLAGA and SWCNT/PLAGA composites. Cells adhered and grew on both the composites surface.**

Immunofluorescence Staining

The β-actin staining revealed that the MC3T3-E1 cells adhered, grew and exhibited a normal, non-stressed morphological pattern (flat and polygonal morphology) on both of the composites surface at day 7 (Figure 4-7). At day 14 and 21, cells were confluent over the entire surface of composites (data not shown).

90
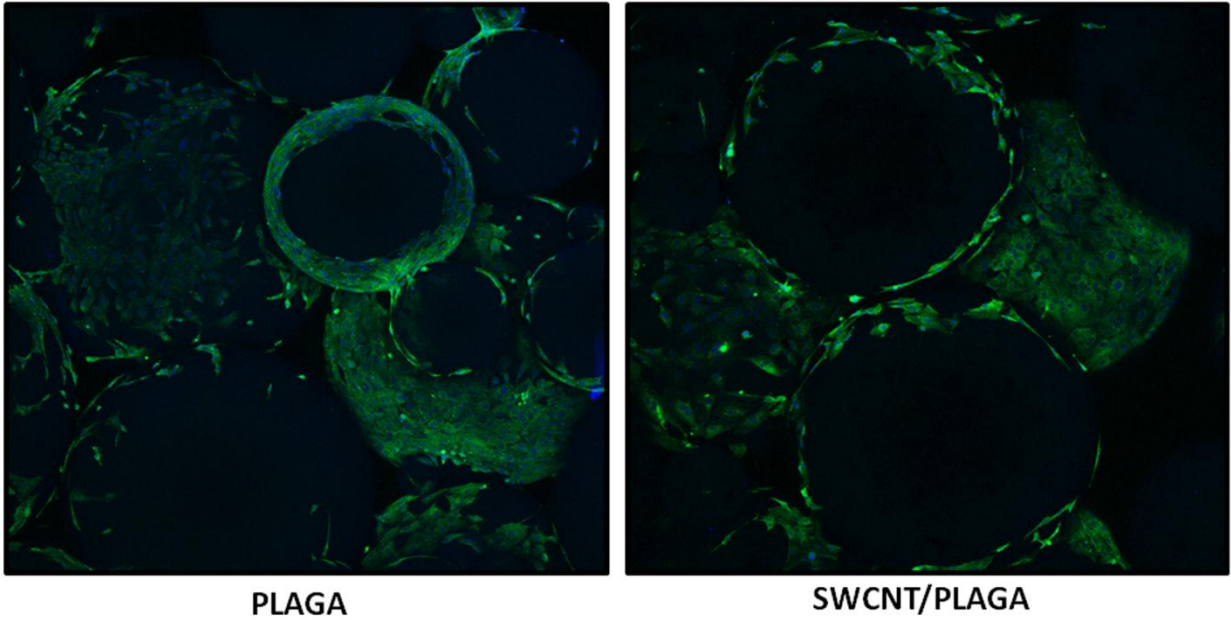
Figure 4-7: **Immunofluorescence staining (green: β-actin, blue: hoechst stain) images captured using a confocal microscope (at 10X 3.1zoom). MC3T3-E1 cells adhered, grew and retained morphology on both PLAGA and SWCNT/PLAGA composites.**

Live/Dead Assay

Live MC3T3-E1 cells were stained green, and adhered and attained their normal morphology on both PLAGA and SWCNT/PLAGA composites. Dead cells were stained red and were very few in number (Figure 4-8). By day 7, the cells adhered and grew on the composites surface. By day 14, the cells began migrating on the surface of composites. By day 21, the cell density increased on both the composites surface.
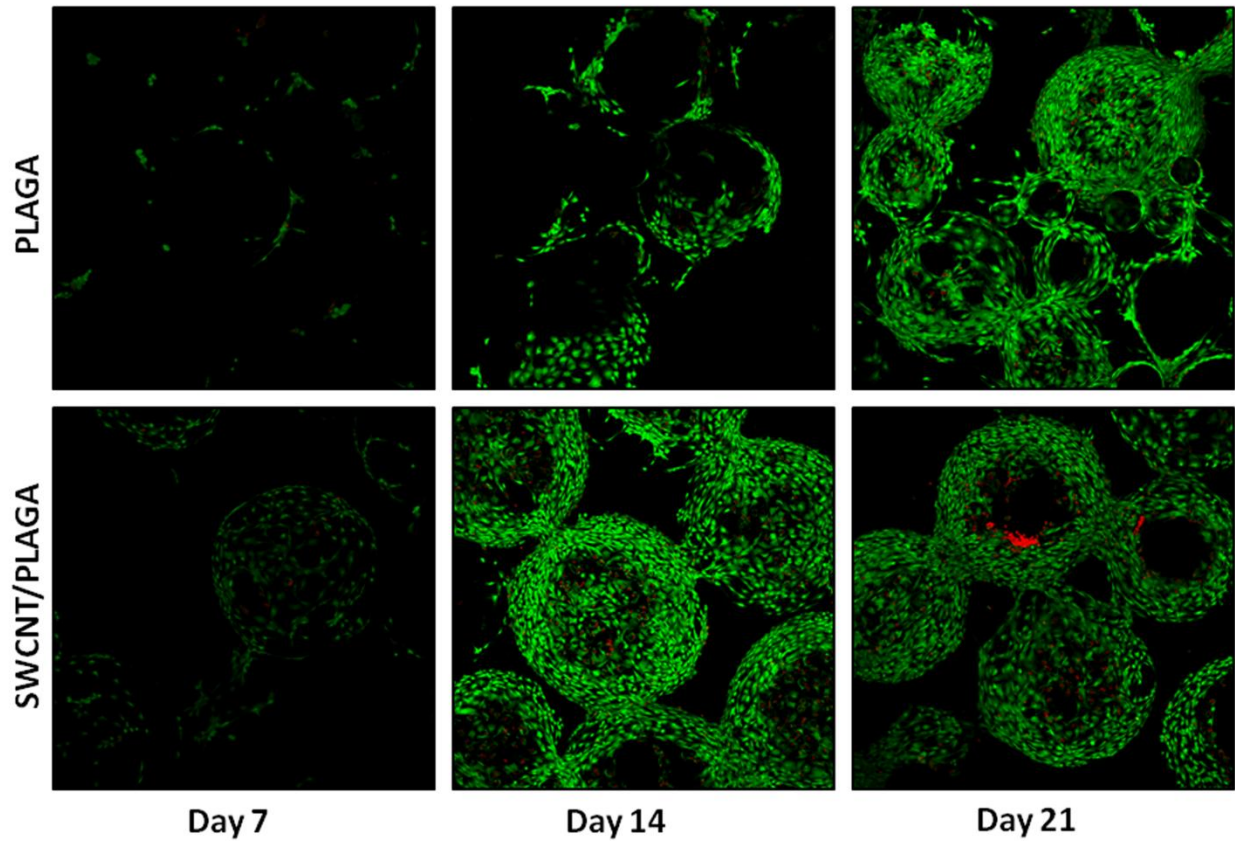
Figure 4-8: **Growth and survival of MC3T3-E1 cells on PLAGA and SWCNT/PLAGA composites (at 10X 3.1 zoom) at day 7, 14 and 21. Images show live (green) and dead (red) cells.**

Cell Proliferation

A significantly higher MC3T3-E1 cell proliferation rate was observed on SWCNT/PLAGA compared to PLAGA composites and the negative control BGS at all time intervals (day 7, 14 and 21). At day 21, the cell proliferation rate for SWCNT/PLAGA composites was significantly greater than all other groups. For PLAGA, the cell proliferation rate significantly increased from day 7 to 14 and plateaued by day 21; whereas, for SWCNT/PLAGA, the cell proliferation rate significantly increased from day 7 to 14 and day 14 to 21 (Figure 4-9).
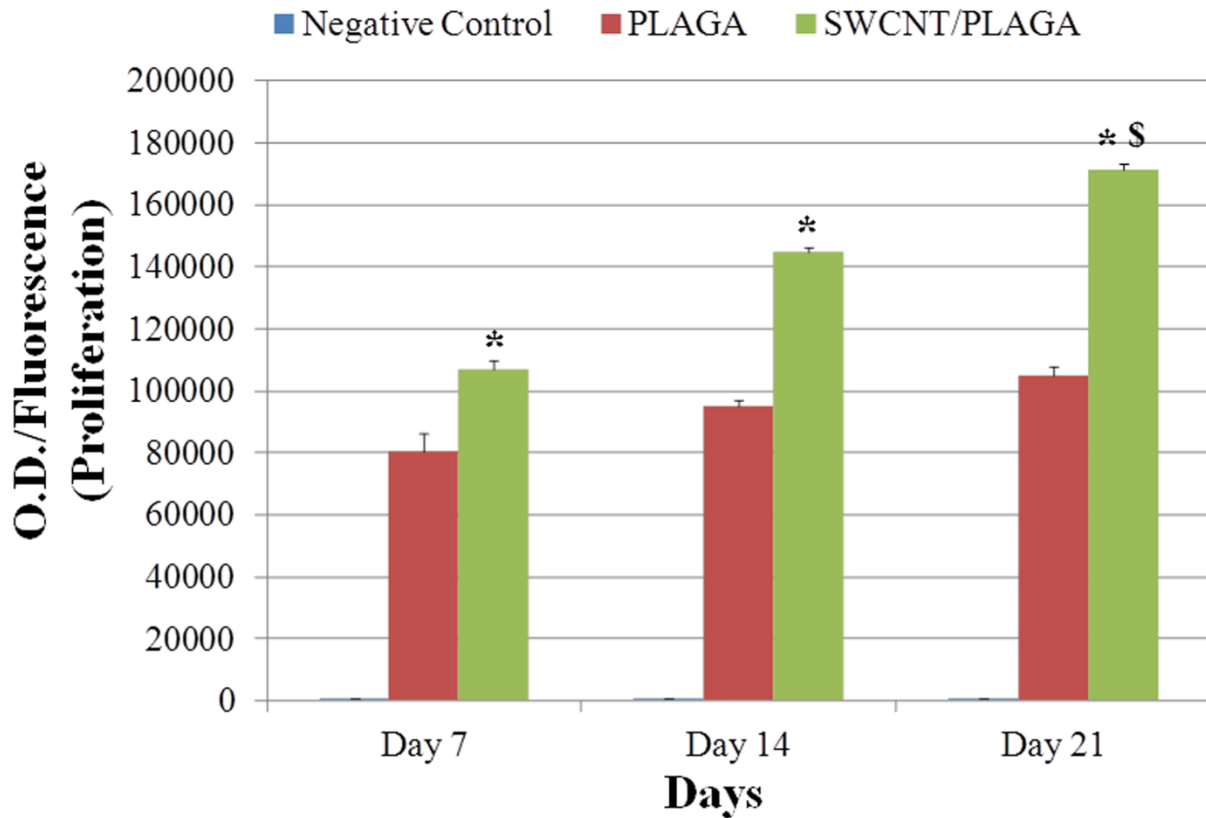
Figure 4-9: **CyQUANT® cell proliferation assay for proliferation of MC3T3-E1 cells cultured on PLAGA and SWCNT/PLAGA composites. Data represents Mean ± SEM and * represents significant difference in proliferation on SWCNT/PLAGA composites compared to PLAGA composites at the same time point at significance level $p < 0.05$. $ is significant over all groups.**

Gene Expression Analysis

The results demonstrated the expression of osteoblast phenotypic markers (Col I, OPN), mineralization markers (ALP1, OC, BSP) and differentiation marker (RUNX2) on PLAGA and SWCNT/PLAGA composites normalized to control TCPS at day 7, 14 and 21 (Figure 4-10). There was a non-significant trend of increased gene expression levels on SWCNT/PLAGA compared to PLAGA composites on day 7 for Col I, OPN, ALP1, BSP and OC, with the difference being significant for RUNX2 only. By day 14, gene expression levels showed a trend toward increased levels for all genes, with only Col I, ALP and RUNX2 showing a significant increase. By day 21 again all genes showed a trend for increased mRNA expression levels, with only Col I, ALP, OC and RUNX2 showing a significant increase.
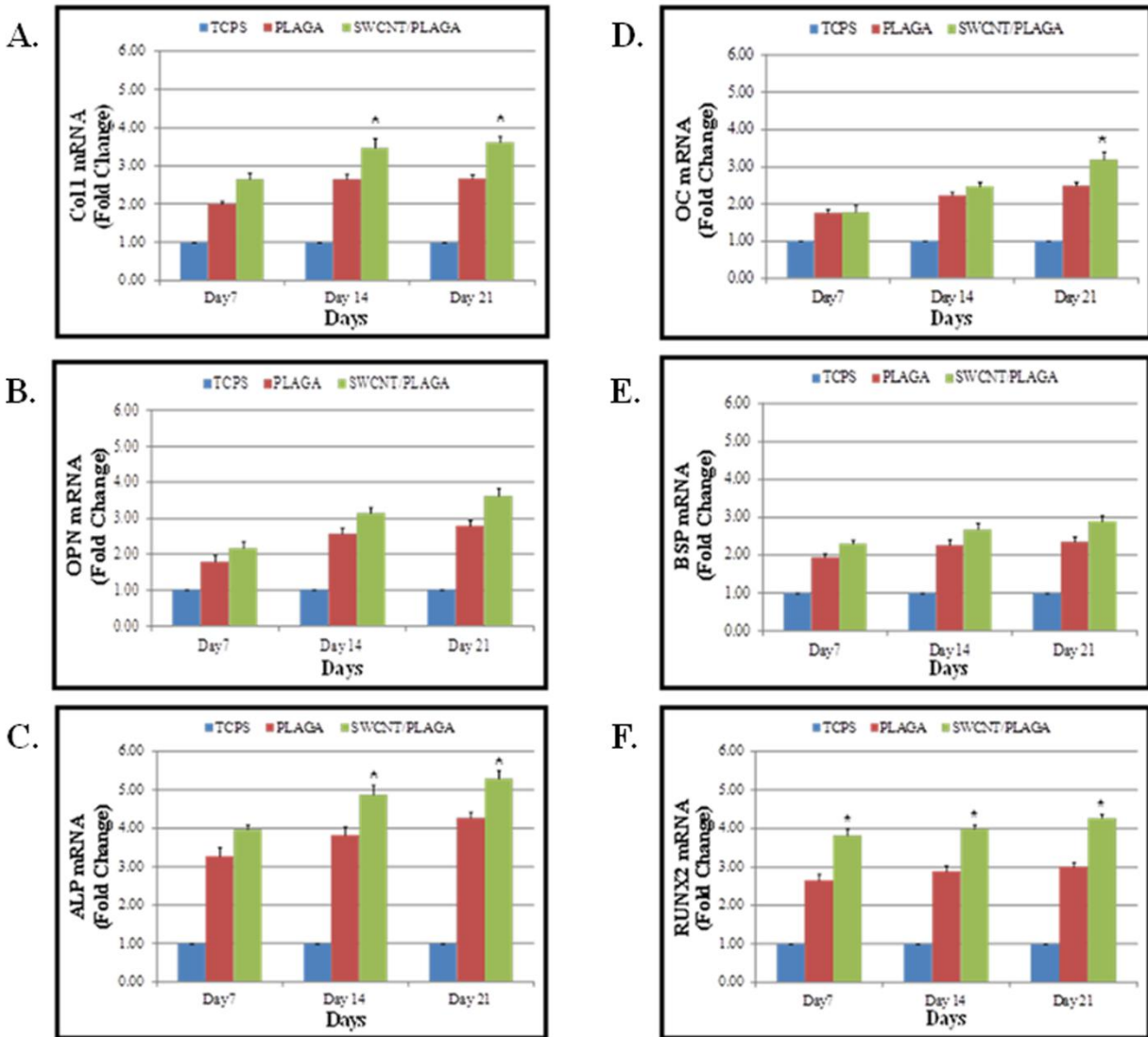
Figure 4-10: **Gene expression profile of MC3T3-E1 cells grown on PLAGA and SWCNT/PLAGA composites. Panels showing mRNA levels detected by qPCR for Col I (A), OPN (B), ALP (C), OC (D), BSP (E), and RUNX2 (F). Data represents Mean $\pm$ SEM and * represents significant difference in gene expression on SWCNT/PLAGA composites compared to PLAGA composites at the same time point at significance level $p < 0.05$.**

CHAPTER 4-4

DISCUSSION

Fabricating a tissue engineered scaffold with appropriate mechanical strength and biocompatibility poses many difficulties in the field of BTE. Bone is a highly organized tissue with a complex macrostructure, microstructure, nanostructure, and ECM (Rho, Kuhn-Spearing, & Zioupos, 1998). Designing an ideal scaffold that mimics the complex physiognomy of native bone is an impossible task; however, our lab has developed a novel 3-D SWCNT/PLAGA composite fabricated by sintering microspheres that resembles bone microstructure and macrostructure. We hypothesized that the 3-D SWCNT/PLAGA composite would be able to support MC3T3-E1 cell growth, possess appropriate mechanical strength, and be applied for use in BTE.

In this study, we fabricated PLAGA and SWCNT/PLAGA microspheres with uniform shape and smooth surface using o/w emulsion method. Sintering PLAGA and SWCNT/PLAGA microspheres of varying sizes (250-750µm) led to microspheres arranged in a random packing manner with their spacing maintained. This uneven size distribution of microspheres produced highly porous networks that resemble the microstructure of the bone. The highly porous network allowed for optimal nutrient perforation, and the addition of SWCNT to the PLAGA composite increased the mechanical properties of the composite. In support of our hypothesis, the results demonstrated a 3-fold increase in compressive modulus and 4-fold increase in ultimate compressive strength with addition of 10mg SWCNT to PLAGA. The increased stress value at which the SWCNT/PLAGA failed can be likely contributed to the addition of the SWCNT. SWCNT are flexible nanotube bundles, which absorb energy and forces from multiple directions without failing. The structure of these nanotubes can be described as a continuous fiber that

98

allows for the release of stresses in the composite without breaking, and will provide toughness to the composite. This absorption of energy is evident with increased compressive modulus and ultimate compressive strength when the SWCNT are incorporated into PLAGA. Without SWCNT, the PLAGA composite failed and plastically deformed at a lower stress values.

In addition to mechanical strength, the composite must allow for cell adhesion and proliferation. Several studies have demonstrated cell adhesion and proliferation on CNT and PLAGA composites (Hu et al., 2004; Cheng, Rutledge, & Jabbarzadeh, 2013). In line with our previously published study, our recent results demonstrated that the addition of 10mg SWCNT to PLAGA imparted beneficial MC3T3-E1 cell adhesion and proliferation. Qualitative analysis via immunofluorescence staining and SEM demonstrated MC3T3-E1 cells adhered and exhibited normal, healthy morphology on these composites by day 7. At day 14 and 21 cells were confluent, covering the entire surface of the composites. Quantitative analysis via CyQUANT® cell proliferation assay confirmed larger cell density on the SWCNT/PLAGA composites compared to PLAGA composites at day 7, 14 and 21. These results are in accordance with a study performed by Cheng et al., which also showed addition of CNT increased both cell proliferation and mechanical strength (Cheng et al., 2013). Additionally, cell proliferation and differentiation may be enhanced by the incorporation of growth and differentiation factors to our SWCNT/PLAGA composites. Previous studies have incorporated biological agents into PLAGA microspheres for applications in BTE (Ambrose et al., 2004; Fei et al., 2008). Future studies must evaluate whether the incorporation of growth and differentiation factors to our SWCNT/PLAGA composites will impact cell proliferation and differentiation.

Furthermore, the potential of SWCNT/PLAGA composites to promote osteogenic differentiation was observed. The results demonstrated significantly increased expression of

genes on SWCNT/PLAGA compared to PLAGA composites. A significant increase in amount of Col I, ALP1 and RUNX2 was observed at day 14 and 21. In addition, upregulation of late mineralization marker, Osteocalcin (OC), at day 21 showed an osteoinductive potential for the SWCNT/PLAGA composites. Significantly higher expression of osteoblast differentiation marker, RUNX2, at all intervals is consistent with increased cell proliferation at all intervals. We believe that this upregulation of gene expression in SWCNT/PLAGA composites is due to increased integrin receptor expression. Future studies will evaluate the expression of integrin receptors involved in the initial adhesion of cells on the composites and to determine the role of integrin ligand RGD in the cellular adhesion on these composites.

The synthetic polymer PLAGA is an attractive composite for BTE due to its attractive degradation profile; but lacks mechanical strength to provide adequate support as a bone graft (Lu et al., 1999). In our previous study (Gupta et al., 2013), we determined that SWNCT completely integrated with the PLAGA matrix without altering the degradation profile of PLAGA. In this study we build on that analysis, demonstrating that the addition of SWCNT to PLAGA increases the compressive modulus and ultimate compressive strength of PLAGA along with cell proliferation rate. These results further demonstrate the effectiveness of SWCNT/PLAGA composites as potential scaffolds for BTE and musculoskeletal regeneration. Future studies will involve pore size and pore volume determination using mercury intrusion porosimetry. Future studies will also involve assessing mineral formation to determine composites' ability to induce bone formation. Future studies must evaluate the in-vivo biocompatibility and toxicity of SWCNT/PLAGA composites, and test its ability to regenerate bone in an animal model. While it is first important to understand the biocompatibility of these

novel composites, successful future studies will likely represent the clinical applicability of

SWCNT/PLAGA in BTE.

CHAPTER 5

IN-VIVO BIOCOMPATIBILITY AND TOXIXITY OF SINGLE WALLED CARBON NANOTUBES COMPOSITES FOR BONE TISSUE ENGINEERING

CHAPTER 5-1

INTRODUCTION

Bone defects and non-unions caused by trauma, tumor-resection, pathological deformation and peri-prosthetic fractures occur within both young and aging populations accounting for more than three million surgeries annually (Korompilias, Lykissas, Soucacos, Kostas, & Beris, 2009; Borrelli, Prickett, & Ricci, 2003; Giannoudis et al., 2005). With this high level of demand, the repair of these bone defects poses a great challenge to the field of orthopaedics. Current methods for bone repair rely heavily on the use of autografts and allografts. However, the many disadvantages surrounding their use have influenced researchers to study other alternatives for bone growth and repair (Soucacos, Johnson, & Babis, 2008; Beris et al., 2004; Soucacos, Kokkalis, Piagkou, & Johnson, 2013). Bone tissue engineering (BTE) has evolved as an alternative that relies on the use of biodegradable polymers with or without the use of cells and growth factors (Petite et al., 2000). Biodegradable polymers are of interest in medicine and are an ideal candidate for BTE because of their commercial availability, biocompatibility, ease of use, degradation into non-toxic products and the ability to control the material's characteristics such as mechanical properties, porosity and surface charges (C. T. Laurencin et al., 1999).

Poly lactic-co-glycolic acid (PLAGA) is widely used as a composite material for BTE as it can be easily processed into the desired configuration, and its mechanical, physical, chemical and degradation properties can be engineered to fit a particular need (Lu & Mikos, 1996).

PLAGA exhibits the properties of an ideal bone graft but lacks adequate mechanical strength (Athanasiou et al., 1996; Lu et al., 1999). Reinforcing PLAGA with a second-phase material can increase the mechanical properties of PLAGA. Carbon based biomaterials such as diamond-like carbon, carbon nitride, pyrolytic carbon and carbon fibers, all have been used as fillers and coatings in implants due to intrinsic properties like a low coefficient of friction, chemical inertness, hardness, and high wear and corrosion resistance (Lu et al., 1999). These materials are relevant to medicine due to their biocompatibility. Carbon Nanotubes (CNT) have also been researched for their use in biomedical systems due to their unique properties in terms of size, strength and surface area. CNT also possess high tensile strength, are ultra-light weight, have excellent thermal and chemical stability, and act as an exceptional substrate for cell growth and differentiation (N. Sinha & Yeow, 2005; Armentano et al., 2008; N. Saito et al., 2009; Hu et al., 2004). These properties make CNT an excellent candidate for use as nanofillers in polymeric materials to increase mechanical properties.

In our previous study (Gupta et al., 2013), we demonstrated that reinforcing PLAGA with Single Walled Carbon Nanotubes (SWCNT), producing a novel SWCNT/PLAGA composite, imparted beneficial cell growth, gene expression and mineralization. The results demonstrated that degradation rate of PLAGA remained unaffected by the addition of SWCNT, and the addition of 10mg SWCNT resulted in the highest rate of cell proliferation. In our another study (Gupta et al., 2014), we demonstrated that the addition of 10mg SWCNT to fabricate three dimensional SWCNT/PLAGA composites led to a greater compressive modulus and ultimate compressive strength in addition to a higher cell proliferation rate and gene expression compared to PLAGA alone. These results demonstrated the potential use of SWCNT/PLAGA composites for musculoskeletal regeneration and BTE with promising applications for orthopedic

103

procedures.

Although, *in-vitro* results indicated the biocompatibility of SWCNT/PLAGA composites, adequate testing of their biocompatibility *in-vivo* is necessary for their use in biological systems because factors such as shape, texture, vasculature of the surrounding tissue, and the location of the implant affect biocompatibility (Sethuraman et al., 2006). Cellular response to biomaterials range from localized inflammation to no response, and the degree of cellular response is determined by the extent of fibrous tissue encapsulation of the implant (Kasemo & Lausmaa, 1994). Inert biomaterials often cause fibrous tissue encapsulation, while toxic biomaterials lead to cell death (Hench & Wilson, 1984). Composites must be certified as biocompatible and non-toxic to ensure that they are safe for use in clinical applications. The goal of this study was to evaluate the *in-vivo* biocompatibility and toxicity of SWCNT/PLAGA composites via subcutaneous implant in a rat model. We hypothesized that SWCNT/PLAGA composites are biocompatible, non-toxic, and are ideal candidates for bone regeneration.

CHAPTER 5-2

METHOD

Fabrication of PLAGA and SWCNT/PLAGA Composites

SWCNT (Sigma Aldrich, USA) and PLAGA (Purasorb PLG8523, Purac Biomaterials, Netherlands) were obtained and stored in the desiccator and at -80^0C, respectively. PLAGA composites were fabricated by dissolving 1g PLAGA in 12ml solution of dichloromethane (Fisher Scientific, USA) in a 20ml scintillation vial. The solution was vortexed for 8hrs at a constant speed to dissolve the polymer, poured in a glass Petri-plate with Bytac paper and kept under a vacuum hood for 30min. For SWCNT/PLAGA composites, once the PLAGA was dissolved, 10mg of SWCNT was added to the polymer solution and the vials were vortexed for an additional 8hrs. The uniform mixture of PLAGA and SWCNT was then poured in a glass Petri-plate with Bytac paper and kept under a vacuum hood for 30min. For both composites, the plates were then kept at -20^0C overnight and then brought to room temperature for complete evaporation of the solvent. The thin films obtained were bored into circular disks (12mm diameter) and placed in a desiccator for 24hrs to remove the residual solvent.

Animals, Housing and Implantation of Scaffolds

All animal experiments were performed after receiving approval from the Laboratory Animal Care and Use Committee (LACUC) of Southern Illinois University, School of Medicine. NIH guidelines for the care and use of laboratory animals were observed. Sixty (5animals/group/time point), 36-40 day old male Sprague-Dawley rats were purchased from Harlan, USA. Animals were acclimatized for a week before surgical procedures were performed. The animals were housed individually in animal rooms with environmentally controlled temperature, relative humidity and 12hr light/dark cycle. Animals were anaesthetized using isoflurane which was

105

delivered using an anesthetic vaporizer. The dorsa of the animals were shaved and sterile prepped with betadine and alcohol. Two incisions approximately 15mm in length (about 15mm apart) were made laterally on the dorsum using a No. 10 surgical blade. A subcutaneous pouch on opposite sides of each incision was made using blunt-dissection technique. The PLAGA and SWCNT/PLAGA disks were unsealed in a sterilized environment (previously sterilized with UV light) and each animal was implanted with 2 polymer disks of same type. Sham implanted rats were used as negative controls. Following implantation the skin was closed using sterile auto-clips (Figure 5-1). The animals were given buprenorphine (0.05mg/kg subcutaneously) for pain management and were allowed to recover. At specific time points post implantation (2, 4, 8 and 12 weeks); the animals were euthanized by carbon dioxide inhalation. The implants and surrounding tissues in addition to major organs were excised for further evaluation.

Morbidity and Clinical Signs

All the animals were observed for signs of morbidity and overt toxicity once daily post-implantation throughout the study. The clinical signs included visual examination in addition to physical examination of the animal and/or palpation. They were observed for any lesions or abnormalities in behavior or function.

Body Weights

Individual body weights were recorded prior to the study (before surgery) and at day 1, 3 and 7 after surgery for the first week and then weekly thereafter.

Food Consumption

Food consumption was measured for individual rats at day 1, 3 and 7 after surgery for the first week and then weekly thereafter. The amount of food was measured before it was supplied to

106

each cage and its remnants were measured at the next time point to calculate the difference. Amounts were then used to calculate the daily food consumption (g/animal/day).

Urinalysis

Urine was collected from 5animals/group once at 12 weeks post implantation. Animals were placed in metabolic racks on the day of collection for 4 hours with access to water and the urine was collected in the collection container at the bottom of the racks. The parameters determined in the urinalysis included pH, specific gravity, leucocytes, nitrite, protein, ketone, ascorbic acid, urobilinogen, bilirubin, glucose and occult blood using a Urispec[TM] 11-way test strips (Henry Schein, USA).

Hematology

Blood samples were collected in EDTA-containing tubes using cardiac puncture after euthanasia. The parameters including WBC count, RBC count, hemoglobin concentration, mean corpuscular volume, mean corpuscular hemoglobin, platelet count etc. were determined using an automated hematology machine (VetScan HM2, Abaxis, Union City, CA). WBC differential counts including neutrophil, lymphocyte, eosinophil, basophil and monocyte were determined from blood smears stained with Wright-Giemsa.

Necropsy

The animals were euthanized as described at the specified intervals and were observed for macroscopic abnormalities. Major organs including heart, lungs, liver, spleen, kidneys and adrenal glands were collected, weighed (absolute and relative to body weights) and observed for abnormalities. All the organs and implant areas were fixed using 10% neutral-buffered formalin.

Histopathology

The collected organs along with the polymer and the surrounding tissues were fixed in 10% neutral-buffered formalin solution for at least 7 days. The samples were embedded in paraffin, sectioned using a microtome to 4-5µm thickness, and stained with hemotoxylin and eosin. All organs and the implant sites were analyzed by a veterinary pathologist blinded to the treatment group. Two implant sites were evaluated for each animal. For the implant sites, a scoring system utilizing 11 parameters was used to calculate a final summary toxicity score for each animal. Scores for the 11 individual parameters ranged from 0 (no finding) to 4 (severe) with the parameters including necrosis, inflammation, polymorphonuclear neutrophils, macrophages, lymphocytes, plasma cells, giant cells, fibroplasia, fibrosis, presence of lipid material and relative size. Summary toxicity scores could range from 0 (no findings) to a maximum score of 44.

Statistical Analysis

Mean ± SEM values along with statistical analysis using one-way ANOVA with Tukey post hoc test were performed for body weight, food consumption, hematology, absolute and relative organ weights, and histopathology. For urinalysis, qualitative interpretations was presented descriptively and mean ± SEM values along with statistical analysis using one-way ANOVA with Tukey post hoc test were performed for urine volume. The results were considered significant when $p < 0.05$.
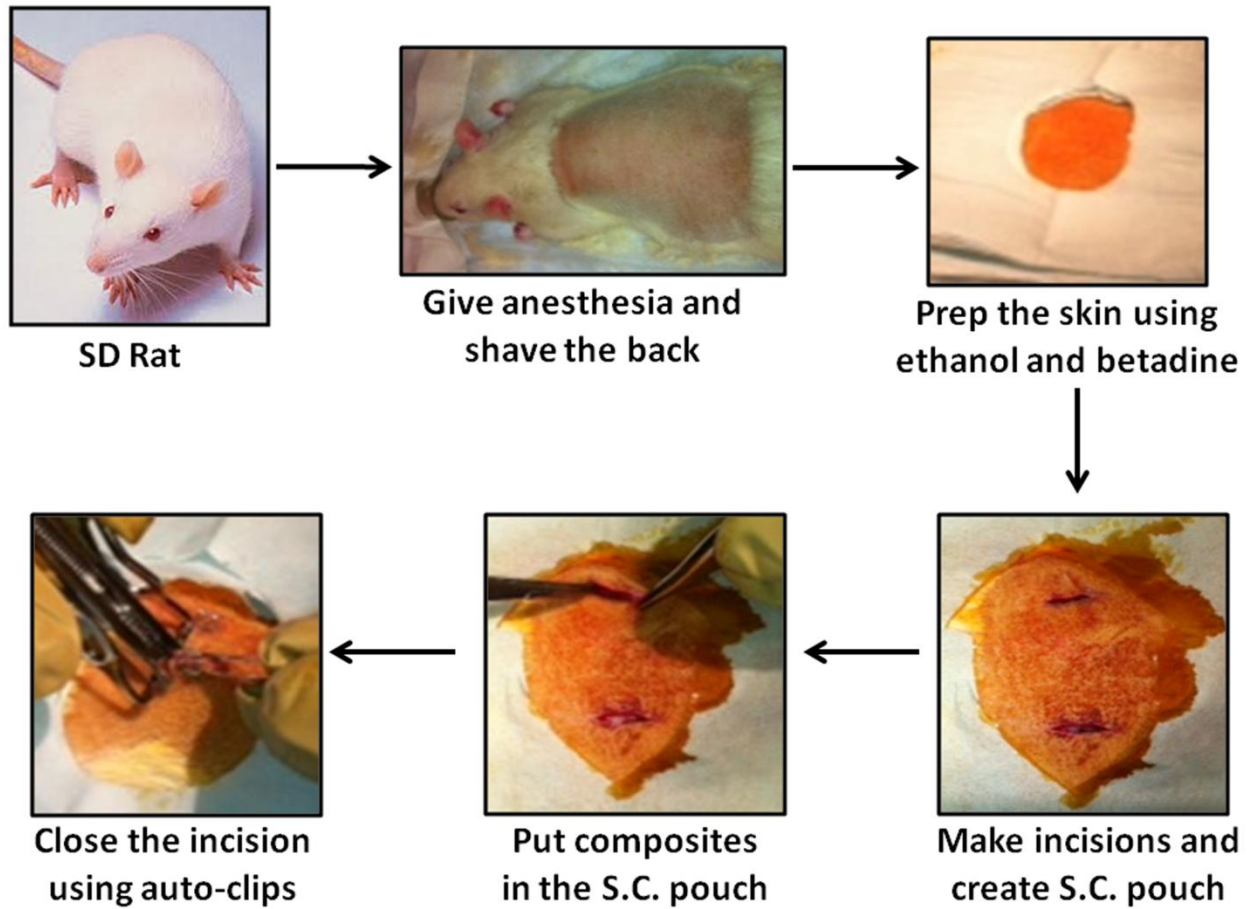
Figure 5-1: **Schematic representation of surgical procedure involved in subcutaneous implantation of Sham, PLAGA and SWCNT/PLAGA composites in the rat.**

Morbidity and Clinical Signs

No mortality occurred during the study. No behavioral changes or visible signs of physical self-mutilation indicating localized or neurological toxicity were observed during the post-op examinations or at the time of euthanasia. No treatment-related signs were observed for any of the animals.

Body Weights

All the groups i.e. Sham; PLAGA; and SWCNT/PLAGA showed consistent weight gain and

followed the same pattern of rate-of-gain throughout the study period (Figure 5-2).

111
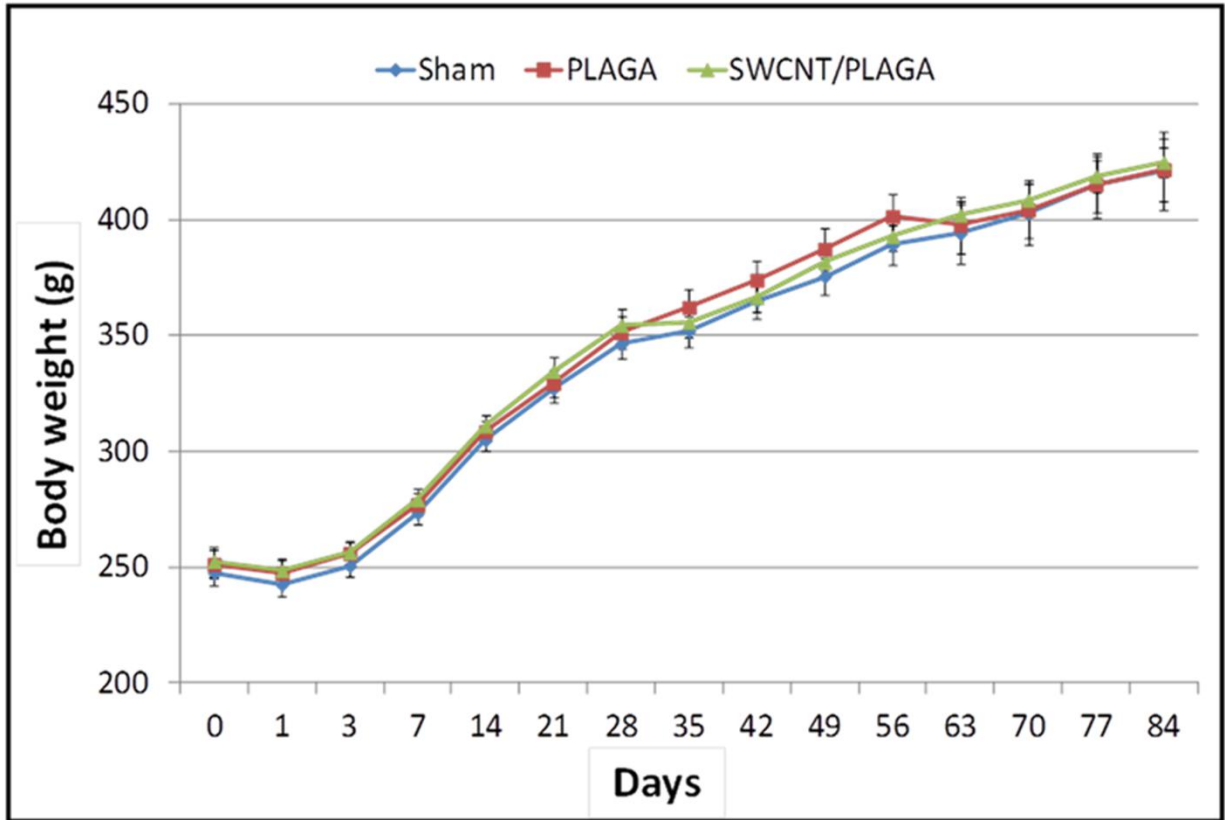
Figure 5-2: **Body weight changes in rats implanted with Sham, PLAGA and SWCNT/PLAGA composites. Data represents mean ± SEM and $p < 0.05$ was considered significant.**

Food Consumption

The food consumption for male rats implanted with Sham, PLAGA and SWCNT/PLAGA exhibited a similar pattern by 14 days (2 weeks) (Figure 5-3A), 28 days (4 weeks) (Figure 5-3B) and 84 days (12 weeks) (Figure 5-3D). All treatment groups showed a significant increase in food consumption initially following the post surgical period and then food consumption plateaued. However, the food consumption of rats implanted with PLAGA was significantly higher than that of Sham at day 35 of 56 days (8 weeks) period (Figure 5-3C).

113
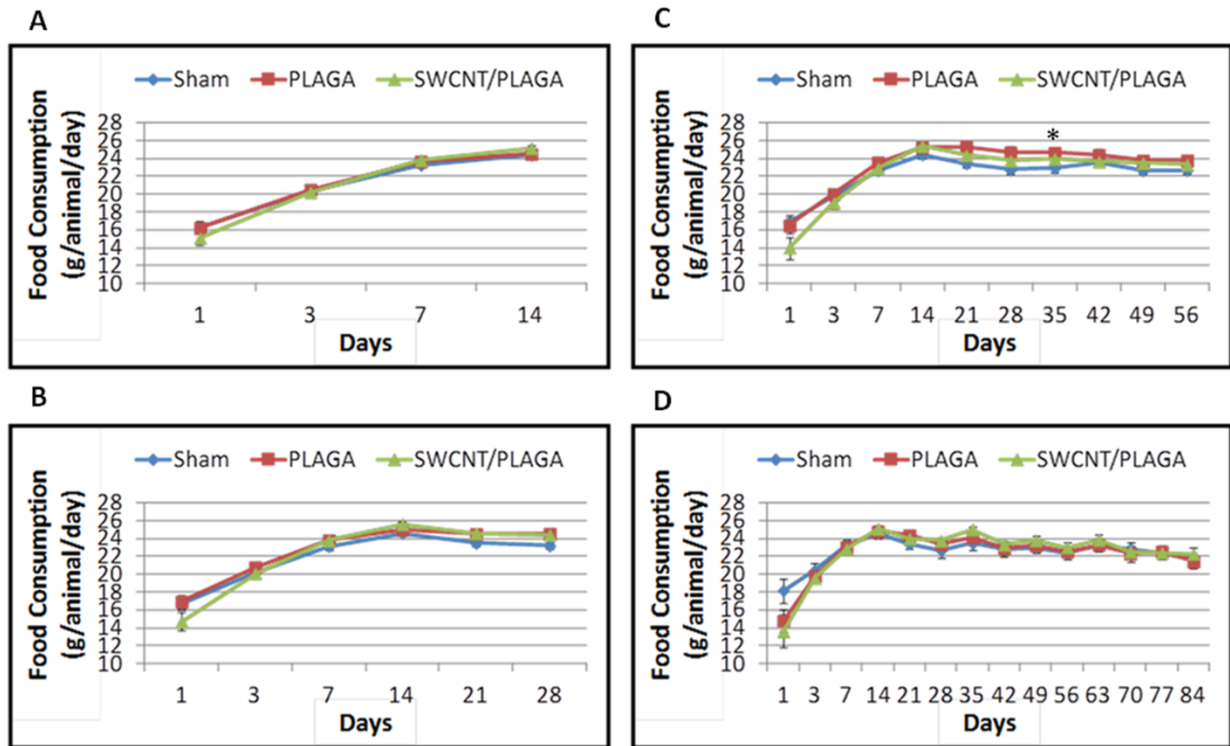
Figure 5-3: **Food consumption in rats implanted with Sham, PLAGA and**

SWCNT/PLAGA composites at 2 weeks (A), 4 weeks (B), 8 weeks (C) and 12 weeks (D)

post-implantation. Data represents mean ± SEM and p < 0.05 was considered significant.

*, PLAGA was significantly different from Sham.

114

www.manaraa.com

Urinalysis

No significant difference between the Sham, PLAGA and SWCNT/PLAGA occurred for any of

the urinalysis parameters (Table 5-1). However, the urine volume collected for the

SWCNT/PLAGA group was significantly higher compared to the PLAGA group. There was no

significant difference for urine volume collected between Sham and PLAGA; and Sham and

SWCNT/PLAGA groups.

Table 5-1

Urinalysis values of rats implanted with Sham, PLAGA and SWCNT/PLAGA composites at 12 weeks post-implantation.

PARAMETERS	GROUP	RATS		
		SHAM $(5)^n$	PLAGA (5)	SWCNT/PLAGA (5)
Blood, hemolyzed (Ery/µl)	ca. 10	-	-	-
	ca. 50	-	-	-
	ca. 250	-	-	-
Blood, non-hemolyzed (Ery/µl)	negative	5	5	4
	ca. 5-10	-	-	1
	ca. 50	-	-	-
	ca.250	-	-	-
Urobilinogen (mg/dl)	normal	5	5	5
	2	-	-	-
	4	-	-	-
	8	-	-	-
	12	-	-	-
Bilirubin	negative	4	4	5
	+	1	1	-
	++	-	-	-
	+++	-	-	-
Protein (mg/dl)	negative	-	-	-
	30	2	2	1
	100	3	3	4
	500	-	-	-
Nitrite	negative	5	5	5
	positive	-	-	-
	every pink color	-	-	-
Ketones	negative	5	5	5
	+	-	-	-
	++	-	-	-
	+++	-	-	-
Ascorbic acid	negative	1	2	2
	+	4	2	3
	++	-	1	-
Glucose (mg/dl)	negative	5	5	5
	normal	-	-	-

116

	50	-	-	-
	150	-	-	-
	500	-	-	-
	≥1000	-	-	-
pH	5	-	-	-
	6	-	-	-
	7	5	5	4
	8	-	-	1
	9	-	-	-
Specific gravity	1	-	-	-
	1.005	3	1	2
	1.01	-	-	2
	1.015	1	2	1
	1.02	1	2	-
	1.025	-	-	-
	1.03	-	-	-
Leucocytes (leuco/µl)	negative	-	-	-
	ca. 25	-	-	-
	ca. 75	1	1	1
	ca.500	4	4	4

[n], number in parentheses represents the number of animals examined.

Hematology

In rats a significantly higher value for mean corpuscular hemoglobin (MCH) was observed for Sham and SWCNT/PLAGA compared to PLAGA at 4 weeks (Table 5-3); and higher granulocyte percent (GR %) value for Sham compared to SWCNT/PLAGA at 12 weeks (Table 5-5). No significant difference was observed for any of the hematological parameters at 2 weeks (Table 5-2) and 8 weeks (Table 5-4).

For WBC differential count (Figure 5-4), segmented neutrophils count was significantly higher for rats implanted with PLAGA compared to Sham at 4 weeks (Figure 5-4A). No other significant difference was observed for any of parameters at 2 weeks, 8 weeks and 12 weeks. All of these statistically significant differences observed were within the normal range of values reported for rats.

118

Table 5-2

Hematological values of rats implanted with Sham, PLAGA and SWCNT/PLAGA composites at 2 weeks post-implantation.

	2 Weeks		
	Sham (5)[n]	PLAGA (5)	SWCNT/PLAGA (5)
WBC (10^9/l)	9.258 ± 1.81	8.988 ± 1.20	11.074 ± 0.72
LYM (10^9/l)	7.556 ± 1.48	6.678 ± 0.88	8.964 ± 0.59
MON (10^9/l)	0.264 ± 1.12	0.158 ± 0.06	0.32 ± 0.10
GRA (10^9/l)	1.436 ± 0.34	2.154 ± 0.36	1.79 ± 0.10
LY% (%)	81.46 ± 3.09	74.3 ± 1.41	80.9 ± 0.96
MO% (%)	2.68 ± 1.02	1.6 ± 0.61	2.72 ± 0.69
GR% (%)	15.86 ± 3.24	24.06 ± 1.96	16.36 ± 1.20
RBC (10^{12}/l)	8.4 ± 0.12	8.314 ± 0.24	8.264 ± 0.15
HGB (g/dl)	15.52 ± 0.38	15.22 ± 0.64	15.82 ± 0.35
HCT (%)	47.154 ± 0.25	45.418 ± 1.02	46.072 ± 0.84
MCV (fl)	56.2 ± 0.66	54.6 ± 0.60	55.6 ± 0.87
MCH (pg)	18.5 ± 0.32	18.28 ± 0.36	19.16 ± 0.20
MCHC (g/dl)	32.92 ± 0.77	33.46 ± 0.75	34.34 ± 0.25
RDWc (%)	16.68 ± 0.09	16.4 ± 0.12	16.46 ± 0.29
PLT (10^9/l)	435.6 ± 86.19	523.6 ± 126.94	506 ± 91.27
PCT (%)	0.344 ± 0.06	0.374 ± 0.09	0.376 ± 0.07
MPV (fl)	8.36 ± 0.56	7.54 ± 0.42	7.48 ± 0.04
PDWc (%)	32.8 ± 1.72	31.46 ± 1.18	30.14 ± 0.51

Each value represents mean ± SEM. [n], number in parentheses represents the number of animals examined. $p < 0.05$ was considered significant.

Table 5-3

Hematological values of rats implanted with Sham, PLAGA and SWCNT/PLAGA composites at 4 weeks post-implantation.

	4 Weeks		
	Sham (5)[n]	PLAGA (5)	SWCNT/PLAGA (5)
WBC (10^9/l)	7.908 ± 1.58	9.57 ± 0.84	9.19 ± 0.57
LYM (10^9/l)	6.272 ± 1.29	7.596 ± 0.67	8.254 ± 0.63
MON (10^9/l)	0.222 ± 0.12	0.124 ± 0.05	0.114 ± 0.03
GRA (10^9/l)	1.41 ± 0.42	1.85 ± 0.17	0.824 ± 0.30
LY% (%)	80.44 ± 3.43	79.44 ± 1.14	89.8 ± 3.30
MO% (%)	2.5 ± 0.94	1.18 ± 0.36	1.28 ± 0.34
GR% (%)	17.04 ± 4.08	19.36 ± 1.25	8.98 ± 3.14
RBC (10^12/l)	8.61 ± 0.08	9.032 ± 0.13	8.9 ± 0.04
HGB (g/dl)	15.84 ± 0.16	16.14 ± 0.17	16.62 ± 0.12
HCT (%)	48.056 ± 0.57	49.06 ± 0.54	49.798 ± 0.46
MCV (fl)	55.8 ± 0.66	54.2 ± 0.58	56 ± 0.63
MCH (pg)	18.4 ± 0.08*	17.84 ± 0.13	18.68 ± 0.19*
MCHC (g/dl)	32.98 ± 0.22	32.84 ± 0.20	33.38 ± 0.19
RDWc (%)	15.78 ± 0.17	16 ± 0.25	15.88 ± 0.18
PLT (10^9/l)	664.2 ± 29.27	736.4 ± 43.08	683.8 ± 30.53
PCT (%)	0.508 ± 0.02	0.546 ± 0.03	0.522 ± 0.02
MPV (fl)	7.66 ± 0.09	7.44 ± 0.09	7.64 ± 0.10
PDWc (%)	30.6 ± 0.19	29.96 ± 0.15	30.9 ± 0.25

Each value represents mean $\pm$ SEM. [n], number in parentheses represents the number of animals examined. $p < 0.05$ was considered significant. *, Sham and SWCNT/PLAGA were significantly different from PLAGA.

120

Table 5-4

Hematological values of rats implanted with Sham, PLAGA and SWCNT/PLAGA composites at 8 weeks post-implantation.

	8 Weeks		
	Sham (5)[n]	PLAGA (5)	SWCNT/PLAGA (5)
WBC (10^9/l)	6.672 ± 1.13	7.08 ± 0.85	5.136 ± 0.38
LYM (10^9/l)	5.194 ± 0.68	5.706 ± 0.50	4.162 ± 0.36
MON (10^9/l)	0.132 ± 0.05	0.202 ± 0.03	0.062 ± 0.01
GRA (10^9/l)	1.342 ± 0.53	1.17 ± 0.36	0.91 ± 0.09
LY% (%)	80.1 ± 3.88	81.9 ± 2.87	80.8 ± 1.61
MO% (%)	2.42 ± 0.92	2.88 ± 0.56	1.32 ± 0.32
GR% (%)	17.5 ± 4.58	15.22 ± 3.17	17.86 ± 1.65
RBC (10^12/l)	8.782 ± 0.21	9.208 ± 0.14	8.774 ± 0.09
HGB (g/dl)	16.26 ± 0.31	16.64 ± 012	15.96 ± 0.20
HCT (%)	47.806 ± 1.01	49.518 ± 0.84	47.198 ± 0.75
MCV (fl)	54.6 ± 0.75	53.8 ± 0.58	53.6 ± 0.51
MCH (pg)	18.56 ± 0.18	18.1 ± 0.19	18.2 ± 0.08
MCHC (g/dl)	34.04 ± 0.46	33.62 ± 0.42	33.84 ± 0.35
RDWc (%)	15.78 ± 0.16	15.88 ± 0.18	16.38 ± 0.09
PLT (10^9/l)	730 ± 112.88	757.6 ± 36.24	723.8 ± 25.42
PCT (%)	0.62 ± 0.12	0.584 ± 0.03	0.564 ± 0.02
MPV (fl)	8.4 ± 0.37	7.68 ± 0.06	7.78 ± 0.18
PDWc (%)	32.12 ± 0.79	30.58 ± 0.35	30.8 ± 0.29

Each value represents mean ± SEM. [n], number in parentheses represents the number of animals examined. $p < 0.05$ was considered significant.

121

Table 5-5

Hematological values of rats implanted with Sham, PLAGA and SWCNT/PLAGA composites

at 12 weeks post-implantation.

	12 Weeks		
	Sham (5)[n]	**PLAGA (5)**	**SWCNT/PLAGA (5)**
WBC (10^9/l)	4.548 ± 0.90	6.546 ± 1.50	5.838 ± 1.24
LYM (10^9/l)	3.536 ± 0.68	5.402 ± 1.18	4.98 ± 1.13
MON (10^9/l)	0.046 ± 0.01	0.138 ± 0.05	0.174 ± 0.09
GRA (10^9/l)	0.966 ± 0.23	1.006 ± 0.29	0.684 ± 0.07
LY% (%)	78.14 ± 1.20	83.1 ± 1.82	84.08 ± 1.81
MO% (%)	1.12 ± 0.34	1.9 ± 0.51	2.42 ± 0.86
GR% (%)	20.72 ± 1.09*	15 ± 1.65	13.5 ± 2.51
RBC (10^12/l)	8.934 ± 0.18	8.896 ± 0.17	8.984 ± 0.19
HGB (g/dl)	15.98 ± 0.28	16.24 ± 0.08	16.3 ± 0.19
HCT (%)	46.902 ± 1.10	46.97 ± 0.55	46.684 ± 0.66
MCV (fl)	52.8 ± 0.49	53 ± 0.89	52.4 ± 0.87
MCH (pg)	17.88 ± 0.14	18.3 ± 0.35	18.18 ± 0.21
MCHC (g/dl)	34.08 ± 0.40	34.6 ± 0.30	35 ± 0.33
RDWc (%)	16.84 ± 0.10	16.64 ± 0.18	16.52 ± 0.23
PLT (10^9/l)	648.2 ± 65.05	553.774 ± 140.93	657.2 ± 19.67
PCT (%)	0.494 ± 0.05	0.504 ± 0.04	0.502 ± 0.02
MPV (fl)	7.64 ± 0.07	7.78 ± 0.16	7.62 ± 0.08
PDWc (%)	30.48 ± 0.27	31.3 ± 0.33	30.78 ± 0.41

Each value represents mean ± SEM. [n], number in parentheses represents the number of animals examined. $p < 0.05$ was considered significant. *, Sham was significantly different from SWCNT/PLAGA.
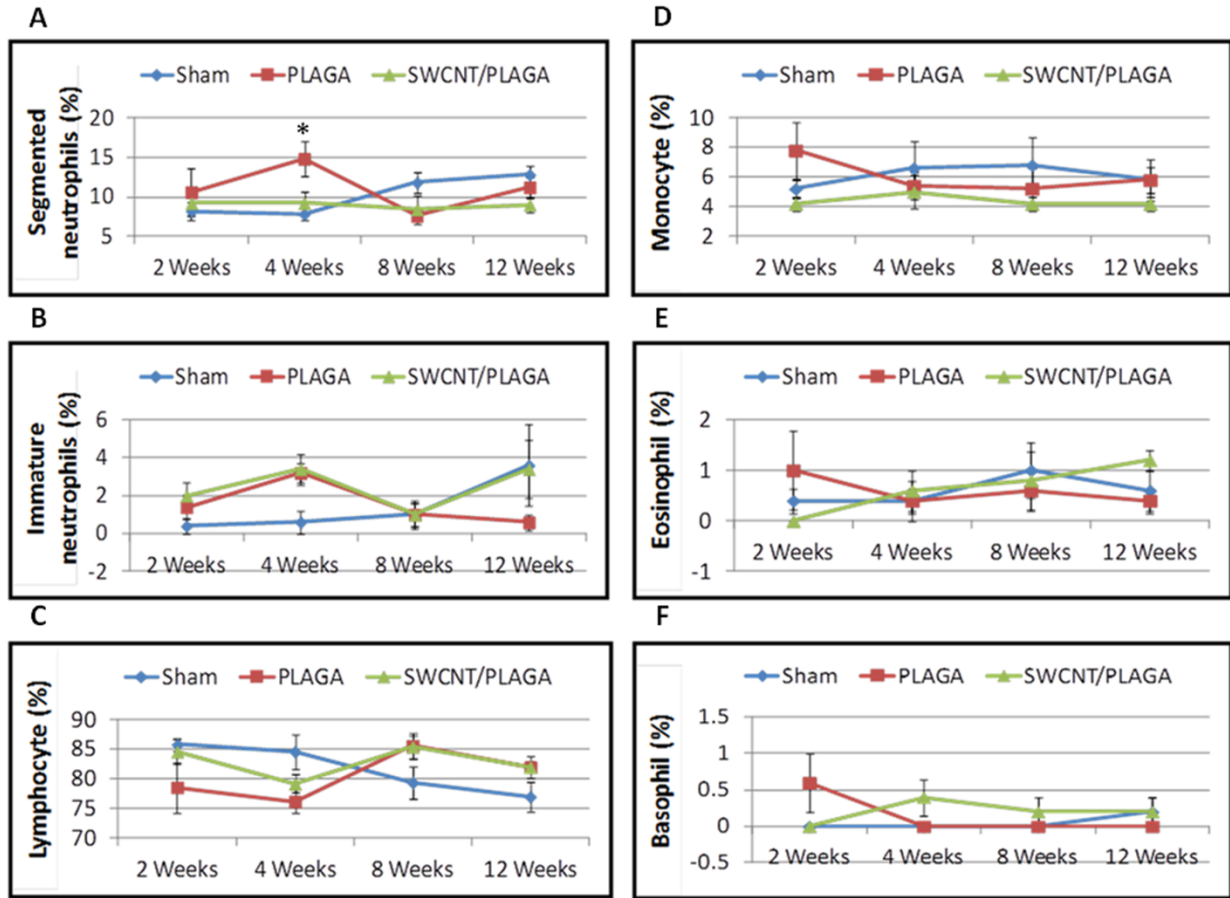
Figure 5-4: **WBC differential count of rats implanted with Sham, PLAGA and**

SWCNT/PLAGA composites. The parameters include segmented neutrophils (A),

immature neutrophils (B), lymphocyte (C), monocyte (D), eosinophil (E) and basophil (F).

Data represents mean ± SEM and $p < 0.05$ was considered significant. *, PLAGA was

significantly different from Sham.

Gross findings at necropsy, absolute and relative organ weights

Implants did not migrate from their original location even though no immobilization (sutures, adhesives etc.) was used. No macroscopic abnormalities were noted in any of the animals (Sham, PLAGA and SWCNT/PLAGA) at 2, 4, 8 and 12 weeks. Subcutaneous tissue surrounding the implants appeared grossly normal with no overt evidence of inflammation and all incision sites were healed (Figure 5-5) (data shown for 8 and 12 weeks only).

No significant differences in absolute and relative organ weights were observed in the rats post-implantation with Sham, PLAGA or SWCNT/PLAGA composites at 2, 4, 8 and 12 weeks (Figure 5-6 and 5-7).
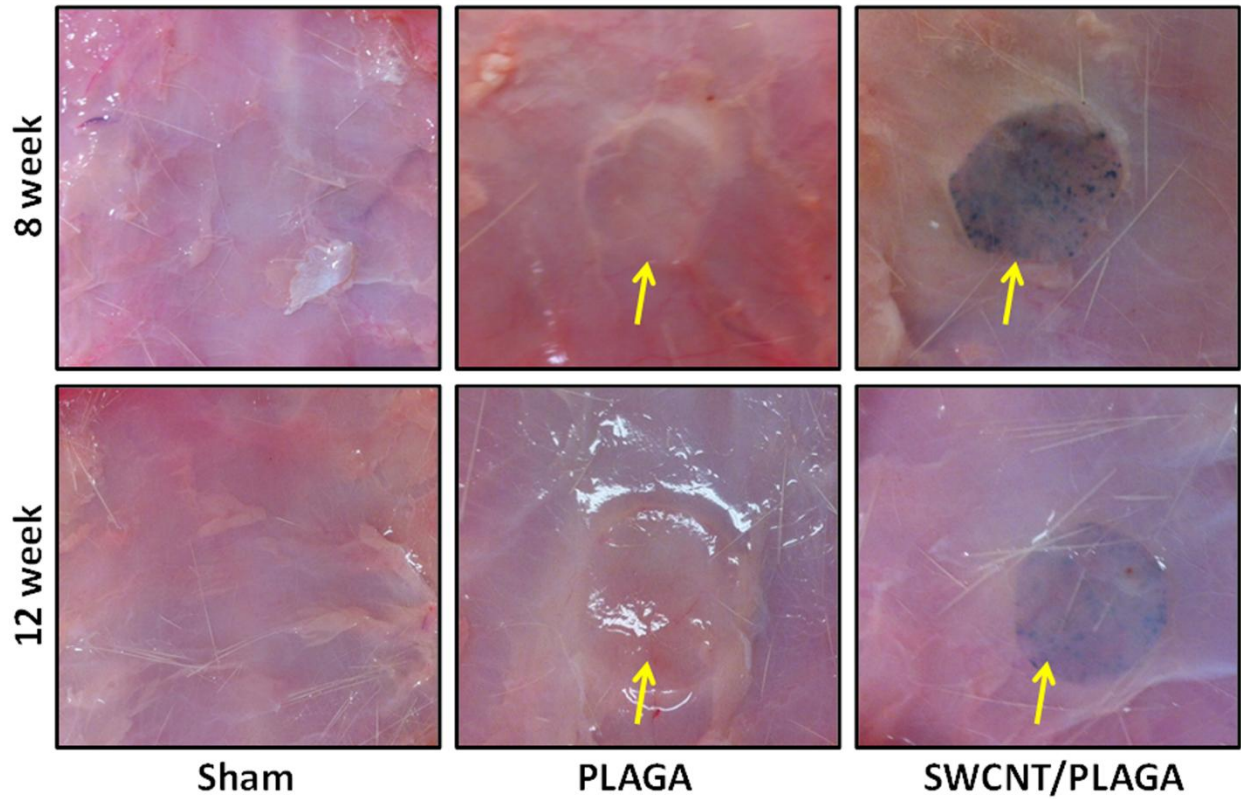
Figure 5-5: **Gross pathology images of subcutaneous tissue surrounding the implants (Sham, PLAGA and SWCNT/PLAGA) at 8 and 12 weeks post-implantation. All incision sites were healed and the tissue surrounding the implants appeared grossly normal with no overt evidence of inflammation.**
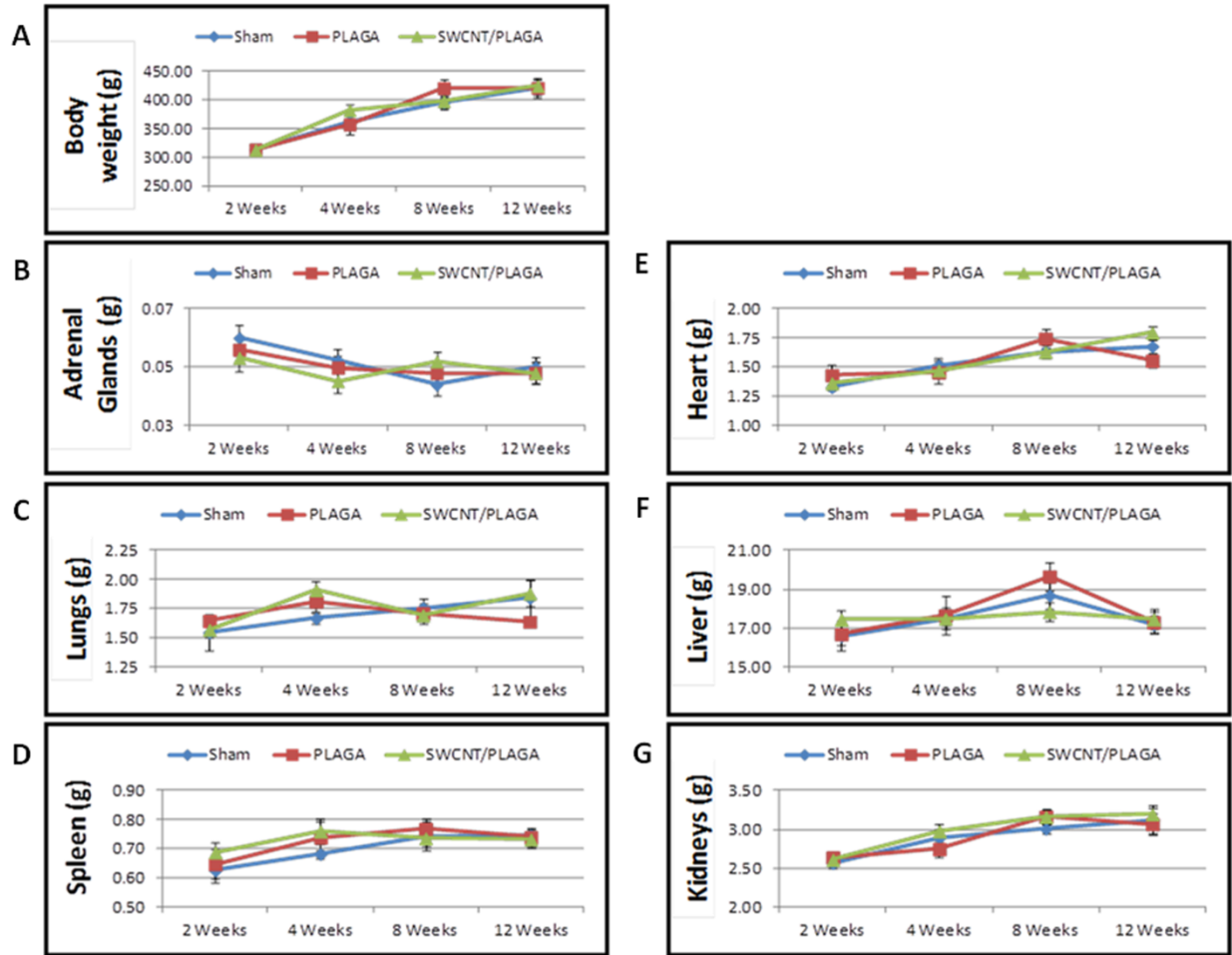
Figure 5-6: **Absolute organ weight in rats implanted with Sham, PLAGA and**

SWCNT/PLAGA composites. The parameters include body weight (A), adrenal glands

(B), Lungs (C), spleen (D), heart (E), liver (F) and Kidneys (G). Data represents mean ±

SEM and $p < 0.05$ was considered significant.
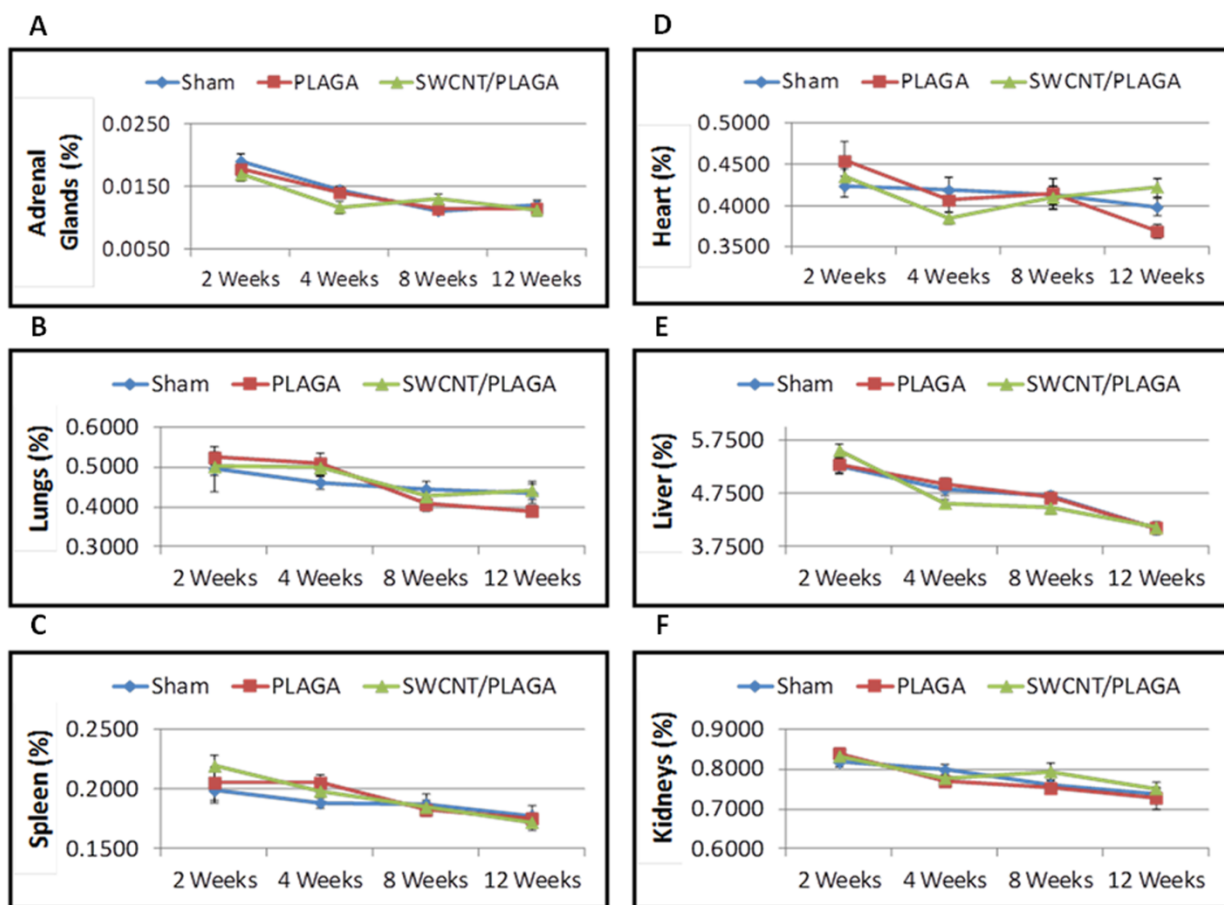
Figure 5-7: **Relative organ weight in rats implanted with Sham, PLAGA and SWCNT/PLAGA composites. The parameters include adrenal glands (A), Lungs (B), spleen (C), heart (D), liver (E) and Kidneys (F). Data represents mean ± SEM and $p < 0.05$ was considered significant.**

Histopathology

There were no lesions observed in the major organs of the rats related to implantation of PLAGA and SWCNT/PLAGA. The sham animals were uniformly without observable response to the sham operation, with a summary toxicology (sumtox) of zero for all four time periods following surgery. Animals treated with the both the PLAGA composite and SWCNT/PLAGA composite tended to have mild to moderate sumtox scores. Both PLAGA and SWCNT/PLAGA composites showed a significant decrease in sumtox score from week 2-4 and no change was observed for weeks 4-8 and 8-12 and between weeks 2 and 8, and 2 and 12. Also, at all the time intervals both PLAGA and SWCNT/PLAGA showed a significantly higher sumtox score compared to Sham group. However, there was no significant difference between PLAGA and SWCNT/PLAGA at all the time intervals (Figures 5-8, 5-9, 5-10, 5-11, and 5-12).
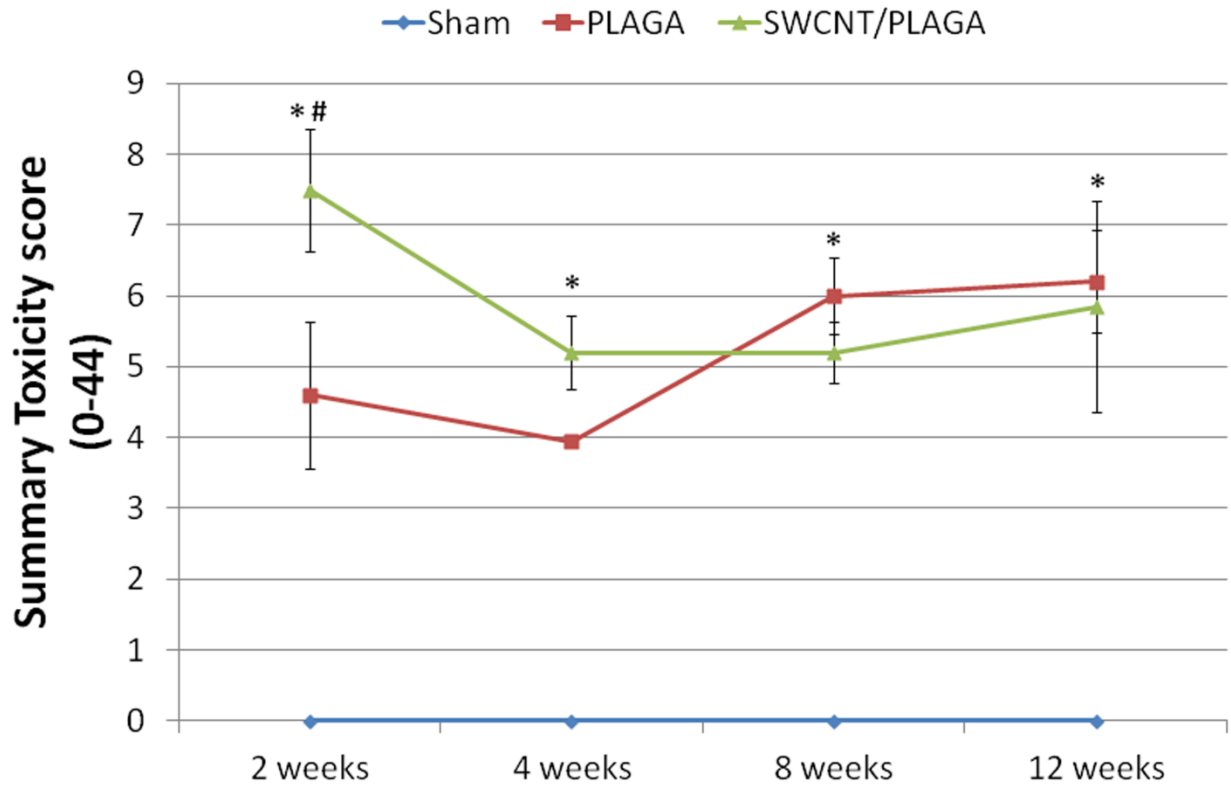
Figure 5-8: **Histopathology changes to Sham, PLAGA and SWCNT/PLAGA in rat subcutaneous tissue as a function of summary toxicity score on a scale of 0-44 over a period of 12 weeks post-implantation. Data represents mean ± SEM and $p < 0.05$ was considered significant. *, PLAGA and SWCNT/PLAGA were significantly different from Sham; #, Both PLAGA and SWCNT/PLAGA showed significant decrease from week 2 to week 4.**
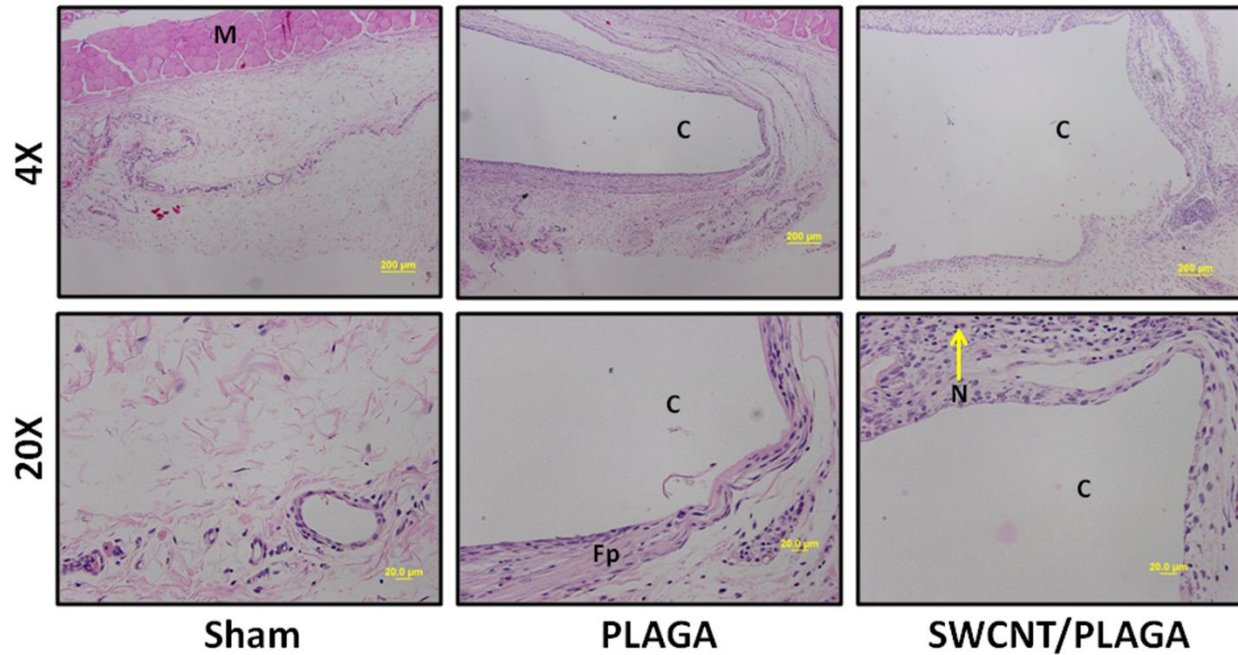
Figure 5-9: **Micrograph of subcutaneous skin tissues of rats implanted with Sham, PLAGA and SWCNT/PLAGA at 2 weeks post-implantation stained with H&E (at X4 and X20 magnification). C= composite (PLAGA or SWCNT/PLAGA) implant site, M= muscular tissue, N= polymorphonuclear neutrophils, Fp= fibroplasia.**
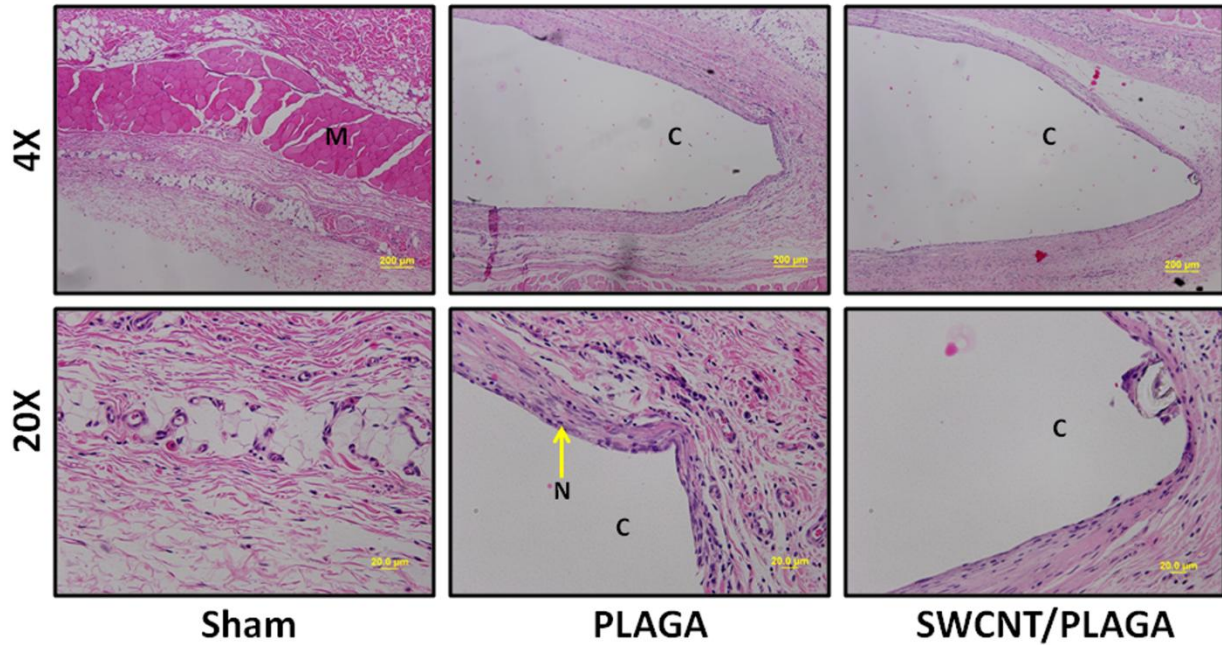
Figure 5-10: **Micrograph of subcutaneous skin tissues of rats implanted with Sham, PLAGA and SWCNT/PLAGA at 4 weeks post-implantation stained with H&E (at X4 and X20 magnification). C= composite (PLAGA or SWCNT/PLAGA) implant site, M= muscular tissue, N= polymorphonuclear neutrophils, Fp= fibroplasia.**

Figure 5-11: **Micrograph of subcutaneous skin tissues of rats implanted with Sham, PLAGA and SWCNT/PLAGA at 8 weeks post-implantation stained with H&E (at X4 and X20 magnification). C= composite (PLAGA or SWCNT/PLAGA) implant site, M= muscular tissue, Fb= fibrosis.**

Figure 5-12: **Micrograph of subcutaneous skin tissues of rats implanted with Sham, PLAGA and SWCNT/PLAGA at 12 weeks post-implantation stained with H&E (at X4 and X20 magnification). C= composite (PLAGA or SWCNT/PLAGA) implant site, M= muscular tissue, Fb= fibrosis.**
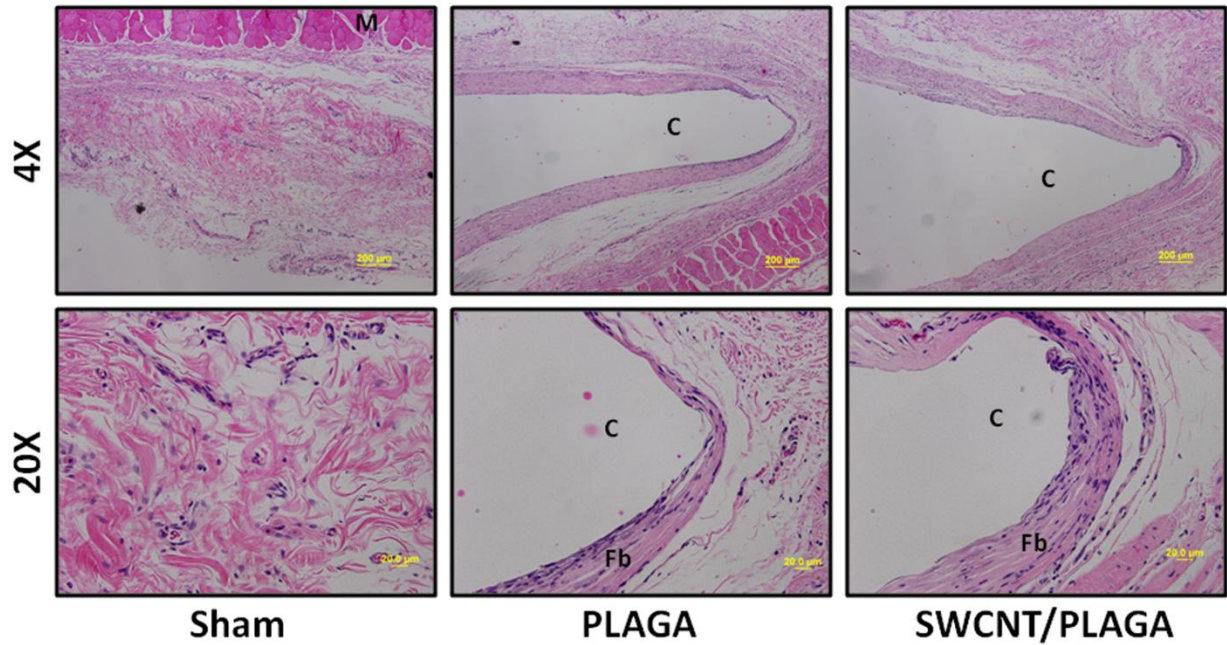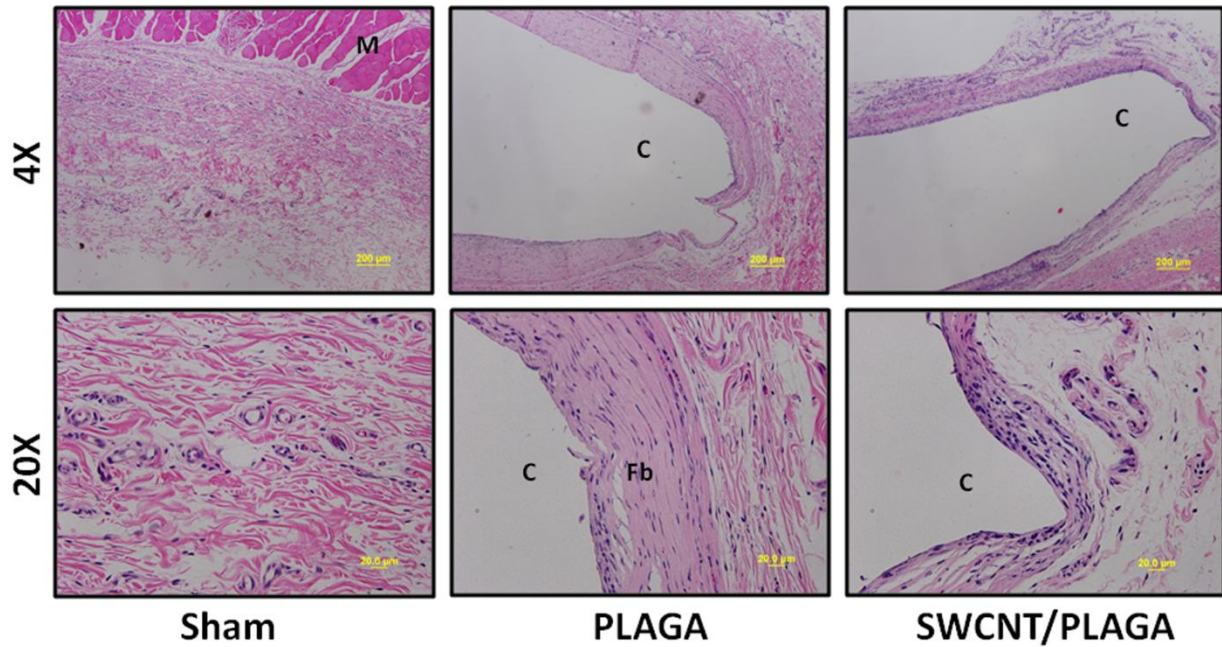
CHAPTER 5-4

DISCUSSION

Biodegradable composites are of interest in clinical medicine because of their biocompatibility, bioresorbability, non-immunogenicity, high mechanical strength, and essentially circumvent the need to surgically remove the implanted scaffold (Ibim et al., 1998). The introduction of biodegradable synthetic polymers has increased considerably by researchers in the area of tissue engineering in recent years. Copolymers such as PLAGA are ideal biodegradable scaffolds for tissue engineering applications and are currently used in the biomedical industry (C. T. Laurencin, Attawia, Elgendy, & Herbert, 1996; Lim, Poh, & Wang, 2009). PLAGA scaffolds exhibit excellent biocompatibility, bioresorbability, non-immunogenicity, and high mechanical strength. In our previous published studies we demonstrated that incorporation of SWCNT to PLAGA significantly enhanced cell proliferation and mechanical strength against a PLAGA control (Gupta et al., 2014; Gupta et al., 2013). Before a composite can be applied in a clinical application, it has to be certified as biocompatible and non-toxic (Khouw et al., 2000).

The goal of this study was to evaluate tissue biocompatibility and toxicity of a SWCNT/PLAGA composite in Sprague-Dawley (SD) rats for 12 weeks to demonstrate that SWCNT/PLAGA composites are biocompatible, non-cytotoxic, and potentially safe for clinical use. Rats were implanted with Sham, PLAGA and SWCNT/PLAGA composites subcutaneously and 5 rats from each group were euthanized at 2, 4, 8, and 12 weeks. No mortality, inflammation, behavioral changes or visible signs of physical self-mutilation indicating localized, systemic or neurological toxicity were observed during the post-op examinations and at the time of euthanasia. No treatment-related signs were observed for any animals. All the

134

groups showed consistent weight gain throughout the study appropriate for the age of the animals and the rate-of-gain for each group was similar. The food consumption by the animals in all the groups followed the same pattern. All treatment groups showed a significant increase in food consumption initially following the post surgical period and then food consumption plateaued. This pattern can be attributed to necessity of more food consumption during wound healing period. The urinalysis showed no significant difference between the Sham, PLAGA and SWCNT/PLAGA for any of the urinalysis parameters. For the hematology analysis, the statistically significant differences observed were all for values that nonetheless were within the normal range of values reported for rats. Therefore, it was considered that there were no hematological effects due to implantation of SWCNT/PLAGA composite compared to Sham and PLAGA.

It is documented that inflammation around implants is a process of normal host defense mechanisms brought about by the result of surgical implantation along with the presence of the implanted material (Menei et al., 1993; Ibim et al., 1998). In a polymeric implant the inflammatory reaction is dependent on several factors such as the extent of injury or defect, size, shape, degradation rates of the polymers, as well as the physical, chemical and mechanical properties of the implant material (Homsy, 1970; LITTLE & PARKHOUSE, 1962; Wood, Kaminski, & Oglesby, 1970). Biodegradable polymers such as polyphosphazenes, polyanhydrides, PLAGA and many non-degradable polymers have been shown to produce inflammatory responses (Leong, D'Amore, Marletta, & Langer, 1986; C. Laurencin et al., 1990; Brady, Cutright, Miller, & Barristone, 1973; Turner, Lawrence, & Autian, 1973). In this study, no macroscopic abnormalities were observed in any of the animals at any time interval. Subcutaneous tissue surrounding the implants appeared grossly normal with no overt evidence of

inflammation and all incision sites were healed. There were no lesions observed in the major organs of the rats related to implantation of PLAGA and SWCNT/PLAGA. The absolute and relative organ weight of the animals in all the groups at all the intervals was similar and did not show any significant difference. The sham animals did not show any response to the sham operation, with a sumtox score of zero for all four time periods following implantation. A mild to moderate sumtox score was observed for animals treated with the PLAGA and SWCNT/PLAGA composites. At all the time intervals both PLAGA and SWCNT/PLAGA showed a significantly higher sumtox score compared to the relative Sham group however, there was no significant difference between PLAGA and SWCNT/PLAGA implanted groups.

In conclusion, our SWCNT/PLAGA composites, which possess high mechanical strength and mimic the microstructure of human trabecular bone (Gupta et al., 2014), displayed tissue compatibility similar to PLAGA, a well known biocompatible polymer over the 12 week study. Thus, the results obtained demonstrate the potential of SWCNT/PLAGA composites for application in BTE and musculoskeletal regeneration. Future studies will be designed to evaluate the efficacy of SWCNT/PLAGA composites in bone regeneration in a non-union ulnar bone defect rabbit model. As interest in carbon nanotube technology increases, studies must be performed to fully evaluate these novel materials at a nonclinical level to assess their safety. The ability to produce composites capable of promoting bone growth will have a significant impact on tissue regeneration and will allow greater functional recovery in injured patients.

REFERENCES

Albelda, S. M., & Buck, C. A. (1990). Integrins and other cell adhesion molecules. *FASEB J, 4*(11), 2868-2880.

Ambrose, C. G., Clyburn, T. A., Louden, K., Joseph, J., Wright, J., Gulati, P., . . . Mikos, A. G. (2004). Effective treatment of osteomyelitis with biodegradable microspheres in a rabbit model. *Clin Orthop Relat Res*(421), 293-299.

Apte, U. M., Banerjee, A., McRee, R., Wellberg, E., & Ramaiah, S. K. (2005). Role of osteopontin in hepatic neutrophil infiltration during alcoholic steatohepatitis. *Toxicol Appl Pharmacol, 207*(1), 25-38. doi: 10.1016/j.taap.2004.12.018

Armentano, I., Dottori, M., Puglia, D., & Kenny, J. M. (2008). Effects of carbon nanotubes (CNTs) on the processing and in-vitro degradation of poly(DL-lactide-co-glycolide)/CNT films. *J Mater Sci Mater Med, 19*(6), 2377-2387. doi: 10.1007/s10856-007-3276-2

Arsecularatne, J. A., & Zhang, L. C. (2007). Carbon nanotube reinforced ceramic composites and their performance. *Recent Pat Nanotechnol, 1*(3), 176-185.

Ashizawa, N., Graf, K., Do, Y. S., Nunohiro, T., Giachelli, C. M., Meehan, W. P., . . . Hsueh, W. A. (1996). Osteopontin is produced by rat cardiac fibroblasts and mediates A(II)-induced DNA synthesis and collagen gel contraction. *J Clin Invest, 98*(10), 2218-2227. doi: 10.1172/JCI119031

Athanasiou, K. A., Niederauer, G. G., & Agrawal, C. M. (1996). Sterilization, toxicity, biocompatibility and clinical applications of polylactic acid/polyglycolic acid copolymers. *Biomaterials, 17*(2), 93-102.

Attawia, M. A., Uhrich, K. E., Botchwey, E., Langer, R., & Laurencin, C. T. (1996). In vitro bone biocompatibility of poly (anhydride-co-imides) containing pyromellitylimidoalanine. *J Orthop Res, 14*(3), 445-454. doi: 10.1002/jor.1100140315

Aubin, J. E., Liu, F., Malaval, L., & Gupta, A. K. (1995). Osteoblast and chondroblast differentiation. *Bone, 17*(2 Suppl), 77S-83S.

Babensee, J. E., McIntire, L. V., & Mikos, A. G. (2000). Growth factor delivery for tissue engineering. *Pharm Res, 17*(5), 497-504.

Bagambisa, F. B., Kappert, H. F., & Schilli, W. (1994). Cellular and molecular biological events at the implant interface. *J Craniomaxillofac Surg, 22*(1), 12-17.

Banerjee, A., Apte, U. M., Smith, R., & Ramaiah, S. K. (2006). Higher neutrophil infiltration mediated by osteopontin is a likely contributing factor to the increased susceptibility of females to alcoholic liver disease. *J Pathol, 208*(4), 473-485. doi: 10.1002/path.1917

Berggren, A., Weiland, A. J., & Dorfman, H. (1982). Free vascularized bone grafts: factors affecting their survival and ability to heal to recipient bone defects. *Plast Reconstr Surg, 69*(1), 19-29.

Beris, A. E., Payatakes, A. H., Kostopoulos, V. K., Korompilias, A. V., Mavrodontidis, A. N., Vekris, M. D., . . . Soucacos, P. N. (2004). Non-union of femoral neck fractures with osteonecrosis of the femoral head: treatment with combined free vascularized fibular grafting and subtrochanteric valgus osteotomy. *Orthop Clin North Am, 35*(3), 335-343, ix. doi: 10.1016/j.ocl.2004.02.008

Borrelli, J., Prickett, W. D., & Ricci, W. M. (2003). Treatment of nonunions and osseous defects with bone graft and calcium sulfate. *Clin Orthop Relat Res*(411), 245-254. doi: 10.1097/01.blo.0000069893.31220.6f

Brady, J. M., Cutright, D. E., Miller, R. A., & Barristone, G. C. (1973). Resorption rate, route, route of elimination, and ultrastructure of the implant site of polylactic acid in the abdominal wall of the rat. *J Biomed Mater Res, 7*(2), 155-166. doi: 10.1002/jbm.820070204

Brekke, J. H., & Toth, J. M. (1998). Principles of tissue engineering applied to programmable osteogenesis. *J Biomed Mater Res, 43*(4), 380-398.

Burg, K. J., Porter, S., & Kellam, J. F. (2000). Biomaterial developments for bone tissue engineering. *Biomaterials, 21*(23), 2347-2359.

Butler, W. T. (1989). The nature and significance of osteopontin. *Connect Tissue Res, 23*(2-3), 123-136.

Cancela, L., Hsieh, C. L., Francke, U., & Price, P. A. (1990). Molecular structure, chromosome assignment, and promoter organization of the human matrix Gla protein gene. *J Biol Chem, 265*(25), 15040-15048.

Chang, J., Lei, H., Liu, Q., Qin, S., Ma, K., Luo, S., . . . Xia, Y. (2012). Optimization of culture of mesenchymal stem cells: a comparison of conventional plate and microcarrier cultures. *Cell Prolif, 45*(5), 430-437. doi: 10.1111/j.1365-2184.2012.00836.x

Cheng, Q., Rutledge, K., & Jabbarzadeh, E. (2013). Carbon nanotube-poly(lactide-co-glycolide) composite scaffolds for bone tissue engineering applications. *Ann Biomed Eng, 41*(5), 904-916. doi: 10.1007/s10439-012-0728-8

Coelho, M. J., & Fernandes, M. H. (2000). Human bone cell cultures in biocompatibility testing. Part II: effect of ascorbic acid, beta-glycerophosphate and dexamethasone on osteoblastic differentiation. *Biomaterials, 21*(11), 1095-1102.

Cohen, S., Alonso, M. J., & Langer, R. (1994). Novel approaches to controlled-release antigen delivery. *Int J Technol Assess Health Care, 10*(1), 121-130.

Da Silva, A. P., Pollett, A., Rittling, S. R., Denhardt, D. T., Sodek, J., & Zohar, R. (2006). Exacerbated tissue destruction in DSS-induced acute colitis of OPN-null mice is associated with downregulation of TNF-alpha expression and non-programmed cell death. *J Cell Physiol, 208*(3), 629-639. doi: 10.1002/jcp.20701

Dai, H. (2002). Carbon nanotubes: synthesis, integration, and properties. *Acc Chem Res, 35*(12), 1035-1044.

Denhardt, D. T., & Guo, X. (1993). Osteopontin: a protein with diverse functions. *FASEB J, 7*(15), 1475-1482.

Denhardt, D. T., Noda, M., O'Regan, A. W., Pavlin, D., & Berman, J. S. (2001). Osteopontin as a means to cope with environmental insults: regulation of inflammation, tissue remodeling, and cell survival. *J Clin Invest, 107*(9), 1055-1061. doi: 10.1172/JCI12980

Di Lullo, G. A., Sweeney, S. M., Korkko, J., Ala-Kokko, L., & San Antonio, J. D. (2002). Mapping the ligand-binding sites and disease-associated mutations on the most abundant protein in the human, type I collagen. *J Biol Chem, 277*(6), 4223-4231. doi: 10.1074/jbc.M110709200

Dias, M. R., Fernandes, P. R., Guedes, J. M., & Hollister, S. J. (2012). Permeability analysis of scaffolds for bone tissue engineering. *J Biomech, 45*(6), 938-944. doi: 10.1016/j.jbiomech.2012.01.019

Elgendy, H. M., Norman, M. E., Keaton, A. R., & Laurencin, C. T. (1993). Osteoblast-like cell (MC3T3-E1) proliferation on bioerodible polymers: an approach towards the

development of a bone-bioerodible polymer composite material. *Biomaterials, 14*(4), 263-269.

Fan, J., Li, Y., Jiang, H., Tang, G., & Wang, L. (2008). In vivo Degradation and histocompatibility of a novel class of fluorescent copolyanhydrides, poly{[di(p-carboxyphenyl) succinate]-co-(sebacic anhydride)}. *Macromol Biosci, 8*(5), 384-392. doi: 10.1002/mabi.200700280

Fei, Z., Hu, Y., Wu, D., Wu, H., Lu, R., Bai, J., & Song, H. (2008). Preparation and property of a novel bone graft composite consisting of rhBMP-2 loaded PLGA microspheres and calcium phosphate cement. *J Mater Sci Mater Med, 19*(3), 1109-1116. doi: 10.1007/s10856-007-3050-5

Fernandez, C., Clark, K., Burrows, L., Schofield, N. R., & Humphries, M. J. (1998). Regulation of the extracellular ligand binding activity of integrins. *Front Biosci, 3*, d684-700.

Field, R. A., Riley, M. L., Mello, F. C., Corbridge, M. H., & Kotula, A. W. (1974). Bone composition in cattle, pigs, sheep and poultry. *J Anim Sci, 39*(3), 493-499.

Fisher, L. W., McBride, O. W., Termine, J. D., & Young, M. F. (1990). Human bone sialoprotein. Deduced protein sequence and chromosomal localization. *J Biol Chem, 265*(4), 2347-2351.

Fulzele, K., Riddle, R. C., DiGirolamo, D. J., Cao, X., Wan, C., Chen, D., . . . Clemens, T. L. (2010). Insulin receptor signaling in osteoblasts regulates postnatal bone acquisition and body composition. *Cell, 142*(2), 309-319. doi: 10.1016/j.cell.2010.06.002

Giannoudis, P. V., Dinopoulos, H., & Tsiridis, E. (2005). Bone substitutes: an update. *Injury, 36 Suppl 3*, S20-27. doi: 10.1016/j.injury.2005.07.029

Green, R. E., Krause, J., Briggs, A. W., Maricic, T., Stenzel, U., Kircher, M., . . . Pääbo, S. (2010). A draft sequence of the Neandertal genome. *Science, 328*(5979), 710-722. doi: 10.1126/science.1188021

Greenwald, A. S., Boden, S. D., Goldberg, V. M., Khan, Y., Laurencin, C. T., Rosier, R. N., & Implants, A. A. o. O. S. T. C. o. B. (2001). Bone-graft substitutes: facts, fictions, and applications. *J Bone Joint Surg Am, 83-A Suppl 2 Pt 2*, 98-103.

Grizzi, I., Garreau, H., Li, S., & Vert, M. (1995). Hydrolytic degradation of devices based on poly(DL-lactic acid) size-dependence. *Biomaterials, 16*(4), 305-311.

Groessner-Schreiber, B., & Tuan, R. S. (1992). Enhanced extracellular matrix production and mineralization by osteoblasts cultured on titanium surfaces in vitro. *J Cell Sci, 101 (Pt 1)*, 209-217.

Gronowicz, G., & McCarthy, M. B. (1996). Response of human osteoblasts to implant materials: integrin-mediated adhesion. *J Orthop Res, 14*(6), 878-887. doi: 10.1002/jor.1100140606

Gullberg, D., Velling, T., Lohikangas, L., & Tiger, C. F. (1998). Integrins during muscle development and in muscular dystrophies. *Front Biosci, 3*, D1039-1050.

Gupta, A., Main, B. J., Taylor, B. L., Gupta, M., Whitworth, C. A., Cady, C., . . . El-Amin, S. F. (2014). In vitro evaluation of three-dimensional single-walled carbon nanotube composites for bone tissue engineering. *J Biomed Mater Res A*. doi: 10.1002/jbm.a.35088

Gupta, A., Woods, M. D., Illingworth, K. D., Niemeier, R., Schafer, I., Cady, C., . . . El-Amin, S. F. (2013). Single walled carbon nanotube composites for bone tissue engineering. *J Orthop Res, 31*(9), 1374-1381. doi: 10.1002/jor.22379

Hautanen, A., Gailit, J., Mann, D. M., & Ruoslahti, E. (1989). Effects of modifications of the RGD sequence and its context on recognition by the fibronectin receptor. *J Biol Chem, 264*(3), 1437-1442.

Hench, L. L., & Wilson, J. (1984). Surface-active biomaterials. *Science, 226*(4675), 630-636.

Homsy, C. A. (1970). Bio-compatibility in selection of materials for implantation. *J Biomed Mater Res, 4*(3), 341-356. doi: 10.1002/jbm.820040306

Horikawa, A., Okada, K., Sato, K., & Sato, M. (2000). Morphological changes in osteoblastic cells (MC3T3-E1) due to fluid shear stress: cellular damage by prolonged application of fluid shear stress. *Tohoku J Exp Med, 191*(3), 127-137.

Hu, H., Ni, Y., Montana, V., Haddon, R. C., & Parpura, V. (2004). Chemically Functionalized Carbon Nanotubes as Substrates for Neuronal Growth. *Nano Lett, 4*(3), 507-511. doi: 10.1021/nl035193d

Hughes, D. E., Salter, D. M., Dedhar, S., & Simpson, R. (1993). Integrin expression in human bone. *J Bone Miner Res, 8*(5), 527-533. doi: 10.1002/jbmr.5650080503

Hunter, G. K., & Goldberg, H. A. (1994). Modulation of crystal formation by bone phosphoproteins: role of glutamic acid-rich sequences in the nucleation of hydroxyapatite by bone sialoprotein. *Biochem J, 302 (Pt 1)*, 175-179.

Hutmacher, D. W. (2000). Scaffolds in tissue engineering bone and cartilage. *Biomaterials, 21*(24), 2529-2543.

Hynes, R. O. (1992). Integrins: versatility, modulation, and signaling in cell adhesion. *Cell, 69*(1), 11-25.

Ibim, S. M., Uhrich, K. E., Bronson, R., El-Amin, S. F., Langer, R. S., & Laurencin, C. T. (1998). Poly(anhydride-co-imides): in vivo biocompatibility in a rat model. *Biomaterials, 19*(10), 941-951.

Ignatius, A. A., & Claes, L. E. (1996). In vitro biocompatibility of bioresorbable polymers: poly(L, DL-lactide) and poly(L-lactide-co-glycolide). *Biomaterials, 17*(8), 831-839.

Igwe, J. C., Mikael, P. E., & Nukavarapu, S. P. (2012). Design, fabrication and in vitro evaluation of a novel polymer-hydrogel hybrid scaffold for bone tissue engineering. *J Tissue Eng Regen Med*. doi: 10.1002/term.1506

Ikeda, T., Shirasawa, T., Esaki, Y., Yoshiki, S., & Hirokawa, K. (1993). Osteopontin mRNA is expressed by smooth muscle-derived foam cells in human atherosclerotic lesions of the aorta. *J Clin Invest, 92*(6), 2814-2820. doi: 10.1172/JCI116901

Jackson, D. W., & Simon, T. M. (1999). Tissue engineering principles in orthopaedic surgery. *Clin Orthop Relat Res*(367 Suppl), S31-45.

Jalil, R., & Nixon, J. R. (1990). Biodegradable poly(lactic acid) and poly(lactide-co-glycolide) microcapsules: problems associated with preparative techniques and release properties. *J Microencapsul, 7*(3), 297-325. doi: 10.3109/02652049009021842

Janicki, P., & Schmidmaier, G. (2011). What should be the characteristics of the ideal bone graft substitute? Combining scaffolds with growth factors and/or stem cells. *Injury, 42 Suppl 2*, S77-81. doi: 10.1016/j.injury.2011.06.014

Johansson, S., Svineng, G., Wennerberg, K., Armulik, A., & Lohikangas, L. (1997). Fibronectin-integrin interactions. *Front Biosci, 2*, d126-146.

Kasemo, B., & Lausmaa, J. (1994). Material-tissue interfaces: the role of surface properties and processes. *Environ Health Perspect, 102 Suppl 5*, 41-45.

Khouw, I. M., van Wachem, P. B., Molema, G., Plantinga, J. A., de Leij, L. F., & van Luyn, M. J. (2000). The foreign body reaction to a biodegradable biomaterial differs between rats and mice. *J Biomed Mater Res, 52*(3), 439-446.

Koh, L. B., Rodriguez, I., & Venkatraman, S. S. (2009). A novel nanostructured poly(lactic-co-glycolic-acid)-multi-walled carbon nanotube composite for blood-contacting applications: thrombogenicity studies. *Acta Biomater, 5*(9), 3411-3422. doi: 10.1016/j.actbio.2009.06.003

Korompilias, A. V., Lykissas, M. G., Soucacos, P. N., Kostas, I., & Beris, A. E. (2009). Vascularized free fibular bone graft in the management of congenital tibial pseudarthrosis. *Microsurgery, 29*(5), 346-352. doi: 10.1002/micr.20649

Langer, R. (1995). 1994 Whitaker Lecture: polymers for drug delivery and tissue engineering. *Ann Biomed Eng, 23*(2), 101-111.

Langer, R., & Vacanti, J. P. (1993). Tissue engineering. *Science, 260*(5110), 920-926.

Langer, R. S., & Vacanti, J. P. (1999). Tissue engineering: the challenges ahead. *Sci Am, 280*(4), 86-89.

Laurencin, C., Domb, A., Morris, C., Brown, V., Chasin, M., McConnell, R., . . . Langer, R. (1990). Poly(anhydride) administration in high doses in vivo: studies of biocompatibility and toxicology. *J Biomed Mater Res, 24*(11), 1463-1481. doi: 10.1002/jbm.820241105

Laurencin, C. T., Ambrosio, A. M., Borden, M. D., & Cooper, J. A. (1999). Tissue engineering: orthopedic applications. *Annu Rev Biomed Eng, 1*, 19-46. doi: 10.1146/annurev.bioeng.1.1.19

Laurencin, C. T., Attawia, M. A., Elgendy, H. E., & Herbert, K. M. (1996). Tissue engineered bone-regeneration using degradable polymers: the formation of mineralized matrices. *Bone, 19*(1 Suppl), 93S-99S.

Laurencin, C. T., El-Amin, S. F., Ibim, S. E., Willoughby, D. A., Attawia, M., Allcock, H. R., & Ambrosio, A. A. (1996). A highly porous 3-dimensional polyphosphazene polymer matrix for skeletal tissue regeneration. *J Biomed Mater Res, 30*(2), 133-138. doi: 10.1002/(SICI)1097-4636(199602)30:2<133::AID-JBM1>3.0.CO;2-S

Laurencin, C. T., & Langer, R. (1987). Polymeric controlled release systems: new methods for drug delivery. *Clin Lab Med, 7*(2), 301-323.

Lee, N. K., Sowa, H., Hinoi, E., Ferron, M., Ahn, J. D., Confavreux, C., . . . Karsenty, G. (2007). Endocrine regulation of energy metabolism by the skeleton. *Cell, 130*(3), 456-469. doi: 10.1016/j.cell.2007.05.047

Legros, R., Balmain, N., & Bonel, G. (1987). Age-related changes in mineral of rat and bovine cortical bone. *Calcif Tissue Int, 41*(3), 137-144.

Leong, K. W., D'Amore, P. D., Marletta, M., & Langer, R. (1986). Bioerodible polyanhydrides as drug-carrier matrices. II. Biocompatibility and chemical reactivity. *J Biomed Mater Res, 20*(1), 51-64. doi: 10.1002/jbm.820200106

Lim, T. Y., Poh, C. K., & Wang, W. (2009). Poly (lactic-co-glycolic acid) as a controlled release delivery device. *J Mater Sci Mater Med, 20*(8), 1669-1675. doi: 10.1007/s10856-009-3727-z

Liopo, A. V., Stewart, M. P., Hudson, J., Tour, J. M., & Pappas, T. C. (2006). Biocompatibility of native and functionalized single-walled carbon nanotubes for neuronal interface. *J Nanosci Nanotechnol, 6*(5), 1365-1374.

LITTLE, K., & PARKHOUSE, J. (1962). Tissue reactions to polymers. *Lancet, 2*(7261), 857-861.

Lu, L., Garcia, C. A., & Mikos, A. G. (1999). In vitro degradation of thin poly(DL-lactic-co-glycolic acid) films. *J Biomed Mater Res, 46*(2), 236-244.

Lu, L., & Mikos, A. G. (1996). The importance of new processing techniques in tissue engineering. *MRS Bull, 21*(11), 28-32.

Luginbuehl, V., Meinel, L., Merkle, H. P., & Gander, B. (2004). Localized delivery of growth factors for bone repair. *Eur J Pharm Biopharm, 58*(2), 197-208. doi: 10.1016/j.ejpb.2004.03.004

Mattson, M. P., Haddon, R. C., & Rao, A. M. (2000). Molecular functionalization of carbon nanotubes and use as substrates for neuronal growth. *J Mol Neurosci, 14*(3), 175-182. doi: 10.1385/JMN:14:3:175

Menei, P., Daniel, V., Montero-Menei, C., Brouillard, M., Pouplard-Barthelaix, A., & Benoit, J. P. (1993). Biodegradation and brain tissue reaction to poly(D,L-lactide-co-glycolide) microspheres. *Biomaterials, 14*(6), 470-478.

Meng, J., Kong, H., Xu, H. Y., Song, L., Wang, C. Y., & Xie, S. S. (2005). Improving the blood compatibility of polyurethane using carbon nanotubes as fillers and its implications to cardiovascular surgery. *J Biomed Mater Res A, 74*(2), 208-214. doi: 10.1002/jbm.a.30315

Migliaresi, C., Fambri, L., & Cohn, D. (1994). A study on the in vitro degradation of poly(lactic acid). *J Biomater Sci Polym Ed, 5*(6), 591-606.

Mikos, A. G., Sarakinos, G., Leite, S. M., Vacanti, J. P., & Langer, R. (1993). Laminated three-dimensional biodegradable foams for use in tissue engineering. *Biomaterials, 14*(5), 323-330.

147

Mistry, A. S., & Mikos, A. G. (2005). Tissue engineering strategies for bone regeneration. *Adv Biochem Eng Biotechnol, 94*, 1-22.

Miyamoto, S., Takaoka, K., Okada, T., Yoshikawa, H., Hashimoto, J., Suzuki, S., & Ono, K. (1993). Polylactic acid-polyethylene glycol block copolymer. A new biodegradable synthetic carrier for bone morphogenetic protein. *Clin Orthop Relat Res*(294), 333-343.

Murry, C. E., Giachelli, C. M., Schwartz, S. M., & Vracko, R. (1994). Macrophages express osteopontin during repair of myocardial necrosis. *Am J Pathol, 145*(6), 1450-1462.

Müller, W. E. (2003). The origin of metazoan complexity: porifera as integrated animals. *Integr Comp Biol, 43*(1), 3-10. doi: 10.1093/icb/43.1.3

Nagasaka, A., Matsue, H., Matsushima, H., Aoki, R., Nakamura, Y., Kambe, N., . . . Shimada, S. (2008). Osteopontin is produced by mast cells and affects IgE-mediated degranulation and migration of mast cells. *Eur J Immunol, 38*(2), 489-499. doi: 10.1002/eji.200737057

Ogata, Y. (2008). Bone sialoprotein and its transcriptional regulatory mechanism. *J Periodontal Res, 43*(2), 127-135. doi: 10.1111/j.1600-0765.2007.01014.x

Oury, F., Sumara, G., Sumara, O., Ferron, M., Chang, H., Smith, C. E., . . . Karsenty, G. (2011). Endocrine regulation of male fertility by the skeleton. *Cell, 144*(5), 796-809. doi: 10.1016/j.cell.2011.02.004

Pellegrini, G., Seol, Y. J., Gruber, R., & Giannobile, W. V. (2009). Pre-clinical models for oral and periodontal reconstructive therapies. *J Dent Res, 88*(12), 1065-1076. doi: 10.1177/0022034509349748

Petite, H., Viateau, V., Bensaïd, W., Meunier, A., de Pollak, C., Bourguignon, M., . . . Guillemin, G. (2000). Tissue-engineered bone regeneration. *Nat Biotechnol, 18*(9), 959-963. doi: 10.1038/79449

148

Pi, M., Wu, Y., & Quarles, L. D. (2011). GPRC6A mediates responses to osteocalcin in β-cells in vitro and pancreas in vivo. *J Bone Miner Res, 26*(7), 1680-1683. doi: 10.1002/jbmr.390

Pierschbacher, M. D., & Ruoslahti, E. (1984). Cell attachment activity of fibronectin can be duplicated by small synthetic fragments of the molecule. *Nature, 309*(5963), 30-33.

Pockwinse, S. M., Kota, K. P., Quaresma, A. J., Imbalzano, A. N., Lian, J. B., van Wijnen, A. J., . . . Nickerson, J. A. (2011). Live cell imaging of the cancer-related transcription factor RUNX2 during mitotic progression. *J Cell Physiol, 226*(5), 1383-1389. doi: 10.1002/jcp.22465

Puchacz, E., Lian, J. B., Stein, G. S., Wozney, J., Huebner, K., & Croce, C. (1989). Chromosomal localization of the human osteocalcin gene. *Endocrinology, 124*(5), 2648-2650. doi: 10.1210/endo-124-5-2648

Puleo, D. A., & Nanci, A. (1999). Understanding and controlling the bone-implant interface. *Biomaterials, 20*(23-24), 2311-2321.

Pytela, R., Pierschbacher, M. D., & Ruoslahti, E. (1985). Identification and isolation of a 140 kd cell surface glycoprotein with properties expected of a fibronectin receptor. *Cell, 40*(1), 191-198.

Qin, C., Brunn, J. C., Jones, J., George, A., Ramachandran, A., Gorski, J. P., & Butler, W. T. (2001). A comparative study of sialic acid-rich proteins in rat bone and dentin. *Eur J Oral Sci, 109*(2), 133-141.

Reinholt, F. P., Hultenby, K., Oldberg, A., & Heinegård, D. (1990). Osteopontin--a possible anchor of osteoclasts to bone. *Proc Natl Acad Sci U S A, 87*(12), 4473-4475.

Rho, J. Y., Kuhn-Spearing, L., & Zioupos, P. (1998). Mechanical properties and the hierarchical structure of bone. *Med Eng Phys, 20*(2), 92-102.

Royals, M. A., Fujita, S. M., Yewey, G. L., Rodriguez, J., Schultheiss, P. C., & Dunn, R. L. (1999). Biocompatibility of a biodegradable in situ forming implant system in rhesus monkeys. *J Biomed Mater Res, 45*(3), 231-239.

Ruoslahti, E. (1996). RGD and other recognition sequences for integrins. *Annu Rev Cell Dev Biol, 12*, 697-715. doi: 10.1146/annurev.cellbio.12.1.697

Saito, N., Usui, Y., Aoki, K., Narita, N., Shimizu, M., Hara, K., . . . Endo, M. (2009). Carbon nanotubes: biomaterial applications. *Chem Soc Rev, 38*(7), 1897-1903. doi: 10.1039/b804822n

Saito, T., Albelda, S. M., & Brighton, C. T. (1994). Identification of integrin receptors on cultured human bone cells. *J Orthop Res, 12*(3), 384-394. doi: 10.1002/jor.1100120311

Schwartz, Z., Lohmann, C. H., Oefinger, J., Bonewald, L. F., Dean, D. D., & Boyan, B. D. (1999). Implant surface characteristics modulate differentiation behavior of cells in the osteoblastic lineage. *Adv Dent Res, 13*, 38-48.

Sekiya, I., Larson, B. L., Smith, J. R., Pochampally, R., Cui, J. G., & Prockop, D. J. (2002). Expansion of human adult stem cells from bone marrow stroma: conditions that maximize the yields of early progenitors and evaluate their quality. *Stem Cells, 20*(6), 530-541. doi: 10.1634/stemcells.20-6-530

Sethuraman, S., Nair, L. S., El-Amin, S., Farrar, R., Nguyen, M. T., Singh, A., . . . Laurencin, C. T. (2006). In vivo biodegradability and biocompatibility evaluation of novel alanine ester based polyphosphazenes in a rat model. *J Biomed Mater Res A, 77*(4), 679-687. doi: 10.1002/jbm.a.30620

150

Shi Kam, N. W., Jessop, T. C., Wender, P. A., & Dai, H. (2004). Nanotube molecular transporters: internalization of carbon nanotube-protein conjugates into Mammalian cells. *J Am Chem Soc, 126*(22), 6850-6851. doi: 10.1021/ja0486059

Shoulders, M. D., & Raines, R. T. (2009). Collagen structure and stability. *Annu Rev Biochem, 78*, 929-958. doi: 10.1146/annurev.biochem.77.032207.120833

Sinha, N., & Yeow, J. T. (2005). Carbon nanotubes for biomedical applications. *IEEE Trans Nanobioscience, 4*(2), 180-195.

Sinha, R. K., & Tuan, R. S. (1996). Regulation of human osteoblast integrin expression by orthopedic implant materials. *Bone, 18*(5), 451-457.

Soucacos, P. N., Johnson, E. O., & Babis, G. (2008). An update on recent advances in bone regeneration. *Injury, 39 Suppl 2*, S1-4. doi: 10.1016/S0020-1383(08)70009-3

Soucacos, P. N., Kokkalis, Z. T., Piagkou, M., & Johnson, E. O. (2013). Vascularized bone grafts for the management of skeletal defects in orthopaedic trauma and reconstructive surgery. *Injury, 44 Suppl 1*, S70-75. doi: 10.1016/S0020-1383(13)70016-0

Standal, T., Borset, M., & Sundan, A. (2004). Role of osteopontin in adhesion, migration, cell survival and bone remodeling. *Exp Oncol, 26*(3), 179-184.

Tandon, M., Gokul, K., Ali, S. A., Chen, Z., Lian, J., Stein, G. S., & Pratap, J. (2012). Runx2 mediates epigenetic silencing of the bone morphogenetic protein-3B (BMP-3B/GDF10) in lung cancer cells. *Mol Cancer, 11*, 27. doi: 10.1186/1476-4598-11-27

Thein-Han, W. W., & Misra, R. D. (2009). Biomimetic chitosan-nanohydroxyapatite composite scaffolds for bone tissue engineering. *Acta Biomater, 5*(4), 1182-1197. doi: 10.1016/j.actbio.2008.11.025

151

Thomson, R. C., Yaszemski, M. J., Powers, J. M., & Mikos, A. G. (1995). Fabrication of biodegradable polymer scaffolds to engineer trabecular bone. *J Biomater Sci Polym Ed, 7*(1), 23-38.

Turner, J. E., Lawrence, W. H., & Autian, J. (1973). Subacute toxicity testing of biomaterials using histopathologic evaluation of rabbit muscle tissue. *J Biomed Mater Res, 7*(1), 39-58. doi: 10.1002/jbm.820070104

Uaesoontrachoon, K., Yoo, H. J., Tudor, E. M., Pike, R. N., Mackie, E. J., & Pagel, C. N. (2008). Osteopontin and skeletal muscle myoblasts: association with muscle regeneration and regulation of myoblast function in vitro. *Int J Biochem Cell Biol, 40*(10), 2303-2314. doi: 10.1016/j.biocel.2008.03.020

Uhrich, K. E., Ibim, S. E., Larrier, D. R., Langer, R., & Laurencin, C. T. (1998). Chemical changes during in vivo degradation of poly(anhydride-imide) matrices. *Biomaterials, 19*(22), 2045-2050.

Vandrovcová, M., Douglas, T., Hauk, D., Grössner-Schreiber, B., Wiltfang, J., Bačáková, L., & Warnke, P. H. (2011). Influence of collagen and chondroitin sulfate (CS) coatings on poly-(lactide-co-glycolide) (PLGA) on MG 63 osteoblast-like cells. *Physiol Res, 60*(5), 797-813.

Vert, M., Li, S. M., & Garreau, H. (1994). Attempts to map the structure and degradation characteristics of aliphatic polyesters derived from lactic and glycolic acids. *J Biomater Sci Polym Ed, 6*(7), 639-649.

Vert, M., Mauduit, J., & Li, S. (1994). Biodegradation of PLA/GA polymers: increasing complexity. *Biomaterials, 15*(15), 1209-1213.

Waldrop, F. S., Puchtler, H., Meloan, S. N., & Younker, T. D. (1980). Histochemical investigations of different types of collagen. *Acta Histochem Suppl, 21*, 23-31.

Wang, K. X., & Denhardt, D. T. (2008). Osteopontin: role in immune regulation and stress responses. *Cytokine Growth Factor Rev, 19*(5-6), 333-345. doi: 10.1016/j.cytogfr.2008.08.001

Wang, X., Li, Q., Xie, J., Jin, Z., Wang, J., Li, Y., . . . Fan, S. (2009). Fabrication of ultralong and electrically uniform single-walled carbon nanotubes on clean substrates. *Nano Lett, 9*(9), 3137-3141. doi: 10.1021/nl901260b

Webb, K., Hlady, V., & Tresco, P. A. (2000). Relationships among cell attachment, spreading, cytoskeletal organization, and migration rate for anchorage-dependent cells on model surfaces. *J Biomed Mater Res, 49*(3), 362-368.

Wood, N. K., Kaminski, E. J., & Oglesby, R. J. (1970). The significance of implant shape in experimental testing of biological materials: disc vs. rod. *J Biomed Mater Res, 4*(1), 1-12. doi: 10.1002/jbm.820040102

Zanello, L. P., Zhao, B., Hu, H., & Haddon, R. C. (2006). Bone cell proliferation on carbon nanotubes. *Nano Lett, 6*(3), 562-567. doi: 10.1021/nl051861e

Zhang, Q., Mochalin, V. N., Neitzel, I., Hazeli, K., Niu, J., Kontsos, A., . . . Gogotsi, Y. (2012). Mechanical properties and biomineralization of multifunctional nanodiamond-PLLA composites for bone tissue engineering. *Biomaterials, 33*(20), 5067-5075. doi: 10.1016/j.biomaterials.2012.03.063

Zhang, R., & Ma, P. X. (1999). Porous poly(L-lactic acid)/apatite composites created by biomimetic process. *J Biomed Mater Res, 45*(4), 285-293.

Graduate School

Southern Illinois University

Ashim Gupta

Email: ashim6786@gmail.com

University of Delhi, Delhi, INDIA
Bachelor of Pharmacy, June 2008

Southern Illinois University Carbondale, IL, USA
Master of Science, Molecular Biology, Microbiology and Biochemistry, August 2010

Dissertation Title: EVALUATION OF NON-FUNCTIONALIZED SINGLE WALLED

CARBON NANOTUBES COMPOSITES FOR BONE TISSUE ENGINEERING.

Major Professor: Saadiq F. El-Amin III, M.D., PhD

Publications:

Gupta, A., Main, B.J., Taylor, B.L., Gupta, M., Whitworth, C.A., Cady, C., Freeman, J.W., El-Amin, S.F. (2014) In-vitro Evaluation of Three Dimensional Single Walled Carbon Nanotube Composites for Bone Tissue Engineering. J Biomed Mater Res A. doi: 10.1002/jbm.a.35088.

Gupta, A., Woods, M.D., Illingworth, K.D., Niemeier, R., Schafer, I., Cady, C., Filip, P., El-Amin, S.F. (2013). Single walled carbon nanotubes composites for bone tissue engineering. *J Orthop Res*, 31(9), 1374-1381. doi: 10.1002/jor.22379.

El-Amin, S.F., Thomas, J.W., Hekweazu, U.N., Woods, M.D., Gupta, A. (2013) Regenerative Engineering- The Future of Medicine. *Regenerative Engineering*, CRC Press.

Kukkar, N., Gupta, A., Banerjee, D., Bedi, N., Main, B.J., Freitag, P. (2013). Alterations in disc height, foraminal height and foraminal width following one and two level AxiaLIF® – A radiological analysis. *J Spine*, 2, S5-008. doi: 10.4172/2165-7939.S5-008.

Kukkar, N., Mai, M.C., Gupta, A., Banerjee, D., Bedi, N., Main, B.J., Freitag, P. (2013). Sagittal Lumbar Alignment Following Axial Lumbar Interbody Fusion with TranS1. *J Spine*, 2, 143. doi: 10.4172/2165-7939.1000143.

Gupta, A., Mo, Y.Y. (2011). Detection of microRNAs in both cultured cells and paraffin-embedded tissue specimens by in situ hybridization. *Methods Mol Biol*, 676, 73-83. doi: 10.1007/978-1-60761-863-8_6.